THE EFFECT OF BACTERIAL FLAGELLIN ON VIRUS INFECTION

Elizabeth Kristin Benedikz

A thesis submitted to the University of Birmingham for the degree of Doctor of Philosophy

Institute of Immunology and Immunotherapy

College of Medical and Dental Sciences

University of Birmingham

November 2016

Abstract

Coinfection with bacteria and viruses is an understudied area of microbiology, despite its potential to modulate pathogen abundance and host survival. We investigated the effect of bacteria on virus infection and developed an *in vitro* system to study the first step: viral internalization. Our studies show that multiple bacterial species promote the entry of a diverse panel of viruses into lung and gut epithelial cells. Bacteria expressing the toll-like receptor (TLR)5 agonist, flagellin, are most efficient at inducing viral uptake and studies using recombinant flagellin or aflagellate bacterial strains confirm that flagellin has pro-viral activity. Flagellin promotes epithelial cells to support virus entry via TLR5-dependent activation of NF-κB. To extend these observations and study the role of flagellin in the complete viral replicative lifecycle, we studied human immunodeficiency virus (HIV)-1 replication in T cells. Flagellin augments HIV-1 entry and promoter activity and increases the production of extracellular virus. The data presented in this thesis highlight a new role for bacterial flagellin to promote diverse virus infection of epithelial barriers and enhance the spread of HIV-1. This has significant implications for understanding how exposure to multiple pathogens can alter susceptibility to infection and its associated pathogenesis.

Dedication

To Adam Cunningham and Jane McKeating, who made me a scientist

and

To Anna Benedikz and Steve Brown, who made me

Acknowledgements

Firstly, thank you to everyone who has ever helped me in the lab, especially Dave Mason, who taught me how to work with bacteria, and Nicola Fletcher, who taught me how to work with pseudoparticles. Everyone who has worked in Jane's group and Adam's group over the last 4 years has helped with this thesis. Also to Dalan Bailey and Daniel Gonçalves-Carniero for their advice and measles, and the Institute of Microbiology and Infection who always let me join in - so many people were generous with their time and bacterial strains. Thank you to my family, friends and Morris Symington, who encouraged me when doing a PhD was sometimes overwhelming. And finally, thank you to Jane and Adam, for giving me this opportunity and the Medical Research Council for funding me. I've had a brilliant time.

Table of contents

List of figures

List of tables

List of common abbreviations

CF	Cystic fibrosis
CFU	Colony forming units
CM	Conditioned medium
COPD	Chronic obstructive pulmonary disease
DC	Dendritic cell
EP	Enteropathogenic
GFPpp	Pseudoparticle containing a GFP reporter
HBGA	Histo-blood group antigen
HIV	Human immunodeficiency virus
HSPG	Heparan sulfate proteoglycan
IFN	Interferon
IL	Interleukin
LPS	Lipopolysaccharide
LTR	Long terminal repeat
MAMP	Microbe-associated molecular pattern
MeV	Measles virus
MHC	Major histocompatibility complex
MMTV	Mouse mammary tumour virus
MOI	Multiplicity of infection
NEpp	Non-enveloped pseudoparticle
PERT	Product-enhanced reverse transcriptase
PGN	Peptidoglycan
PrK	Proteinase K
RLU	Relative light units
RTase	Reverse transcriptase
SCV	*Salmonella* containing vacuole
SLAMF1	Signaling lymphocytic activation molecule
SPI	*Salmonella* pathogenicity island
STm	*Salmonella enterica* serovar Typhimurium
Tat	Transactivator of transcription
TJ	Tight junction
TLR	Toll-like receptor
TNF	Tumour necrosis factor
VSV	Vesicular stomatitis virus
VSV-Gpp	Pseudoparticles carrying VSV glycoprotein

1. INTRODUCTION

1.1 The importance of coinfection

The human body hosts a variety of microbes: including bacteria, viruses, fungi and parasites. However, the majority of publications report on the mechanisms underlying a single infectious agent causing disease. Coinfection, also called polymicrobial or dual-species infection, refers to the occurrence of two or more microbes that interact synergistically. Coinfections are more likely to increase pathogen abundance and have a negative effect on host health, than the inverse (Griffiths et al., 2011). Interestingly, one infection can affect the outcome of a secondary infection even after the first has resolved, due to changes in host immunity (Didierlaurent et al., 2007; Goulding et al., 2007). It is important that we understand coinfection and other interactions between microbes, to better prevent and treat infections that are likely to have increased mortality rates.

Global infectious disease mortality data only report a single cause of death, even if other causes were known, preventing researchers from tracking the prevalence of coinfection (Griffiths et al., 2011). The importance of studying coinfection is evidenced when reading clinical reports of pulmonary and gastrointestinal infections, which often report that 20-30% of cases involve two or more pathogenic microbes (Bhavnani et al., 2012; Hoffmann et al., 2012; Sambe-Ba et al., 2013; Obasi et al., 2014). Analysis of all publications describing coinfections in 2009 determined that the most commonly reported pathogen type was bacterial. However, the most studied coinfecting pairs were virus-virus combinations, such as human immunodeficiency

virus (HIV)-hepatitis C virus (HCV; (Griffiths et al., 2011). There is a need to study the interactions of bacterial pathogens with other microbes.

While virus-virus coinfections often occur though shared transmission routes, many bacterial species able to cause disease are carried by the host and require an opportunity to cause infection. This often occurs following viral infection, when immune cell responses can be altered and immunosuppressive cytokines are present (Didierlaurent et al., 2007). Concurrent and successive infections can be more difficult to treat and have increased mortality rates (Gordon et al., 2002; Karlström et al., 2009; Aaron, 2014). Some coinfection combinations include bacterial species already known to interact synergistically with other microbes, such as respiratory viruses promoting bacterial infection (Bosch et al., 2013) or HIV-induced immunosuppression potentiaing opportunistic infections (Furrer, 2016). There are also disease states known to be associated with coinfection, for example, acute otitis media in children, caused by bacterial-bacterial, viral-viral or viral-bacterial coinfection (Marom et al., 2012).

The transkingdom interactions that have been well characterized will be discussed below. However, further research is required to identify coinfecting pathogens that are frequently understudied, to increase our understanding of microbial interactions. This can aid treatment, or ideally increase preventative strategies, to decrease the high mortality rates associated with coinfection.

1.2 Influenza leads to secondary bacterial infection

The influenza virus is an enveloped, negative sense RNA virus that can be classified as type A, B or C. The majority of human infections are caused by type A (Short et al., 2012). Influenza induces a cytolytic infection that reduces the epithelial barrier function, through necrosis of epithelial cells and apoptosis of inflammatory cells (Hussell and Cavanagh, 2009). Influenza interacts with host cells via two envelope glycoproteins; hemagglutinin (HA) binds to its receptor on host cells, sialic acids, to facilitate entry, and neuraminidase (NA) cleaves sialic acids to allow release of new progeny virus from the infected cell in the late steps of the viral life cycle (Short et al., 2012). Influenza infection has long been known to associate with bacterial pneumonia and the majority of deaths caused by the 1918-1919 influenza pandemic, the most recent pandemic without access to antimicrobial agents, were due to secondary bacterial infections (Morens et al., 2008).

Following the discovery of antimicrobial agents and the introduction of vaccines to some common bacterial pathogens in the lung, secondary bacterial infections are still detected after influenza infection. However, the range of species involved has changed (Morens et al., 2008). Bacterial infection usually occurs between four and 14 days after resolution of an influenza infection, when fever reappears. Although influenza is not associated with one specific bacterial species, secondary infection is most often caused by *Haemophilus influenzae*, *Staphylococcus aureus* and *Streptococcus pneumoniae* (Hussell et al., 2009).

The time between influenza resolution and onset of bacterial pneumonia suggests that the interplay is not mediated via direct interactions between the microbes, but an alteration of the host environment following resolution of the viral Infection. One exception to this occurs in coinfections with influenza and *S. pneumoniae*, which both express NA. *S. pneumoniae* encoded NA cleaves host cell sialic acid and thereby promotes bacterial adhesion. However, following influenza virus exit from epithelial cells, the sialic acid has already been modified and can independently augment bacterial adhesion (Peltola and McCullers, 2004). This shared use of NA helps explain the synergy observed when the two microbes infect the lung epithelia at the same time. Interestingly, administration of the influenza NA inhibitor oseltamivir to influenza-infected individuals can decrease the risk of secondary complications (Viasus et al., 2011; Vardakas et al., 2016).

The species of bacteria most frequently associated with secondary infection often colonize the nasopharynx in healthy individuals. Remodeling of the lung immune environment during influenza infection allows bacteria to colonize the lower lung causing pneumonia (Short et al., 2012). In children, influenza and other respiratory viral infections can lead to otitis media, when bacteria such as *S. pneumoniae* infect the middle ear (Marom et al., 2012). This remodeling has been reported to increase the concentration of interleukin (IL)-10 in the lungs of mice to 20 times higher than mice without influenza infection, allowing increased bacterial growth, as the addition of neutralizing anti-IL-10 monoclonal antibody decreased the bacterial burden (van der Sluijs et al., 2004). This study indicates that the presence of an anti-inflammatory cytokines following virus resolution can allow bacteria to colonize the lung.

Influenza A virus infection prior to *S. aureus* challenge in mice reduces the clearance of either microbe from the lung, despite increased macrophage and neutrophil accumulation and interferon (IFN) expression (Kudva et al., 2011). Kudva et al., 2011, reported that type I IFN produced during the virus infection decreases the ability of dendritic cells (DC) to induce Th17 CD4+ T cells that are major players in bacterial clearance. Th17 cells express high levels of the pro-inflammatory cytokines IL-17 and IL-22 that recruit neutrophils and induce antimicrobial peptide (AMP) expression, respectively (Aujla et al., 2007). Further effects on immune cells include desensitization of alveolar macrophages to bacterial products following influenza infection and decreased pro-inflammatory activity upon secondary challenge (Didierlaurent et al., 2008).

Bacterial pneumonia following influenza infection is more difficult to treat than pneumonia caused by a primary bacterial infection and it has been demonstrated that treatment with different types of antibiotic can improve or worsen the outcome (Karlström et al., 2009). The use of β-lactam antibiotics that are bacteriocidal caused greater inflammation and higher mortality than clindamycin, a bacteriostatic antibiotic that leaves cells intact, in a mouse model of influenza A virus and *S. pneumoniae* coinfection (Karlström et al., 2009). This study suggests a need for bacterial testing following influenza infection, before prescription of antibiotics, if the mortality rate of secondary bacterial infection is to be lowered.

The combination of this respiratory virus with certain bacterial species worsens pneumonia outcome compared to that caused by bacteria alone (Hussell and

Cavanagh, 2009). There are many ways that influenza can lead to enhanced bacterial infection (**Fig.1.1**), including those discussed above: decreased integrity of the lung epithelium caused by the cytopathic effects of the virus but also increased expression of bacterial adhesion molecules on influenza infected cells, decreased immune cells that can control bacterial growth such as alveolar macrophages and neutrophils and upregulation of immune suppressant cytokines following the creation of apoptotic cells. Importantly, it has been found that influenza vaccination can decrease the likelihood of bacterial coinfection (Lee et al., 2015) as well as antiviral drugs also targeting the bacterial neuraminidase to reduce bacterial infection (Viasus et al., 2011; Vardakas et al., 2016). In contrast, there is evidence that *S. pneumoniae* exposure prior to influenza can reduce the viral infection (Short et al., 2012). However, the mechanisms for this are yet to be determined.

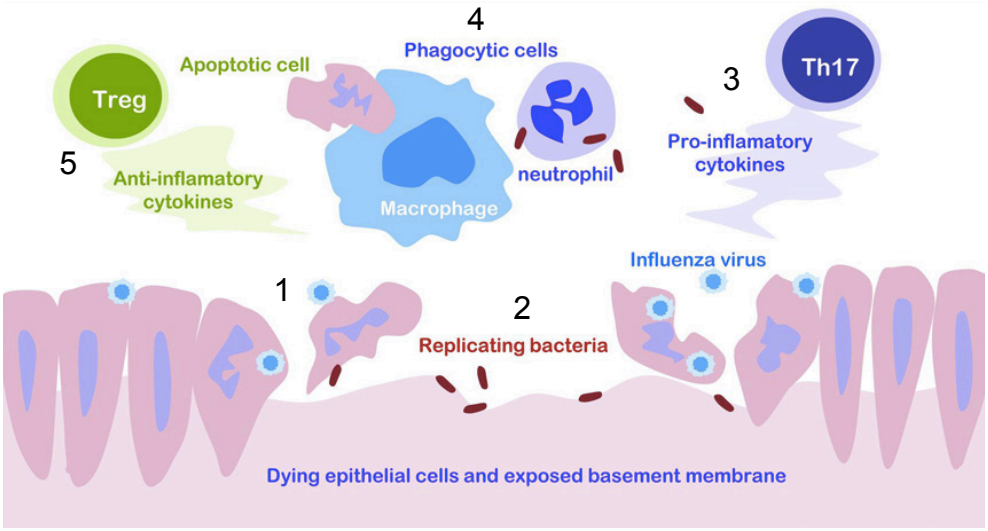

Figure 1.1 **Influenza virus infection predisposes the lung epithelia to secondary bacterial infection.**

Adapted from (Cauley and Vella, 2015) 1. Virus infection of lung epithelia can lead to cell death and damage. 2. Bacteria spread into damaged areas of the lung and replicate. 3. Prolonged pro-inflammatory responses to the virus infection can become toxic and have a negative effect. 4. Phagocytic cells are recruited to clear dying epithelial cells and are less able to phagocytose bacteria. 5. Regulatory T cells can be recruited to dampen the anti-viral response by producing anti-inflammatory cytokines. The combination of steps 3, 4 and 5 allow bacterial growth to continue leading to a secondary infection.

1.3 HIV and opportunistic infections

HIV is a lentivirus and part of the *Retroviridae* family. There are two types of HIV and the majority of HIV-associated deaths are caused by HIV-1, whereas HIV-2 has a lower mortality rate (Prince et al., 2014). HIV is transmitted by sexual intercourse, contaminated blood and vertically from mother-to-child before or during birth, or through breast milk (Cohen et al., 2008). The virus targets CD4+ T cells for depletion, leading to immunodeficiency, which can progress to acquired immune deficiency syndrome (AIDS; (Pantaleo et al., 1993). However, it is now known that the effects are not limited to T cells and there is chronic immune activation that is not reversed by antiretroviral therapy (ART; (Mudd and Brenchley, 2016). Transmission and infection of a new host is dependent on the amount of infectious virus in the bodily fluid transferred. This varies from high levels during the acute infection to undetectable levels from individuals on ART, which is suppressive so does not cure HIV (Cohen et al., 2008). While HIV infection can be controlled to prevent progression to AIDS, it is important to understand factors that can increase HIV transmission to uninfected individuals.

Due to the immunocompromised status of HIV-infected individuals not treated with ART, secondary infections are common. However, they can also occur during ART (Hooshyar et al., 2007). These infections can be bacterial, viral, fungal or parasitic and are often opportunistic pathogens that would not cause disease in a healthy individual. For HIV-infected individuals undergoing treatment in North America, the risk of opportunistic infection is now low (fewer than two in 100 per year) and the main risks are candidiasis, *Pneumocystis jirovecii* pneumonia, mycobacterial

infections including *Mycobacterium tuberculosis* (Mtb), cytomegalovirus, toxoplasmosis and cryptococcosis (Buchacz et al., 2016). In resource-limited settings, tuberculosis is attributable for 40% of HIV-associated deaths (Gupta et al., 2015). The incidence of any opportunistic infection in these settings, even with ART, can be as high as 50%, but is linked to lower T cell numbers due to reduced ART availability (Mitiku et al., 2015).

1.3.1 HIV and Mtb

One third of the global population is reported to encounter Mtb and tuberculosis is the second most common cause of death by an infectious agent (Shankar et al., 2014). Mtb primarily infects the respiratory tract and is detected by innate immune cells such as alveolar macrophages, which phagocytose the bacterium, where it halts lysosomal breakdown to replicate in the immune cell. This infected cell is surrounded by other immune cells that form a granuloma to limit the infection and allow Mtb to establish latency (reviewed by (Ernst, 2012). The bacterium can persist for years in this state, only to be reactivated by alteration of the immune status. As Mtb has an intracellular lifecycle, cell-mediated immunity is necessary for clearance from the host and this allows for interactions with HIV-infected cells (**Fig.1.2**). HIV coinfection can increase the chance of Mtb reactivation by 20-fold and exacerbate associated pathologies (Pawlowski et al., 2012). Conversely, the presence of Mtb increases HIV RNA levels through pro-inflammatory signaling that can augment HIV transcription in infected T cells and macrophages (Deffur et al., 2013).

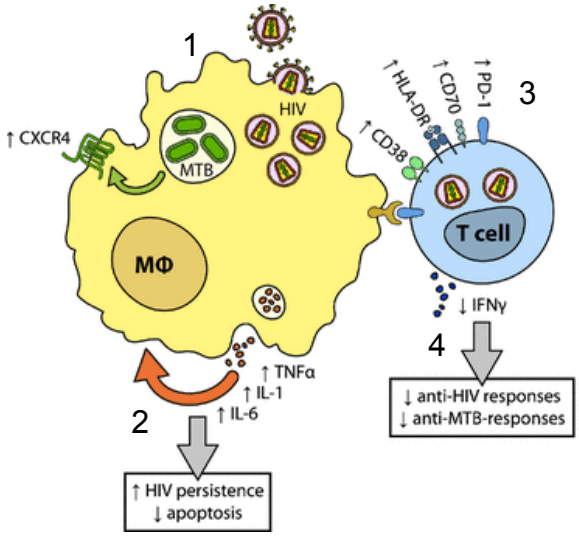

Figure 1.2 **Interactions between HIV and Mtb that can exacerbate both infections.**

Adapted from Shankar et al., 2014. 1. Macrophages (MΦ) infected with *Mycobacterium tuberculosis* (MTB) can upregulate expression of an HIV co-receptor, CXCR4, allowing increased virus infection. 2. Altered cytokine secretion from MTB-infected macrophages also has effects on immune cell functionality and prevents apoptosis of infected cells. Furthermore, HIV-infected T cells have increased expression of immune activation markers (3), reduced anti-viral and anti-bacterial responses and less IFNγ release (4), which is one of the responses required for maintaining a granuloma around MTB-infected cells.

Deffur et al., 2013, reported that HIV infection can deplete Mtb specific T cells and thereby increase the risk of reactivation. Furthermore, both microbes can infect macrophages, and Mtb has a greater growth rate in HIV infected macrophages through increased tumour necrosis factor (TNF) signaling (Imperiali et al., 2001). This pro-inflammatory signaling increases HIV replication and, interestingly, Mtb can increase expression of a viral co-receptor, CXCR4, which promotes infection of naïve target cells (Shankar et al., 2014). A humanized mouse model of HIV-Mtb coinfection has identified that the microbes can act synergistically and this is dependent on the timing of infection. HIV-infected cells localized to Mtb replication sites and pro-inflammatory signaling led to granuloma breakdown (Nusbaum et al., 2016).

1.3.2 HIV and fungal infections

While fungal infections are rare in the immunocompetent host (Schmiedel and Zimmerli, 2016), they are some of the most prevalent infections in HIV-infected hosts (Mitiku et al., 2015; Buchacz et al., 2016). A major opportunistic fungal infection associated with HIV is candidiasis, caused by *Candida spp*. *Candida spp.* are commensal organisms found on the skin and in the oral cavity, gastrointestinal tract and female genital tract that can cause infection upon reaching the bloodstream or deep tissue (Schmiedel and Zimmerli, 2016).

Although increased susceptibility could be solely due to immune suppression, HIV-infected macrophages show a reduced ability to phagocytose *Candida albicans* (Crowe et al., 1994). Furthermore, studies have identified that HIV, through its envelope glycoproteins, can bind to *Candida spp.* cells, which increases their uptake

into HIV-infected host cells (Gruber et al., 2003). Mouse studies have also shown that reduced IL-17 and IL-22 responses during HIV infection lead to decreased innate defences in the oral mucosa (de Repentigny et al., 2015). These mechanisms are similar to those reported for Mtb, indicating that broad effects from one microbe can impact on the outcome of other infections.

Interestingly, *Candida albicans* has been reported to reduce HIV replication in macrophages by promoting the anti-viral response and triggering expression of interferon-stimulated genes such as tetherin (Rodriguez Rodrigues et al., 2013). This interaction highlights the complexity of studying coinfections in more detail. We need to determine whether the microbes in question are likely to meet and act synergistically, and identify whether there's a need for more potent or specific treatments.

1.3.3 Bacterial translocation during HIV infection

HIV infection causes immune activation and inflammation, which is linked to damage to the intestinal tract and gastrointestinal symptoms (reviewed by (Marchetti et al., 2013). CD4+ T cells specific to the gut are lost early in HIV infection, disproportionately to the loss of circulating CD4+ T cells, likely due to increased expression of the HIV-1 co-receptor CCR5 on the gut-resident cells (Mudd and Brenchley, 2016). Other changes associated with gut damage include loss of IL-17 and IL-22 producing cells and enterocyte apoptosis (Shan and Siliciano, 2014). This damage allows bacteria and their products to pass through the epithelial barrier into the local area and beyond to the bloodstream, which is termed microbial

translocation. Furthermore, the immunocompromised status that can occur during HIV infection may reduce phagocytosis of any bacteria breaching the barrier. During translocation of bacteria and their microbial associated molecular patterns (MAMP), inflammation is increased, which may also contribute to breakdown of the barrier (Marchetti et al., 2013).

Although ART can reduce viral RNA in the periphery to undetectable levels, HIV-infected individuals still have increased mortality compared to uninfected individuals. This is most likely explained by chronic immune activation and inflammatory responses induced by microbial translocation, as gastrointestinal damage is not rapidly reversed by ART (Lozupone et al., 2013; Mudd and Brenchley, 2016). Microbial translocation can be detected by measuring levels of bacterial MAMPs such as lipopolysaccharide (LPS) and flagellin in the blood and by levels of antibody to these antigens (Marchetti et al., 2013). Soluble CD14 is a useful marker of monocyte activation that correlates with LPS levels, but may also indicate the presence of Gram-positive bacteria (Shan and Siliciano, 2014). Microbial translocation can affect HIV pathogenesis by increasing inflammation, including T cell activation, potentiating immunodeficiency but also through direct effects on the viral lifecycle. Activation of NF-κB by bacterial products such as flagellin can increase HIV replication (Brichacek et al., 2010; Ferreira et al., 2011), cell-cell transmission (Côté et al., 2013) and reactivation of latent HIV in T cells (Thibault et al., 2009).

Recent studies show that HIV infection can cause profound changes in the virome and bacterial and fungal microbiomes and these changes can contribute to

immunodeficiency, which is only now being realized (Palmer et al., 2016). The most dramatic changes in the intestinal microbiome composition are observed in individuals with low CD4+ T cell counts. Interestingly, expansion of other viruses such as adenovirus may also cause epithelial damage and contribute to microbial translocation (Monaco et al., 2016).

1.3.4 Non-HIV infections can enhance HIV transmission

While HIV can increase the likelihood of opportunistic infections or microbial translocation, there is also evidence for HIV as a secondary infection. Bacterial vaginosis is a condition where the female lower genital tract has an altered microbiome, often with no symptoms. Although the bacterial species involved can vary between individuals, there is an association with increased transmission of HIV and other sexually transmitted infections (Mirmonsef et al., 2012), for which the mechanisms are yet to be determined. It is possible that an increasingly pro-inflammatory environment leads to epithelial damage, allowing HIV easier entry into the host. *Chlamydia trachomatis* is the most common bacterial STI. (Buckner et al., 2016), found that migration of T cells infected with HIV was more successful when the epithelial cells were infected with *C. trachomatis*.

Clinical studies suggest that schistosome infection, a parasitic worm, can increase HIV transmission and progression to AIDS, suggesting that increased used of low-cost treatments for this infection could reduce HIV transmission as well as schistosomiasis (Secor, 2012). *Trichomonas vaginalis* is another parasite associated with increased HIV infection and is the most common non-viral STI in the world

(Mirmonsef et al., 2012). While there is clinical evidence for increased HIV transmission in the presence of other STIs and genital infections, there is little experimental investigation into these interactions. These reports highlight the importance of STI screening, as the most common organisms are largely asymptomatic but can increase the risk of HIV transmission.

1.4 Bacteria can predispose the host to viral infections

The majority of research into coinfection focuses on viral infection preceding bacterial infection. Interactions such as the increased susceptibility to HIV infection when other STIs are present (Mirmonsef et al., 2012) have promoted research to study the effect(s) of bacterial carriage predisposing to viral infections. One interesting and expanding area is the impact of the microbiome on the outcome of viral infections. Two groups reported differences in poliovirus, reovirus and mouse mammary tumour virus (MMTV) infection of germ-free mice, or after pre-treating mice with antibiotics, suggesting a pro-viral role for the microbiome (**Fig.1.3**; (Kane et al., 2011; Kuss et al., 2011). Furthermore, norovirus infection is augmented by the presence of bacterial products (Karst, 2015). However, there are also viruses for which the microbiome exerts an inhibitory effect (Wilks et al., 2013). Several *in vitro* studies have reported that bacterial infection can potentiate virus infection and these studies will be discussed below (Sajjan et al., 2006; Chattoraj et al., 2011a; Verkaik et al., 2011).

1.4.1 Microbiome-viral interactions

The intestinal tract is the most heavily colonized organ in the body and its microbiome is one of the protective mechanisms present to prevent disease, by competing for space and nutrients with potentially pathogenic organisms (Sekirov et al., 2010). However, recent studies suggest that the microbiome can facilitate viral infection. Kuss et al., 2011, reported that antibiotic depletion of intestinal bacteria decreased mortality associated with oral poliovirus and reovirus infection. Further studies showed that Gram-negative bacterial surface expressed LPS binds poliovirus

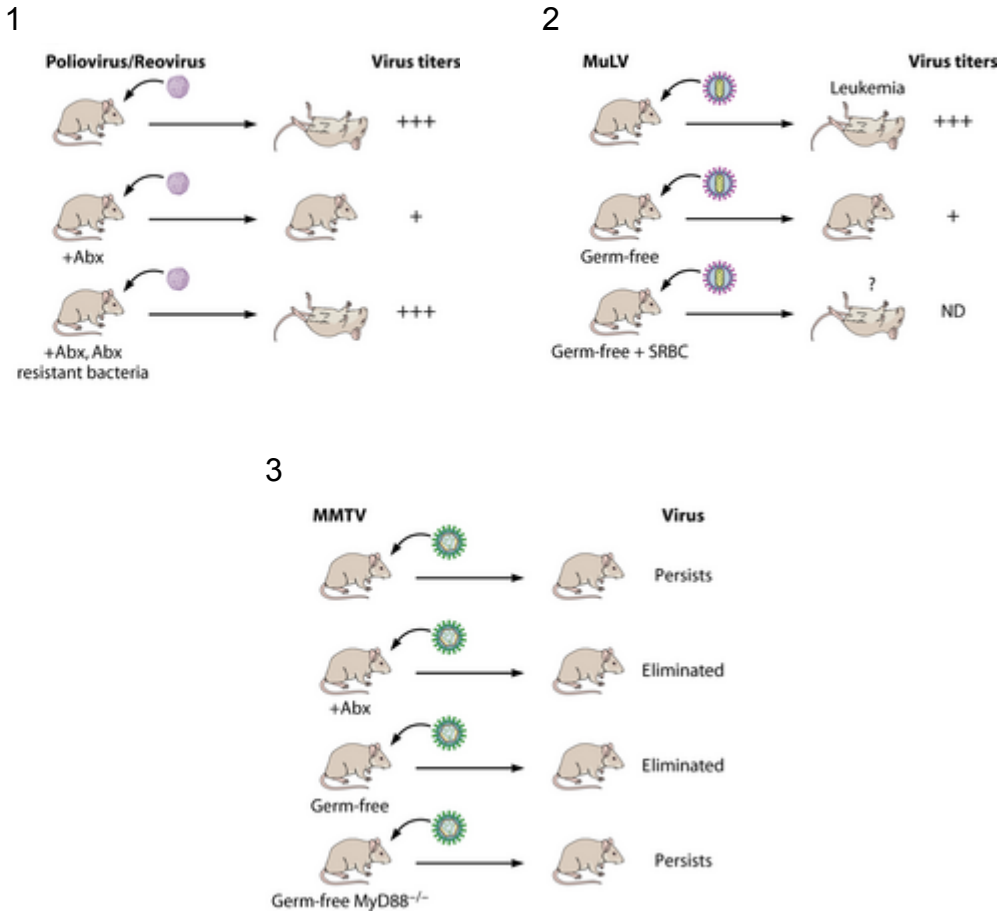

Figure 1.3 **The intestinal microbiome can augment virus infection in mouse models.**

Adapted from (Wilks et al., 2013) 1. Reduction in the intestinal microbiome using antibiotics (Abx) can decrease poliovirus and reovirus infections, improving mouse survival. Addition of Abx resistant bacteria rescues viral pathogenesis. 2. Infection of germ-free mice with murine leukemia virus (MuLV), which in conventionally reared mice causes leukemia and death, leads to increased viremia without leukemia generation. Addition of sheep red blood cells (SRBC) increases mortality for germ-free mice infected with MuLV to the level seen with conventionally reared mice, however without leukemia development. 3. Mouse mammary tumor virus (MMTV) causes a persistent infection in mice. In those treated with Abx or raised germ-free, the infection is eliminated. Germ-free mice without the MyD88 gene infected with MMTV are not able to clear the virus, suggesting a role for TLR signaling.

and this interaction promotes viral stability at higher temperatures, and attachment to host cells via the poliovirus receptor (Kuss et al., 2011; Robinson et al., 2014). Moreover, bacterially expressed peptidoglycan (PGN) was independently reported to increase the stability of poliovirus (Robinson et al., 2014), identifying a direct interaction between poliovirus and a wide range of bacterial species. Rotavirus infection can also be reduced when the microbiota is depleted and the effect is suggested be at the viral entry stage, rather than replication, but further investigation is needed to determine the mechanism (Uchiyama et al., 2014).

MMTV, which is frequently transmitted through milk from mothers to their offspring, can also utilize LPS on mucosal surfaces to its advantage (Wilks et al., 2013). Kane et al., 2011, reported that adult mice exposed to MMTV in milk as neonates failed to mount an anti-MMTV response later in life. However, when neonates were infected with MMTV intraperitoneally, they produced antibody upon subsequent challenge with viral antigens. This occurs through MMTV binding LPS in the stomach of neonates, which induces toll-like receptor (TLR)4 signaling and leads to increased expression of IL-10. The IL-10 produced reduces the anti-viral response to MMTV and potentiates tolerance (Kane et al., 2011). MMTV binds LPS via the incorporation of LPS-specific host cell receptors, TLR4, CD14 and MD-2, into virus particles (Wilks et al., 2015). This study highlights a role for MMTV incorporation of host immune receptors to allow the virus to evade the immune system. In contrast, influenza virus infection in mice is enhanced when the microbiome is depleted with antibiotics (Wilks et al., 2013), which introduces another factor to consider when treating secondary bacterial infections causing pneumonia as discussed earlier.

1.4.2 Noroviruses

Human noroviruses are non-enveloped, positive sense RNA viruses that cause gastroenteritis and are amongst the most prevalent causes of pediatric diarrhea (Koo et al., 2013). However, until recently it has been difficult to study human noroviruses due to a lack of *in vitro* cell culture models that allow virus replication. Murine noroviruses infect macrophages and DCs. However, efforts to infect these cell types with human noroviruses have been unsuccessful and the same is true of intestinal epithelial cells, which would be the logical first point of infection for a gastrointestinal pathogen (Karst, 2015).

(Jones et al., 2014) showed that human noroviruses infect B cells and this can be augmented by bacteria, or bacterial products. Initial experiments identified that murine noroviruses could infect B cells *in vitro* and *in vivo*. To assess this using a human norovirus; filtered and unfiltered stool samples positive for the virus were incubated with B cells and the unfiltered samples supported higher levels of viral replication. Subsequent experiments showed an interaction between the virus and histo-blood group antigens (HBGAs) that are expressed by the host, but also by certain bacterial species present in the gut. Although this mechanism still requires more research, it is hypothesized that the virus particles are coated with HBGAs allowing immune evasion (Karst, 2015).

1.4.3 Bacterial species in the lung predispose to viral infection

In vitro studies have investigated interactions between viruses and bacteria isolated from individuals with chronic obstructive pulmonary disease (COPD) and cystic

fibrosis (CF), as well as pediatric patients with acute respiratory tract infections. Human metapneumovirus (HMPV) antibodies are detected in children by the age of 5, but not all children develop respiratory tract infections from this virus, and the factors responsible for this are not yet understood (Panda et al., 2014). Verkaik et al., 2011, hypothesized that respiratory bacteria could exacerbate HMPV infection. They report an association between HMPV seroconversion and *S. pneumoniae* carriage in young children, which led them to test the interaction *in vitro*. Human bronchial epithelial cells pre-exposed to *S. pneumoniae* support increased levels of HMPV infection by up to 10-fold, whereas *S. aureus, Moraxella catarrhalis* and *H. influenzae* have no effect on virus infection (Verkaik et al., 2011). Further investigations are needed to determine the mechanism of increased HMPV infection following *S. pneumoniae* exposure.

COPD is a chronic condition that can be exacerbated by acute viral and bacterial infections that lead to increased mortality (Aaron, 2014). Coinfection has been identified in 25% of hospitalized patients and is frequently associated with more severe symptoms and outcomes (Papi et al., 2006). Sajjan et al., 2006, investigated the effect of coinfection with *H. influenzae* and rhinovirus, two microbes commonly isolated from COPD patients with clinical symptoms. Primary airway epithelial cells infected with *H. influenzae* prior to rhinovirus secrete higher levels of the pro-inflammatory chemokine IL-8, than when infected with either pathogen alone. Interestingly, heat-killed bacteria do not replicate this effect. Increased IL-8 expression occurs via an upregulation of TLR3 by *H. influenzae*, potentiating the host response to detect viral dsRNA. Furthermore, bacterial exposure upregulates the

viral receptor ICAM-1; allowing more virus particles to bind to host cells. This provides an explanation for the reported increase in the susceptibility of individuals with COPD to rhinovirus infection.

Lung epithelial cells from individuals with CF have impaired innate defenses and, like COPD, CF predisposes to acute episodes of inflammation and viral and bacterial exacerbations (Elborn, 2016). Rhinovirus is associated with up to 60% of CF exacerbations (Chattoraj et al., 2011b). Individuals with CF have increased susceptibility to Gram-negative bacteria and *P. aeruginosa* is the predominant infection (Elborn, 2016). Chattoraj et al., 2011a, infected airway cells with *P. aeruginosa* and allowed the bacteria to form a biofilm to replicate the bacterial burden *in vivo*, rhinovirus was then added and they reported an increased release of bacterial cells from the biofilm in the presence of virus. Further studies identified a role for rhinovirus to disrupt the biofilm via oxidative stress dependent mechanisms. The free bacterial cells then migrate across the epithelial barrier and disrupt tight junctions (TJ) when the virus is coinfected.

Chattoraj *et al*., 2011b, assessed the potential interactions of *P. aeruginosa* and rhinovirus in epithelial cells isolated from individuals diagnosed with CF. They report that IFN responses to rhinovirus are reduced by the presence of *P. aeruginosa* when CF epithelial cells are coinfected, while the reverse occurs in normal epithelial cells. The reduced IFN response increased virus replication in CF epithelial cells co-infected with *P. aeruginosa*. Together, these data identify a complex interaction between rhinovirus and *P. aeruginosa* that may contribute to the exacerbations seen

in individuals with CF, whose lungs often contain *P. aeruginosa* biofilms even after antibiotic therapy (Rybtke et al., 2015).

Collectively, these studies suggest that the role of bacteria in promoting viral infections may be varied and underreported. We were therefore interested to develop an *in vitro* model system to investigate this further and this required identification of a common niche that bacteria and viruses could interact in.

1.5 Epithelial barriers

Epithelial barriers are one of the first defenses against infection. They are often colonized by bacteria and are the first point of infection for many viruses. To prevent infection they form both a physical and biochemical barrier. Polarization of epithelial cells creates a network of cells that are held together by junctional proteins (**Fig.1.4a**; reviewed by (Bergelson, 2009). There are two types of junctional complex between epithelial cells: TJs and adherens junctions (AJ) that prevent the movement of molecules between the apical and basolateral surfaces of the cell (**Fig.1.4b**). They also limit invasion of pathogens, together with mucous layers and antimicrobial peptides (Gallo and Hooper, 2012).

Polarized epithelial surfaces include the respiratory, digestive and reproductive tracts. These sites are frequently exposed to foreign material, including microbial antigens and required to develop a tolerance these antigens whilst retaining the ability to recognize pathogens and mount an inflammatory response (Wissinger et al., 2009). When studying epithelial cells *in vitro*, it is important to remember that unless cells are grown under the correct circumstances to facilitate polarization, there will be less distinction between apically- and basally-localized molecules as found *in vivo* and this may alter the interaction of microbes with the host cell.

1.5.1 The gut epithelium

The intestinal tract is the largest epithelial surface in the body and forms a biochemical barrier at the apical surface of epithelial cells (enterocytes) with mucosal

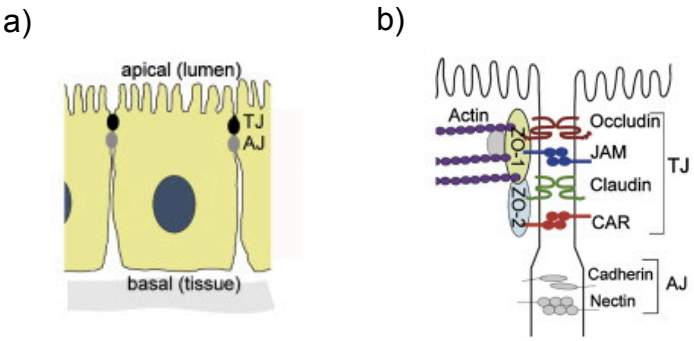

Figure 1.4 **The structure of polarized epithelial cells.**

Adapted from Bergelson, 2009. a) Tight junctions (TJ) and adherens junctions (AJ) are protein complexes that separate the apical and basolateral membranes when epithelial cells are polarized and facilitate the formation of a barrier. b) TJs are composed of four types of protein; claudin, occludin, members of the junction adhesion molecule family including JAM and CAR, and members of the zonula occludens (ZO) protein family, they also interact with the actin network. AJs are composed of cadherin and nectin.

layer(s) that can vary between different sites (**Fig.1.5**; reviewed by (Peterson and Artis, 2014). This allows commensal bacteria to grow and ideally prevents the disruption of homeostasis by pathogenic microbes. While immune cells are present, they are largely localized to the basal side of the epithelia. However, epithelial cells have pattern recognition receptors (PRR) to recognize MAMPs and contribute to inflammatory responses when necessary. They also transport secretory immunoglobulin A (sIgA) that can prevent bacterial-host cell receptor interactions and aid clearance. Secretory goblet cells produce mucins and Paneth cells also contribute to the anti-bacterial environment by secreting AMPs. AMPs, including defensins and cathelicidins, are broadly effective against a variety of bacterial strains and disrupt bacterial membranes. Immune sensing of the apical environment is performed by tissue resident macrophages that form dendrites to sample antigens, goblet cells and microfold (M) cells that can transport antigens to DCs on the basolateral surface.

The bacterial community in the gut is estimated to comprise 70% of the total human microbiome and is supported by the nutrient rich environment, where it is involved in both health and disease (reviewed by (Sekirov et al., 2010). Two phyla are dominant, the Bacteroidetes and the Firmicutes, but the total number of species can be over 1000. Studies using germ-free mice have determined that the gut microbiome is necessary for the development of the immune system, including two contrasting functions; tolerance to the microbiome to prevent continuous inflammation and detection of pathogenic microbes with the induction of inflammation to clear them.

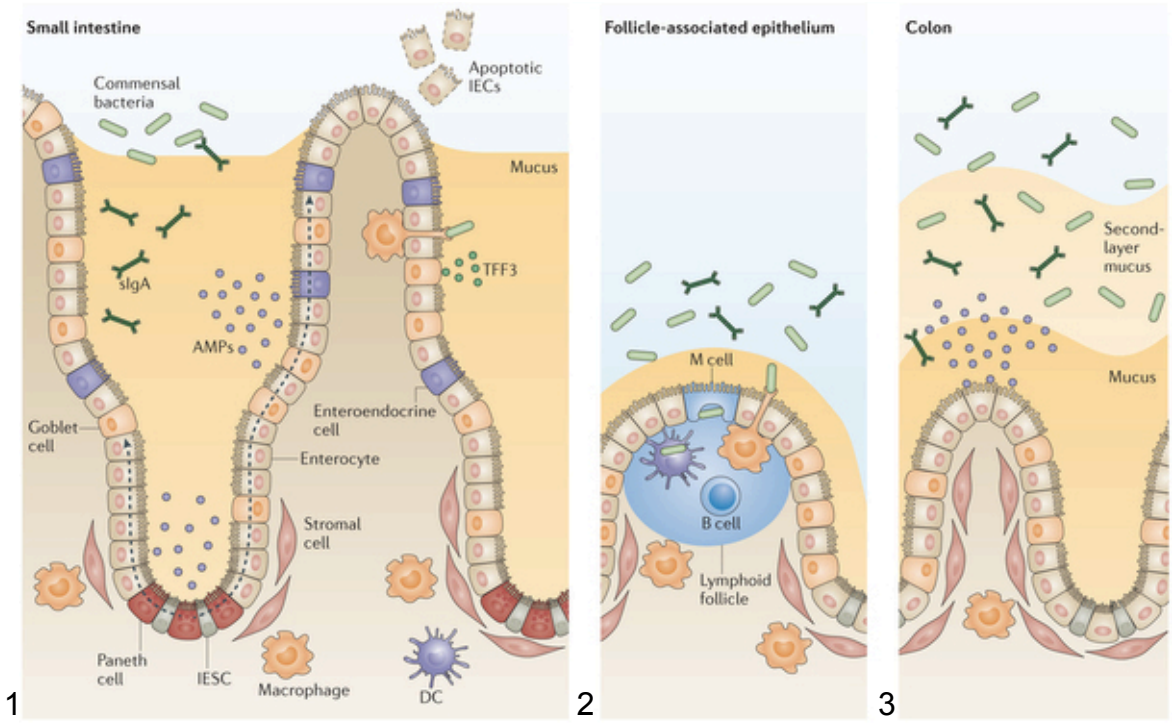

Figure 1.5 **Intestinal epithelial barriers.**

The composition of the epithelial barrier differs along the intestinal tract, from (Peterson and Artis, 2014) 1. In the small intestine there is a thick layer of mucus between villi that contains secretions such as antibody (sIgA), antimicrobial proteins (AMP) and trefoil factor 3 (TFF3), which contribute to the physical and chemical barrier required to regulate bacterial growth. While, apoptotic intestinal epithelial cells (IEC) are shed from the top of villi, intestinal epithelial stem cells (IESC) in the crypts renew many of the cell types present in the epithelium. Immune cells such as macrophages and dendritic cells are present to sample antigens present. 2. The follicle associated epithelial sites contain microfold (M) cells that can sample luminal antigens and present them to underlying immune cells. This requires a thinner mucosal layer. 3. The mucosal layer in the colon is much thicker and comprised of two different layers, as well as AMPs and sIgA. While commensal bacteria can penetrate the outer layer, the inner layer still forms a barrier.

The presence of commensal bacteria also helps to control overgrowth of pathogenic bacterial species by competitive exclusion, which includes competition for nutrients and space. However, if homeostasis is altered then commensal bacteria can cause opportunistic infections or inflammation due to the presence of MAMPs, such as LPS and PGN, as seen during HIV infection.

1.5.2 The lung epithelium

The respiratory tract forms a biochemical barrier that comprises the apical surface of epithelial cells using mucous and AMPs. However, it also uses cilia to move any incoming microbes away from the lungs (**Fig.1.6;** reviewed by (Whitsett and Alenghat, 2015). The respiratory tract is constantly exposed to the environment and requires mucociliary clearance to keep the alveoli, where gas exchange occurs, almost completely sterile. The airways comprise ciliated epithelial cells that can detect MAMPs and secretory cell types such as serous and goblet cells that produce mucous, AMPs and fluids to aid bacterial clearance. To further monitor the environment; DCs and macrophages sample antigens, induce inflammation and phagocytose pathogens. Interestingly, alveolar macrophages can inhibit inflammation to control damage and maintain tissue homeostasis. Of note these macrophages express lower levels of major histocompatibility complex (MHC)II, which allows antigen presentation, compared to non-resident cells, and constitutively express IL-10 (Wissinger et al., 2009). Both functions contribute to the tolerance necessary at epithelial surfaces.

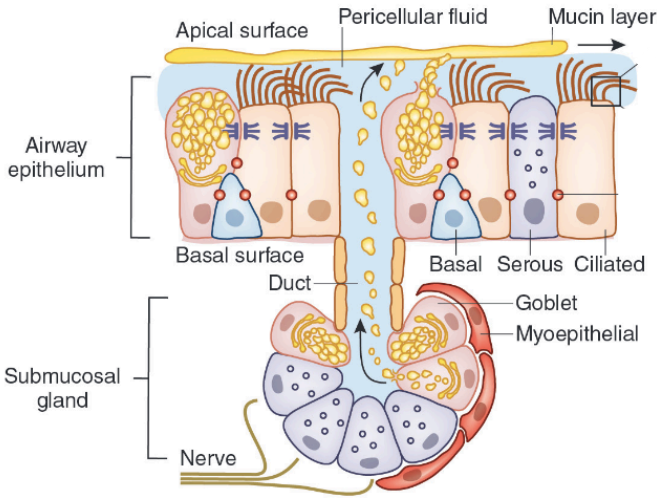

Figure 1.6 **The lung epithelial barrier.**

The composition of the lung epithelial barrier, adapted from (Whitsett and Alenghat, 2015) Both ciliated and mucous-producing goblet epithelial cells form the apical barrier, with serous cells contributing host defense proteins in pericellular fluid. Fluid production and cilial beating are coordinated by the submucosal gland to move mucous and inhaled materials along the epithelium and away from areas of gas exchange. Basal cells are progenitors for ciliated and goblet cells.

The lungs can contain commensal bacteria, at low levels compared to the gut, which can contribute to immune education. Disruption of mucociliary clearance alters the lung microbiome and contributes to exacerbation in conditions including as COPD and CF, where commensal bacteria can cause opportunistic infections (Whitsett and Alenghat, 2015).

1.6 Effects of bacteria on epithelia

Bacterial pathogens adhere to human cells to colonize or invade them. Many bacterial strains can adhere to epithelial monolayers and reduce their barrier function, to aid their cellular invasion or cross the barrier. To achieve this, bacteria commonly secrete effector proteins that interact with TJ proteins or the actin cytoskeleton (Kazmierczak et al., 2001). Examples of the mechanisms used to achieve this alteration in epithelial permeability are discussed below.

Clostridium perfringens expresses an enterotoxin that binds to occludin and claudin TJ proteins and induces their degradation, to disrupt the polarized monolayer (Sonoda et al., 1999; Singh et al., 2000b). This leads to diarrheal symptoms and potentiates bacterial spread to spread to new hosts. A similar mechanism occurs for *Vibrio cholerae*, which uses its toxin to bind and degrade occludin (Wu et al., 2000). *Helicobacter pylori* uses a type IV secretion system to inject an effector protein, CagA, into gastric epithelial cells, where it associates with the TJ protein ZO-1. CagA then recruits the TJ proteins to the site of bacterial attachment, disrupting TJ contacts with neighbouring cells (Amieva et al., 2003).

Enteropathogenic (EP) and enterohemorrhagic strains of *Escherichia coli* encode two proteins that perturb the host actin cytoskeleton and disrupt barrier function to allow bacteria to pass between epithelial cells. This is important for their pathogenicity, unlike other serotypes of *E. coli* that are not associated with pathologies. To disrupt actin structures, the translocated intimin receptor (Tir) is inserted into the host cell membrane where it binds the effector protein, intimin. Upon binding, Tir can

potentiate host tyrosine kinase signaling cascades to bring actin structures towards the bacterial cell and form a pedestal (Campellone, 2010). Interestingly, TJ disruption is well characterized for intestinal pathogens but not respiratory pathogens. However, *P. aeruginosa* is an opportunistic pathogen of the lung that is reported to take advantage of an already disrupted epithelium to initiate infection (Engel and Eran, 2011).

1.6.1 STm perturbs TJs

Salmonella enterica serovar Typhimurium (STm) is a facultative intracellular, Gram-negative bacterium and is associated with a self-limiting gastroenteritis in immune competent hosts (Zhang et al., 2003). However, it can cross the intestine and cause systemic disease. In sub-Saharan Africa, STm is the most common cause of bloodstream infections presenting with fever, with up to 25% mortality (Feasey et al., 2012). In HIV-infected individuals not on ART, this mortality rate can reach 47% (Gordon et al., 2002).

STm can infect epithelial cells, through TJ disruption (Fàbrega and Vila, 2013). It also infects M cells to reach innate immune cells across the epithelial barrier and DCs can form dendrites to capture STm on the apical surface of the epithelia (**Fig.1.7**; (Santos and Bäumler, 2004). These interactions can all lead to inflammation. Of the MAMPs secreted by STm, flagellin, a component of the bacterial flagella, is the major pro-inflammatory determinant that activates NF-κB signalling in host cells (Zeng et al., 2003).

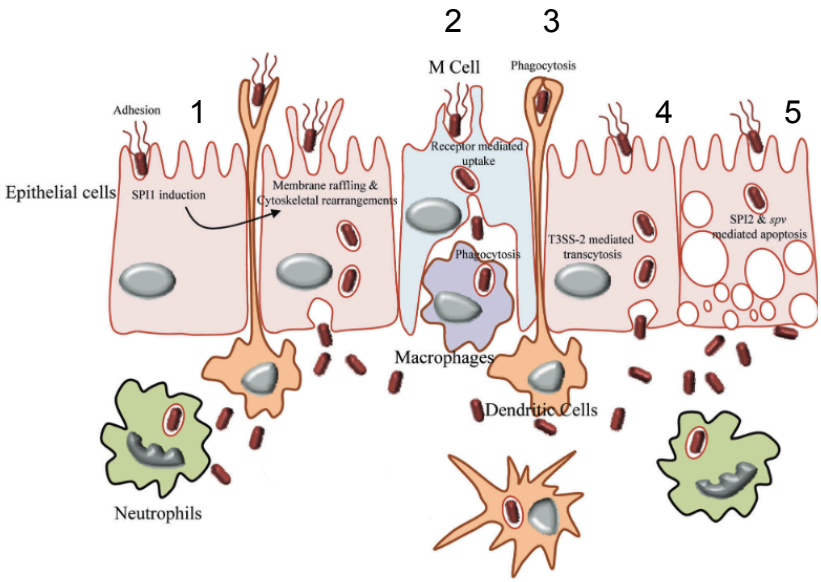

Figure 1.7 **STm crosses gut epithelial cells.**

Salmonella Typhimurium (STm) can invade its host through different pathways, adapted from (Garai et al., 2012) 1. The bacterium adheres to epithelial cells and induces membrane ruffling to facilitate uptake into a vacuole and subsequently release from the basal membrane (4) or apoptosis of the host cell (5), allowing dissemination and phagocytosis by immune cells. 2. Interactions with M cells lead to endocytosis and transport to immune cells on the basal side of the epithelium. 3. Dendrites from dendritic cells can reach between epithelial cells and phagocytose bacteria.

STm uses two type III secretion systems to invade and replicate within host cells that are encoded by *Salmonella* pathogenicity islands (SPI). These type III secretion systems are composed of needle-like protein structures that 'inject' effector proteins into the host cell. SPI-1 effector proteins can augment entry into non-phagocytic cells and SPI-2 effector proteins promote bacterial replication in the *Salmonella* containing vacuole (SCV;(Velge et al., 2012). The SPI-1 type III secretion system injects effector proteins SopB, SopE, SopE2 and SipA to decrease barrier function of polarized epithelia. These proteins alter the localization of TJ proteins ZO-1 and occludin by activation of Rho family GTPases, leading to actin remodelling, as well as decreasing the levels of ZO-1 and occludin in the cell (Boyle et al., 2006; Velge et al., 2012). Additionally, it has recently been reported that *Salmonella* can upregulate TJ protein claudin-2, referred to as the 'leaky' TJ protein. This was determined *in vitro* and in a mouse model of infection to augment bacterial invasion through increased cell permeability (Zhang et al., 2013).

Further interactions between the SPI-1 effector proteins modulate host cell actin to induce ruffling of the cell membrane and allow the bacterium to enter the cell (McGhie et al., 2009). Once entered, STm induces the SCV to survive in host cells and evade immune responses (reviewed by (Steele-Mortimer, 2008). It is a modified phagosome, with SPI-2 effectors preventing lysosomal fusion and destruction of the bacterium.

1.7 Viral entry pathways

Viruses must enter the host cell to replicate and produce new particles. Virus entry is initiated by attachment to specific host cell receptors via the viral glycoprotein(s). This allows internalization and the majority of viruses utilize the host cell endocytic machinery to enter the cell (reviewed by (Yamauchi and Helenius, 2013). This may be either clathrin-dependent or -independent, or via macropinocytosis. The virus particles can then escape into the cytoplasm to replicate (most RNA viruses) or gain transport to the nucleus where they can start replication (most DNA viruses). Escape from endocytic vesicles can occur in the early to late compartments, but also from the endoplasmic reticulum or the macropinosome. Furthermore, viruses can enter the host cell via direct fusion with the plasma membrane to deliver their genome. There is involvement of diverse host cell processes in viral entry mechanisms and some viruses can engage more than one pathway.

1.7.1 Vesicular stomatitis virus (VSV) entry

VSV, although not a common human pathogen, is the prototypic virus in the order *Mononegavirales*, which includes rabies, Ebola and mumps viruses (Bukreyev et al., 2006). VSV entry into host cells has been well characterized and it can enter varied cell types, making it an attractive virus for gene therapy (Lévy et al., 2015). Entry is mediated by the VSV glycoprotein (G), which associates with clathrin-coated pits on the plasma membrane and is rapidly trafficked to early endosomes, also co-opting actin, where low pH causes fusion either in early or late endosomes (**Fig.1.8**;

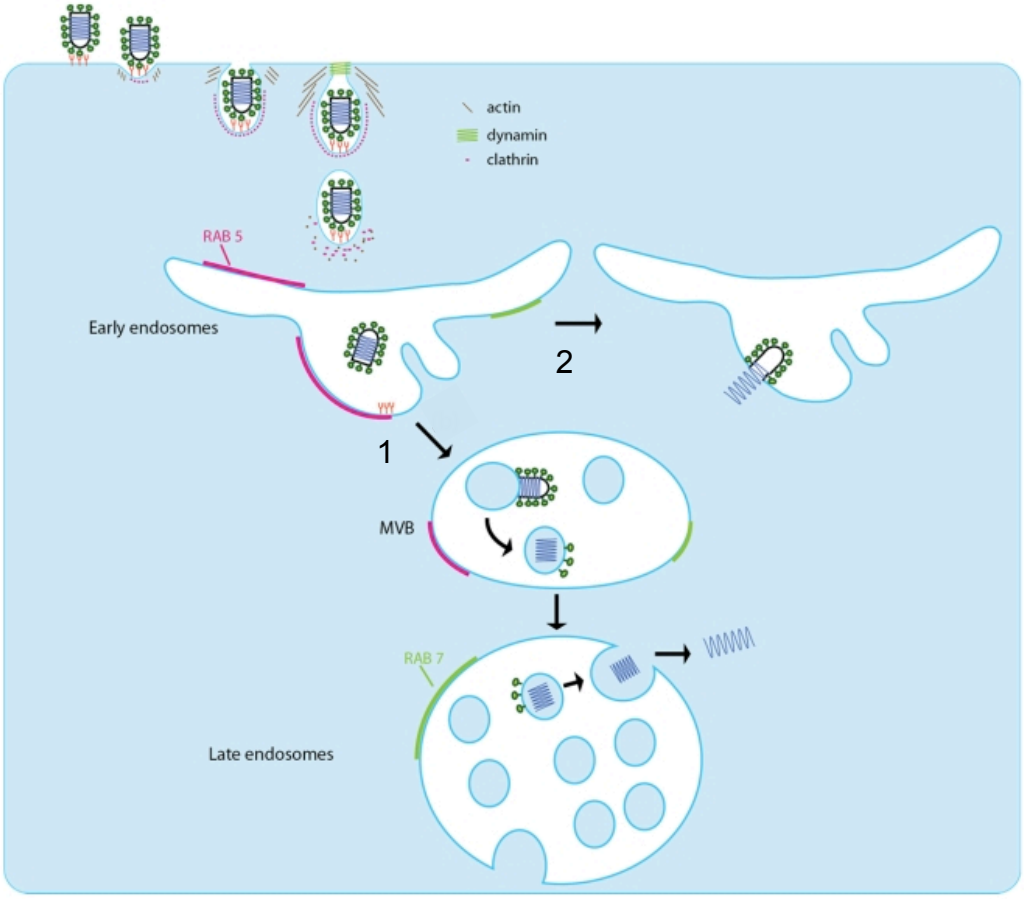

Figure 1.8 **VSV entry.**

From (Albertini et al., 2012) Vesicular stomatitis virus (VSV) particles attach to the host cell via LDL receptor family members and undergo clathrin-mediated endocytosis, which also requires dynamin and actin for efficient entry. Two pathways are proposed for escape from the endosome. 1. As the early endosome becomes a multivesicular body (MVB), particles can fuse with internal vesicles. This fusion releases the viral nucleocapsid. Once the MVB has matured to a late endosome, identified by increased presence of Rab 7 and decreased presence of Rab 5 found earlier in the pathway, vesicle fusion releases the nucleocapsid into the cytoplasm. 2. VSV particles fuse rapidly in early endosomes to release the nucleocapsid into the cytoplasm.

(Cureton et al., 2009; Hastie et al., 2013). It was recently reported that the entry receptor is the low-density lipoprotein (LDL) receptor and family members (Finkelshtein et al., 2013), which elucidates its broad cell tropism. Once VSV enters a host cell and produces new virions it can induce apoptosis, this has allowed it to be developed as an oncolytic virus for cancer therapy in cells without a robust IFN response (Hastie and Grdzelishvili, 2012).

1.7.2 Other virus entry routes of interest

Lassa virus fusion occurs in endosomes and is pH sensitive much like VSV (Cosset et al., 2009). However, entry is via multivesicular bodies as opposed to clathrin-mediated (Pasqual et al., 2011) and α-dystroglycan is the main receptor (Cao et al., 1998), although more entry factors have recently been identified (Shimojima et al., 2012). MeV requires two glycoproteins, hemagglutinin (H) for entry and fusion (F) for fusion of virus-host and host-host membranes. The wild-type virus uses the receptors signalling lymphocyte activation molecule (SLAM)F1 and nectin-4 to enter cells (Mühlebach et al., 2011; Noyce et al., 2011). However, the Edmonston vaccine strain has an altered tropism for CD46 as opposed to nectin-4 (Dörig et al., 1993; Naniche et al., 1993). Fusion of MeV with the host cell surface is poorly defined, but it is reported to occur at neutral pH (Nakatsu et al., 2006). The pro-inflammatory cytokine TNF can promote the entry of MeV, Lassa and VSV pseudoparticles into polarized liver epithelial cells (Fletcher et al., 2014).

The Ebola virus glycoprotein associates with C-type lectins on the host cell membrane, while host phosphatidylserine receptors can interact with

phosphatidylserine in the viral envelope, and the virion enters primarily through macropinocytosis (reviewed by (Moller-Tank and Maury, 2015). Interestingly, Ebola has another receptor in endosomes, Neimann-Pick disease, type C1 (NPC1), which assists virus fusion and release into the cytoplasm. Influenza HA binding to sialic acids has been reported to facilitate entry via various pathways including clathrin-dependent and -independent endocytosis and more recently, macropinocytosis. Irrespective of initial entry pathway, fusion occurs in late endosomes at low pH (Edinger et al., 2014). HIV binds to cells via the receptor CD4 using glycoprotein gp120. Plasma membrane fusion is triggered by HIV gp41 using one of its host cell co-receptors, CCR5 or CXCR4 (Klasse, 2012).

1.7.3 Modelling viral infection of epithelia

Many viruses must cross epithelial barriers to enter the body, and some have been discovered to use TJ proteins as entry receptors (Bergelson, 2009; Fletcher et al., 2012). This route translates into lower infection levels in polarized cells compared to non-polarized cells, due to inaccessibility of receptors. To maximize entry, viruses can alter the permeability of epithelial barriers directly, or by inducing inflammation.

Coxsackievirus B3 and Adenovirus 5 (Ad5) both show limited infection of polarized gut cells via the apical or basal surface, unless ethylenediaminetetraacetic acid (EDTA) is included to disrupt the barrier function. This is due to localization of the coxsackievirus and adenovirus receptor in TJs (Cohen et al., 2001). Coxsackie viruses can induce their own movement to TJs, through interaction with the host cell membrane protein decay-accelerating factor and downstream signaling pathways to

induce actin cytoskeleton rearrangements (Coyne and Bergelson, 2006). Ad5 also shows restricted entry into polarized lung cells, compared to non-polarized cells, with a further decrease when the virus is administered apically rather than basolaterally. Interestingly, Ad5 can successfully infect polarized cells in the presence of macrophages, via induction of IL-8, which relocates the viral co-receptor from TJs to the apical surface (Lütschg et al., 2011).

In a similar mechanism, cytokines secreted by macrophages can promote viral infection of polarized liver cells. Conditioned medium from macrophages stimulated by various agonists, including bacterial LPS, enhances HCV, measles (MeV), Lassa and VSV infection. TNF and IL-1β were determined to be the main effectors (Fletcher et al., 2014). This study used lentiviral pseudoparticles to determine the level of viral entry, without the presence of fully replicating virus. Lentiviral pseudoparticles are formed of an HIV core that packages a luciferase reporter gene, enveloped by host cell membrane containing the viral glycoprotein(s) of interest (Hsu et al., 2003). This allows investigation of viral entry without replication, distribution of new virions and secondary infections.

1.8 Aims

The aim of this study was to further our understanding of bacterial-viral coinfection. Initially, by developing a model system to determine the effect of bacteria on virus infection, as the majority of research currently focuses on viral infection preceding bacterial. Bacteria and viruses both enter the body through epithelial surfaces and we chose to model this *in vitro.* Virus entry is often restricted on polarized epithelia and considering that certain bacteria can affect TJ integrity, we hypothesized that bacterial species able to increase epithelial permeability would increase virus entry. This stage of the viral lifecycle is easily modeled with lentiviral pseudoparticles, which were utilized for this study. Using this model system, we aimed to test various viruses and bacteria, to determine whether certain combinations can act synergistically or there are common interactions that would enable us to define the mechanism(s) leading to increased virus entry. Following the development of this model system using pseudoparticles, we were interested in assessing the role of bacterial stimuli in full-length virus infection.

2. MATERIALS & METHODS

2.1 Cell culture

All cell lines used in this study are described in **Table 2.1**. Unless otherwise stated, cells were maintained at 37°C (20% O_2 and 5% CO_2) in growth medium supplemented with 10% foetal bovine serum (FBS; Thermo Fisher Scientific, USA), 1% non-essential amino acids (Thermo Fisher Scientific), 1% L-glutamine (Thermo Fisher Scientific) and 50 units/mL penicillin and streptomycin (P/S; Thermo Fisher Scientific). To facilitate polarization A549, Caco-2 and Calu-3 cells seeded at $9x10^4$ cells/cm^2 in sterile TC-treated plates or $1x10^5$ cells/transwell (12 mm diameter, 0.4 µm pore size inserts; Corning, USA) for 7-14 days were fed with fresh medium 3x per week, both apically and basolaterally. In case of non-polarized culture, the cells were seeded at $1x10^5$-$3x10^5$ cells/mL one day before use.

2.2 Dextran flux assay

To assess barrier integrity using the permeability coefficient, a protocol previously reported by (Glod et al., 2006), was modified. A549 and Caco-2 cells were grown on transwells for 1, 7 and 14 days as described above. Dulbecco's modified Eagle's medium (DMEM, phenol red-free; Thermo Fisher Scientific) containing 2% FBS and 2 mg/mL 70 kDa Fluorescein isothiocyanate (FITC)-dextran (Sigma-Aldrich) was added at time 0 to the apical side and the insert was moved to a well with fresh medium without FITC-dextran. Subsequent to incubation for 5 min at 37°C, the cells were moved again to a new well and this process was repeated for 30 min. The

basolateral medium was measured with excitation at 485 nm for emission at 520 nm using a microplate reader (Wallac Victor 1420) and compared to a standard curve of dextran movement through an empty transwell, using 2 μg/mL–80 ng/mL. The rate of dextran movement (mg/min) was determined for each cell type at each day post seeding. Rates were compared by calculating the permeability coefficient (cm/min) using the equation (1/((1/sample rate)/(1/standard curve rate)))/transwell surface area.

Name	Tissue of origin	Growth medium	Source
1G5	HIV reporter cell derived from the Jurkat T cell line (Human peripheral blood). Contain a luciferase reporter under transcriptional control of the HIV-1 LTR promoter and express CXCR4 (Aguilar-Cordova et al., 1994)	Roswell Park Memorial Institute (RPMI)-1640	Professor Ariberto Fassati, University College London, London, UK
293T	Human embryonic kidney	DMEM	American Type Culture Collection (ATCC)
A549	Human lung carcinoma	DMEM	ATCC
A549-SLAM	A549 cells stably transfected with human SLAMF1 by HIV-1 based transduction using a puromycin resistant bi-cistronic transcriptional cassette	DMEM supplemented with 1 µg/mL puromycin (Thermo Fisher Scientific)	Dr Dalan Bailey, University of Birmingham, Birmingham, UK
Caco-2	Human colon adenocarcinoma	DMEM	ATCC
Calu-3	Human lung adenocarcinoma	Eagle's minimum essential medium (EMEM; Thermo Fisher Scientific)	ATCC
Detroit 562	Human pharyngeal carcinoma	EMEM	Dr Andrea Mitchell, University of Birmingham, Birmingham, UK
Huh-7	Human hepatoma	DMEM	Dr Charles Rice, Rockerfeller University, New York, USA
PM1	Derivative of HuT 78 human cutaneous T cells	RPMI-1640	NIBSC Centre for AIDS Reagents, UK
SupT1	Human T cell lymphoblastic lymphoma	RPMI-1640	ATCC
TZM-bl	HIV reporter cell derived from HeLa human cervical epithelial cells. Contain a luciferase reporter under transcriptional control of the HIV-1 LTR promoter and express the HIV-1 co-receptors CXCR4 and CCR5 (Wei et al., 2002)	DMEM	Professor Bill Paxton, University of Liverpool, Liverpool, UK

Table 2.1 **Characteristics of the cell lines used in this study.**

The name used throughout this work, tissue of origin, growth medium and source for each cell line cultured.

2.3 Pseudoparticle (pp) generation and infection

Ebola pp, influenza pp, Lassa pp, MeVpp, VSV-Gpp and non-enveloped (NE)pp were produced as described previously (Hsu et al., 2003). 293T cells were plated on poly-L-lysine (Sigma-Aldrich) coated plates and transfected with equal quantities of pNL4.3e⁻r⁻luciferase and envelope construct plasmids (see **Table 2.2**) using fugene 6 (Promega, USA). To make green fluorescent protein (GFP)-tagged pseudoparticles (GFPpp), cells were transfected with plasmids containing the viral glycoprotein of interest, gag-pol and CSGW in optimem medium that was subsequently replaced with 3% FBS/DMEM without P/S 6h post-transfection. Pseudoparticles were collected at 48h and 60h post-transfection, the stocks were pooled, clarified by centrifugation at 2500 rpm for 10 min and passed through 0.22 μM filters before storing at -80°C. Cells were infected in triplicate and incubated for 48h. The supernatant was removed (in some cases used for cytotoxicity assay as described later), cells were lysed and an equal volume of luciferase substrate added (Promega, UK) to be read for 10 s/well in a Centro LB 960 microplate luminometer (Berthold Technologies, UK). Values are plotted as relative light units (RLU), dilution factors removed and where NEpp is not shown it has been subtracted from all samples.

Plasmid name used in text	Description	Reference
pNL4.3e r luciferase	HIV-1 replication-deficient core that packages the luciferase gene	Hsu et al., 2003
For GFPpp: Gag-pol CSGW	HIV-1 replication-deficient core HIV-1 vector that packages the GFP gene	(Hatziioannou et al., 2005)
Ebola	Glycoprotein from the Zaire Mayinga strain	(Long et al., 2015)
HIV-1	Glycoprotein from the LAI strain	Professor Bill Paxton, University of Liverpool, Liverpool, UK
For influenza: Hemagglutinin Neuraminidase	Glycoproteins from the H7N1 strain	(Ohuchi et al., 1994)
Lassa	Glycoprotein from the AV strain	Cosset et al., 2009
For MeV: Hemagglutinin Fusion	Glycoproteins from the Edmonston strain	(Schoenhals et al., 2012)
VSV	Glycoprotein from the Indiana strain	Hsu et al., 2003
Control	Empty vector for NEpp	Hsu et al., 2003

Table 2.2 **Plasmids used for pseudoparticle generation in this study.**

The name used throughout this study, description of genes encoded and reference for each plasmid used to generate lentiviral pseudoparticles.

2.4 Lactate dehydrogenase (LDH) cytotoxicity assay

To determine the effect of drug treatments or bacterial exposure on epithelial cell viability, the CytoTox 96 non-radioactive cytotoxicity assay (Promega) was used to detect LDH release according to manufacturer's instructions. Cell supernatants were collected, clarified and incubated with an equal volume of CytoTox 96 reagent for 30 min at room temperature (r.t.). An equal volume of stop solution was added and the absorbance was measured at 490 nm using a Multiskan Ascent platereader (Thermo Electron Corporation). To determine 100% cell lysis, a positive control was obtained by freeze-thaw lysing untreated cells and measuring released LDH.

2.5 Bacterial culture

Bacterial strains used in this study are described in **Table 2.3**. Bacteria were stored as glycerol stocks in 20% glycerol (v/v) at -80°C or on Luria-Bertani (LB; Thermo Fisher Scientific) agar plates at 4°C. When needed for infection, bacteria were grown overnight in LB broth or DMEM (supplemented with 25 mM HEPES; Thermo Fisher Scientific) containing appropriate antibiotics at 37°C with aeration (200 rpm), inoculated into fresh broth or medium at a ratio of 1:50 and allowed to grow to mid-logarithmic phase (OD_{600} of 0.5). Bacteria grown in LB were washed 3x with phosphate buffered saline (PBS; Thermo Fisher Scientific) and resuspended in 10% FBS/DMEM for addition to epithelial cells. To enumerate the colony forming units (CFU) of the bacterial stock added to epithelial cells, which was then used to determine multiplicity of infection (MOI), the samples were diluted in PBS $x10^{-1}$ to $x10^{-6}$ and 5 µL of each dilution added in triplicate to LB plates. After overnight

Species and strain	Reference and/or source
Bacillus subtilis (NCTC 3610)	Professor Laura Piddock, University of Birmingham, Birmingham, UK
EP *E. coli* (O127:H6 E2348/69)	Professor Laura Piddock
Klebsiella pneumoniae (NCTC 9633)	Professor Laura Piddock
P. aeruginosa (PA14)	Professor Ian Henderson, University of Birmingham, Birmingham, UK
Aflagellate *P. aeruginosa* (PA14 *fliC::Tn* Gm15)	Professor Ian Henderson (Liberati et al., 2006)
STm (SL1344)	(Hoiseth and Stocker, 1981)
Aflagellate STm (SL1344 *fliC::cat fljB::aph*)	Dr Robert Kingsley, Institute of Food Research. Norwich, UK
Attenuated STm (SL3261)	(Hoiseth and Stocker, 1981)
STm ΔSPI-1 (SL1344 SPI-1::*aph*)	Professor Laura Piddock
STm ΔSPI-2 (SL1344 *ssaV::aph*)	(Guy et al., 2000)
S. aureus (NCTC 8532)	Professor Laura Piddock

Table 2.3 **Bacterial strains used in this study.**

The strain details and reference and/or source for each bacterial species assessed.

incubation at 37°C, the colonies were counted for one dilution and multiplied by dilution factors to determine CFU/mL. Bacteria were heat killed at 100°C for 20 min and the absence of viable bacterial cells was verified by overnight culture on LB plates.

Aflagellate STm was constructed by allelic exchange using the method previously described (Datsenko and Wanner, 2000) using primers taacgcagtaaagagaggacgttttgcggaacctggttcgcctgcgccagaacggaCATATGAATATCCTCCT and ggcacaagtcattaatacaaacagcctgtcgctgttgacccagaataacctgaacaaTGTGTAGGCTGGAGCTGCTTC specific for fliC and ttaacgtaacagagacagcacgttctgcgggacctggttagcctgcgccagaacgCATATGAATATCCTCCTTAG and ggcacaagtaatcaacactaacagtctgtcgctgctgacccagaataacctgaacaaTGTGTAGGCTGGAGCTGCTTC for amplification of cat (chloramphenicol resistance) and aph (kanamycin resistance) genes, respectively. Specific replacement of each gene was tested by PCR amplification of the chromosomal region using specific primers flanking the mutation sites. The resultant strain with double gene replacement of fliC and fljB was confirmed as non-motile.

To determine the adhesion and invasion of bacteria into epithelial cells, bacteria were added to cells in 24-well plate and incubated for 1h. Adhered bacteria were quantified by washing epithelial cells 3x with phosphate buffered saline (PBS) and lysing with 1% triton X-100 (Sigma-Aldrich) for 10 min. Lysate was serially diluted and plated to count CFU. Internalized bacteria were quantified by washing the cells and incubating them in 100 µg/mL gentamicin (Thermo Fisher Scientific) for 30 min to kill external bacteria. The cells were lysed and plated to determine CFU as described above.

2.6 Bacterial-viral infection studies

Cells were treated with bacteria, conditioned medium (CM), STm TLR grade LPS (Enzo Life Sciences, UK) or flagellin (STm FliC purified as previously described by Flores-Langarica *et al*., 2015; *P. aeruginosa* PA-Fla, InvivoGen, USA) for 1h using medium without P/S throughout the assay when bacteria were present. Pseudoparticles were added with 34 µg/mL chloramphenicol or 40 µg/mL tobramycin (Sigma-Aldrich) and the cells incubated for 48h prior to lysis and measurement of luciferase activity. When using gentamicin, 30 min post-STm addition the bacteria were removed and antibiotic was added at 50 µg/mL with VSV-Gpp. Cells were incubated for 30 min with the virus and high concentration of antibiotic, washed 1x with medium, and then incubated for 48h with medium containing a low concentration of gentamicin (5 µg/mL). To determine virus entry, cells were lysed and an equal volume of luciferase substrate added (Promega, UK) to be read for 10 s/well in a Centro LB 960 microplate luminometer (Berthold Technologies, UK). Relative pseudoparticle entry was calculated by subtracting the NEpp signal and expressing the treated signal relative to the untreated control.

To determine the rate of virus entry, cells were treated with STm for 1h, VSV-Gpp was added for 1h and the cells were washed three times with medium to remove external virus at time points specified, then incubated with fresh medium for 24h. Cells were lysed to quantify luciferase.

To test GFPpp, cells were treated with bacteria for 1h. Pseudoparticles were added with chloramphenicol and the cells were incubated for 48h. For flow cytometry, cells

were PBS washed, trypsinized and fixed with 4% paraformaldehyde (PFA; TAAB, UK). Fluorescence at 488 nm was measured using a CyAn ADP Analyzer (Beckman Coulter, USA). Using FlowJo 7.6.1 software, the live cell population was selected and the GFP+ population analyzed to determine virus infected cells.

2.7 Confocal microscopy

TJ protein localization: Cells were grown on coverslips overnight and incubated with STm (MOI 10) at 37°C for 1h before fixing with 4% PFA. Cells were permeabilized with 0.1% Triton X-100 and incubated with 2 ug/mL rabbit α-ZO-1 or mouse α-occludin (Thermo Fisher Scientific) followed by goat α-rabbit Alexa fluor 594 or goat α-mouse Alexa fluor 488 (Thermo Fisher Scientific). Nuclei were counterstained with 4′,6-diamidino-2-phenylindole (DAPI; Thermo Fisher Scientific) and coverslips were mounted with ProLong Gold (Thermo Fisher Scientific). Cells were imaged using a Zeiss 510 META confocal microscope with 63x objective and LSM software.

STm and GFPpp coinfection: Cells were grown on coverslips overnight and incubated with STm (MOI 10) at 37°C for 1h before addition of VSV-Gpp containing a GFP reporter and chloramphenicol. After 48h incubation, cells were fixed with PFA and permeabilized. To visualize STm, cells were incubated with mouse α-LPS (1E6; Thermo Fisher Scientific) followed by goat α-mouse Alexa fluor 633 and DAPI. Coverslips were mounted with ProLong Gold and cells were imaged using a Zeiss 510 META confocal microscope with 40x objective and LSM software.

Transferrin or dextran uptake: Cells were grown on coverslips overnight and incubated with 1 µg/mL human transferrin-Alexa Fluor 488 conjugate (Thermo Fisher Scientific) or 250 µg/mL 10 kDa dextran Oregon green 488 (Thermo Fisher Scientific) in serum free medium for 1h. Cells were fixed with PFA, permeabilized and incubated with mouse α-CD81 (2s131, in house) followed by goat α-mouse Alexa fluor 594 (Thermo Fisher Scientific) and DAPI. Coverslips were mounted with ProLong Gold and cells were imaged using a Zeiss 510 META confocal microscope with 100x objective and LSM software.

2.8 IL-8 enzyme linked immunosorbent assay (ELISA)

Supernatants were collected from infected cells and stored at -20°C. IL-8 was measured by ELISA using the manufacturer's instructions (Thermo Fisher Scientific) and absorbance measured at 450 nm using an Multiskan Ascent platereader.

2.9 Luciferase reporter gene transfection

Two protocols were used to test promoter activity of the luciferase plasmid following addition of bacteria. (1) A549 cells seeded in a 6-well plate and transfected with 1.6 µg pNL4.3env^{-}rev^{-}luciferase using fugene 6 were incubated for 24 hr. The cells were trypsinized, re-seeded in a 96-well plate and incubated for a further 24h. Bacteria were prepared as detailed in 2.5 and added in triplicate before incubation at 37°C for 1h when chloramphenicol was added in 10% FBS/DMEM at final concentration of 34 µg/mL and the cells were incubated for a final 24h. The cells were lysed and measured for luciferase signal as detailed earlier. (2) A549 cells were seeded in a 24-well plate, bacteria were added for 1h, 10% FBS/DMEM was removed and

optimem medium with 34 μg/mL chloramphenicol was added for fugene 6 transfection of pNL4.3env^{-}rev^{-}luciferase. Transfection mix was incubated for 6h and removed to culture the cells in 10% FBS/DMEM containing chloramphenicol for the remaining 18h. Cells were lysed to determine luciferase activity.

2.10 Generation of CM

Bacteria were cultured in DMEM overnight, medium was spin clarified and filtered through 0.22 μm. Absence of bacterial cells was verified by overnight culture on LB plates. Proteinase K (PrK) treatment of CM involved incubation of CM with PrK (50 μg/mL; Sigma-Aldrich) for 30 min and heat inactivation of PrK at 100°C for 5 min prior to addition to epithelial cells. CM was prepared for sodium dodecyl sulfate polyacrylamide gel electrophoresis (SDS-PAGE) by concentrating with trichloroacetic acid (TCA) from 30 mL to 100 μL and 10 μL and running in a 12% gel with a prestained protein ladder (Geneflow, UK). Proteins present in the gel were detected by Coomassie staining (Sigma-Aldrich). Size fractionation was achieved using Vivaspin centrifugal concentrators (Sartorius, Germany). CM was added to the top of molecular weight cut-off columns of various pore sizes, spun at 4000 g for 20 min and samples collected from the top and bottom were added to cells for 1h prior to VSV-Gpp. To deplete flagellin from CM, STm was grown in RPMI, spin clarified and filtered through 0.22 μm for affinity chromatography using α-FliC monoclonal antibody by Dr Margaret Goodall at the Monoclonal Production Unit, University of Birmingham.

To prepare CM for mass spectrometry, 50 mL STm CM produced using phenol red free DMEM was centrifuged in a 100 kDa Vivaspin, the top fraction was dialysed in a 10 kDa Slide-A-Lyzer cassette (Thermo Fisher Scientific) in ddH_2O and tested on A549 cells with VSV-Gpp to ensure activity. Samples were sent to the Advanced Mass Spectrometry Facility, University of Birmingham, to assess protein fragments present using an Orbitrap mass spectrometer. The Sequest algorithm was used to determine STm specific proteins.

2.11 Addition of antibody to flagellin and VSV-Gpp

Mouse sera from four PBS-immunized and four STm FliC-immunized mice, and flagellin ELISA data, were provided by Dr Adriana Flores-Langarica, University of Birmingham. The sera were pooled and heat inactivated at 56°C for 20 min. Flagellin was incubated with serially diluted sera for 30 min and added to cells for 1h prior to VSV-Gpp addition.

2.12 Addition of MLN4924 to flagellin and VSV-Gpp

To determine the effect on NF-κB activation, A549 cells were transfected using fugene 6 with plasmid pConA-luciferase (Andrew MacDonald, University of Leeds), which contains a luciferase reporter under the control of NF-κB binding sites. At 24h post-transfection cells were treated with STm, CM or flagellin for 1h and chloramphenicol added. Cells were incubated for 24h prior to lysis and measurement of luciferase activity. To find the optimal concentration of MLN4924 (R&D Systems, USA), A549 cells were transfected with pConA-luc and 24h post-transfection were pre-treated with MLN4924 for 15 min prior to inoculation with STm. To determine the

effect of MLN4924 on pseudoparticle infection studies cells were pretreated with MLN4924 prior to addition of STm, CM or flagellin and pseudoparticle or HIV-1 infection.

2.13 Silencing with siRNA

A549 cells were transfected according to manufacturer's instructions (Dharmafect 1; Thermo Fisher Scientific) with ON-TARGETplus smart pool siRNA to human TLR5, RelA or non-targeting control (Dharmacon, USA) 24h prior to treatment with flagellin and pseudoparticle infection. Subsequently, the cells were incubated for 48h and lysed for luciferase assay, RNA preparation for PCR or western blotting.

PCR: RNA was prepared using the Qiagen RNeasy kit and amplified for TLR5 using human TLR5 primer pair Hs01019558_m1 (Thermo Fisher Scientific) in a quantitative reverse-transcription PCR (qRT-PCR) in accordance with the manufacturer's guidelines (CellsDirect kit; Thermo Fisher Scientific) and fluorescence was monitored in a 7500 real-time PCR machine (Thermo Fisher Scientific). Glyceraldehyde 3-phosphate dehydrogenase (GAPDH) was included as an endogenous control for amplification efficiency, and TLR5 amplification normalized to GAPDH using the ΔΔCt method. Western blotting: Proteins were separated using an 8% SDS-PAGE gel, transferred to PVDF membrane (Merck Millipore, USA) and probed using primary rabbit α-RelA (Cell Signaling Technology, USA) or mouse α-beta-actin (Sigma-Aldrich) and secondary donkey α-rabbit-HRP antibody or sheep α-mouse-HRP (GE Healthcare, USA). Membranes were incubated in EZ-ECL prior to image capture using a PXi multi-application gel imaging system (Syngene, UK).

2.14 Product enhanced reverse transcriptase (PERT) assay

Lentiviral particle associated reverse transcriptase (RTase) activity was detected using the PERT assay as previously described (Pizzato et al., 2009; Vermeire et al., 2012). Supernatant or whole cell samples lysed by equal volume of 2x lysis buffer (0.25% triton X-100, 50 mM KCl, 100 mM TrisHCl pH 7.4, 40% glycerol) was added to the reaction mix (QuantiTect SYBR green buffer; Qiagen, Germany) containing double distilled (ddH_2O) RNase free water, forward and reverse MS2 primers (Thermo Fisher Scientific), MS2 RNA (Roche, Switzerland) and RNase inhibitor (Thermo Fisher Scientific) in a 96-well PCR plate. A standard curve was prepared using HIV-1 RTase (Abnova, Taiwan). Using a Mx3000P qPCR system (Agilent Technologies, USA), the thermal cycler conditions used were 10 min at 45°C, 15 min at 95°C and 50 cycles of amplification, consisting of 10 s at 95°C and 30s at 60°C. The PCR cycle ended with a melting curve cycle of 1 min at 95°C, 30 s at 55°C and 30 s at 95°C. The standard curve was used to determine units (U) of RTase activity.

2.15 HIV-1 generation and infection

293T cells plated on poly-L-lysine coated plates and transfected with the pNL4.3 full-length HIV-1 plasmid using fugene 6 and optimem. As mentioned in section 2.3, the cells were transfected for 6h at 37°C and the media replaced with 3% FBS/DMEM without P/S. Subsequently, virus collected at 48h and 60h post-transfection, the stocks were pooled, clarified by centrifugation at 2500 rpm for 10 min and stored at -80°C. Cells infected in triplicate and incubated for 24h (TZM-bl cells) or 48h (1G5 and SupT1 cells) were lysed to assess luciferase activity. In parallel, the supernatant

collected from each well was clarified and stored at -80°C for PERT assay or titration on TZM-bl cells to quantify HIV-1 produced.

2.16 Flagellin-pseudoparticle binding assay

Flagellin was incubated with pseuodparticles for 1h at 37°C and Ni-NTA agarose beads (Qiagen) were added. This was mixed for 1h at r.t. on a rotary mixer and loaded into a propylene column (Sigma-Aldrich). The flow through was collected and the beads were PBS-washed 5x and samples collected. Flagellin was eluted using 100 mM imidazole and samples were collected from all 5 elutions. The flow through, washes and elutions were assessed for pseudoparticles by PERT assay.

2.17 Inhibitor panel assay

Cytochalasin D (10 μM), jasplakinolide (1 μM), bafilomycin A1 (5 μM), chloroquine (50 μg/mL), blebbistatin (50 μM), 5-(N-ethyl-N-isopropyl) amiloride (EIPA; 50 μM) were kindly donated by Dr Dalan Bailey with data confirming the optimum concentration to use on A549 cells without cytotoxicity from Daniel Gonçalves-Carneiro. Each inhibitor was added to cells at the concentration indicated for 30 min prior to flagellin and maintained throughout flagellin incubation for 1h and the subsequent addition of VSV-Gpp. After 1h virus infection, the cells were washed and fresh medium was added for the remaining 48h. Cells were lysed to determine luciferase activity and supernatant was stored at -20°C for quantification of IL-8 by ELISA.

2.18 Transferrin and dextran uptake assays

To assess clathrin-mediated endocytosis a protocol previously reported by (Junutula et al., 2004) was modified. Two plates of A549 cells were treated with flagellin, while after 1h one plate was moved from 37°C to 4°C, the second plate was maintained at 37°C. Cells in both plates were treated with 1 µg/mL human transferrin-Alexa Fluor 488 conjugate in serum free medium. Cells were PBS washed, trypsinized and PFA fixed at indicated time points for flow cytometry using a CyAn ADP Analyzer. Background fluorescence from cells at 4°C, which would not allow internalization of transferrin, was removed from 37°C samples.

Macropinocytosis was monitored by modifying a protocol previously reported by (Krzyzaniak et al., 2013). Briefly, A549 cells were treated with flagellin or phorbol 12-myristate 13-acetate (PMA; kindly donated by Dr Dalan Bailey with data confirming the optimum concentration to use on A549 cells for macropinocytic uptake from Daniel Gonçalves-Carneiro) for 1h and 250 µg/mL of 10 kDa dextran Oregon green 488 in serum free medium was added. At indicated time points, cells were washed with bleach buffer (10 mM sodium acetate, 50 mM NaCl, pH 5.5) to remove non-internalized dextran and PBS, trypsinized and PFA fixed for flow cytometry using a CyAn ADP Analyzer.

2.19 Isolation of primary CD4+ T cells

CD4+ T cells were isolated using the EasySep human CD4+ T cell enrichment kit (Stemcell Technologies, Canada). Donated human blood was layered over lympholyte-H (Cedarlane, Canada) and centrifuged for 20 min at 800 g, r.t.

Peripheral blood mononuclear cells were removed from the blood-lympholyte interface using a Pasteur pipette, resuspended in RPMI and centrifuged at 800 g for 5 min to wash 3x using fresh RPMI. After the final wash, cells were resuspended in 2% FBS/PBS containing 1 mM EDTA, enrichment cocktail was added and the cells were incubated for 10 min at r.t. Magnetic particles were added, incubated for 5 min at r.t. and the cells were placed into a magnet (Stemcell techinologies). After 5 min, the remaining cells in suspension were removed, centrifuged at 2000 rpm for 3 min and resuspended in 10% FBS/RPMI containing P/S and IL-2 for culture at 37°C until use.

2.20 Statistical Analysis

Statistical analyses were performed using Student t test for bar charts or linear regression for XY graphs in Prism 6.0 (GraphPad, USA) with $P < 0.05$ being considered statistically significant.

We use the term biological replicates to mean measurements of the same protocol run at different times with biologically distinct samples. These account for biological variation. We use the term technical replicates to mean repeated measurements of the same sample. These account for the variation associated with protocols or equipment.

3. DEVELOPMENT OF A MODEL TO STUDY BACTERIAL-VIRAL COINFECTION

3.1 Introduction

Virus entry into polarized epithelial cells can be restricted by the localization of host cell receptors, which can include TJ proteins (Bergelson, 2009; Fletcher et al., 2012). Pro-inflammatory mediators can increase epithelial permeability; this leads to a reorganization of these receptors that can increase virus internalization (Lütschg et al., 2011; Fletcher et al., 2014). Bacteria can also alter epithelial cell permeability to facilitate their own invasion, such as STm effectors SopB, SopE, SopE2 and SipA disrupting TJs (Boyle et al., 2006). Epithelial barriers are frequently colonized by bacteria and provide the first site in the host that viruses encounter. We hypothesized that bacterially induced changes in epithelial permeability promote virus entry.

In this chapter, we present the development of a model system to investigate the effect of bacteria on virus infection. We selected to study virus entry as the first, and often rate-limiting, step in the life cycle and to use lentiviral pseudoparticles to quantify receptor-dependent virus internalization (**Fig.3.1**). This system produces particles comprising an HIV core, enveloped by cell membrane carrying heterologous envelope glycoproteins of the virus of interest that define receptor specific entry into the target cell via receptor-mediated interactions. Once the viral glycoprotein has enabled particle entry and fusion with host cell membranes, the HIV capsid uncoats

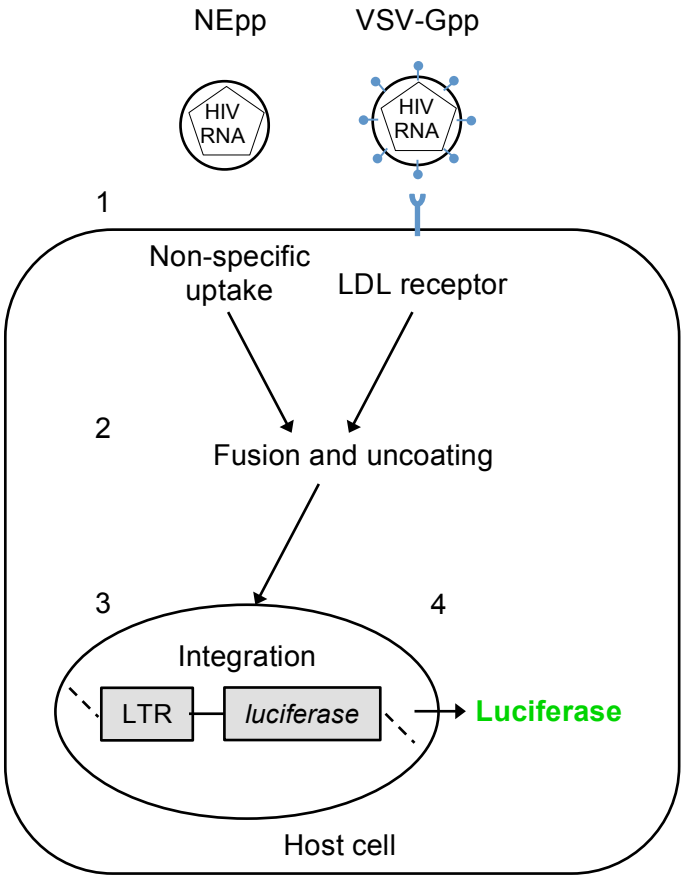

Figure 3.1 **Pseudoparticles as a reporter system for virus entry.**

Pseudoparticles are produced by 293T producer cells transfected with a plasmid encoding the HIV genome; minus the *env* and *rev* genes, with a firefly luciferase reporter gene added; and a plasmid encoding the glycoprotein(s) of the virus of interest such as VSV-G. Assembly of the HIV core, containing HIV RNA with the luciferase gene, at the host cell membrane incorporates the glycoprotein(s) during release. Pseudoparticles are harvested from the supernatant of the producer cells. Pseudoparticle entry into target cells: 1. Pseudoparticles carrying the VSV glycoprotein enter the host cell through low-density lipoprotein (LDL) family receptors (Finkelshtein et al., 2013). Non-enveloped pseudoparticles (NEpp) are a control virus particle from producer cells that are not transfected with a viral envelope glycoprotein. NEpp can be taken up through non-specific routes and all quantification of background particle uptake in each cell line tested. 2. Once particles have entered the cell, the host and viral membranes fuse to release the HIV capsid core, which transports to the nucleus to allow the genome to integrate (3). 4. Expression of the reporter gene, luciferase, is driven by the HIV long-terminal repeat (LTR) promoter and luciferase is produced. To quantify virus entry, target cells are lysed and luciferase substrate is added, allowing measurement of relative light units (RLU) emitted.

and releases viral RNA that is transcribed and encodes a luciferase reporter gene to allow quantification of virus entry by luciferase activity.

We decided to initially focus on VSV-Gpp and STm. VSV has a well-understood entry pathway and broad cell tropism, meaning is frequently used for developing gene therapies (Lévy et al., 2015). STm is a model Gram-negative organism that infects epithelial cells, for which there are many tools for genetic manipulation (Garai et al., 2012). Importantly, STm is able to induce changes in epithelial cell permeability, as discussed above, within 4h (Boyle et al., 2006). However, it can kill cells in culture, reportedly after 12h (Fink and Cookson, 2007). Considering that pseudoparticles require 24h-72h to allow sufficient luciferase production, we chose to model short-term exposure to STm for 1h and to include an antibiotic when adding VSV-Gpp, to prevent bacterial overgrowth and host cell death. In this chapter we present data on establishing and optimizing a model system to study the effects of STm-mediated changes in epithelial permeability on virus entry.

3.2 Modeling epithelial barriers

We chose to study the effect of bacteria on virus entry into epithelial monolayers from the lung and gut, two sites of the body that are frequently colonized by bacteria and represent points of entry for many viruses. There are numerous epithelial cell lines that polarize *in vitro* and model these sites. We selected A549 human lung carcinoma cells and Calu-3 human lung adenocarcinoma cells. While Calu-3 cells are reported to polarize well, there are conflicting reports on the ability of TJs between A549 cells to develop transepithelial electrical resistance, one measure of the formation of barrier integrity required to allow polarization (Törmäkangas et al., 2010). Another technique to assess epithelial barrier integrity is to monitor the flux of a fluorescent molecule from apical to basolateral media using cells grown on transwells. Using this measurement, we demonstrate that both A549 and Calu-3 cells form a barrier within 7 days of seeding on transwells and maintain this for 14 days (**Fig.3.2a-b**).

We also selected to study Caco-2 cells, a well-characterized model of the gut epithelium (Natoli et al., 2012; Dean et al., 2013). Caco-2 cells were previously reported to polarize within 6 days of reaching confluence (Mee et al., 2008). However, our experiments showed that 14 days were required to reach optimal barrier integrity (**Fig.3.2c**). Furthermore, electron microscopy studies have shown that by 14 days an apical brush border forms, mimicking the structure of enterocytes *in vivo* (Hughson and Hopkins, 1990), making these cells a more physiological model than other intestinal cell lines.

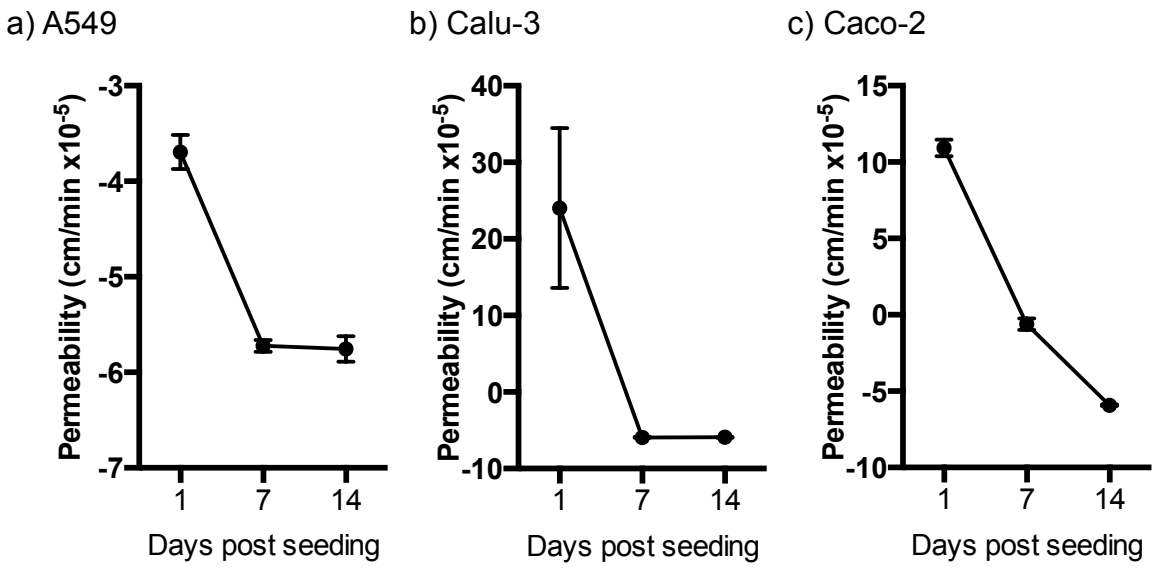

Figure 3.2 **Integrity of epithelial cell barriers over time.**

a-c) Barrier integrity developed per cell type was quantified by monitoring fluorescent dextran movement from the apical to basolateral medium of epithelial cells cultured on transwell inserts for the number of days indicated. The rate of dextran movement through each monolayer was calculated by collecting samples of basolateral medium at 5 min intervals for 30 min, following apical addition of 70 kDa FITC-dextran, and measuring fluorescence in each sample compared to a standard curve. The rate is represented as a permeability coefficient: the amount of dextran that will flow per min per cm of cells. Representative of 2 biological replicates, error bars show standard deviation (SD) of 2 technical replicates.

3.3 STm increases VSV-Gpp entry

First, we assessed whether polarization limits VSV-Gpp infection of A549 and Caco-2 cells. A549 cells supported significantly less virus entry when polarized and Caco-2 cells showed a trend towards less entry (**Fig.3.3a-b**). These data represent the RLU values generated by VSV-Gpp infection of A549 and Caco-2 cells, with NEpp background values removed. Typical NEpp values were between 300 and 500 RLUs. Subsequent data assessing the effect of treatment on pseudoparticle entry will be presented as relative to the untreated control cells.

Bacteria such as STm are often grown in LB broth. Before assessing the effect of bacteria on A549 or Caco-2 cells permissivity to support viral uptake, we assessed the effect of LB on VSV-Gpp infectivity (**Fig.3.4a**). We observed that LB reduced VSV-Gpp entry and in the following experiments bacteria were washed with PBS to remove LB broth and resuspended in cell culture media, prior to adding to epithelial cell cultures.

Co-culturing bacteria and epithelial cells for 24h resulted in bacterial over-growth and cell death (data not shown). We therefore tested two bacteriostatic antibiotics that would halt growth of the bacteria without killing them (Rahal and Simberkoff, 1979; Chopra and Roberts, 2001). Preliminary tests showed that chloramphenicol affected A549 cell permissivity to VSV-Gpp to a lesser extent than tetracycline (**Fig.3.4a**) and we selected chloramphenicol for further experiments.

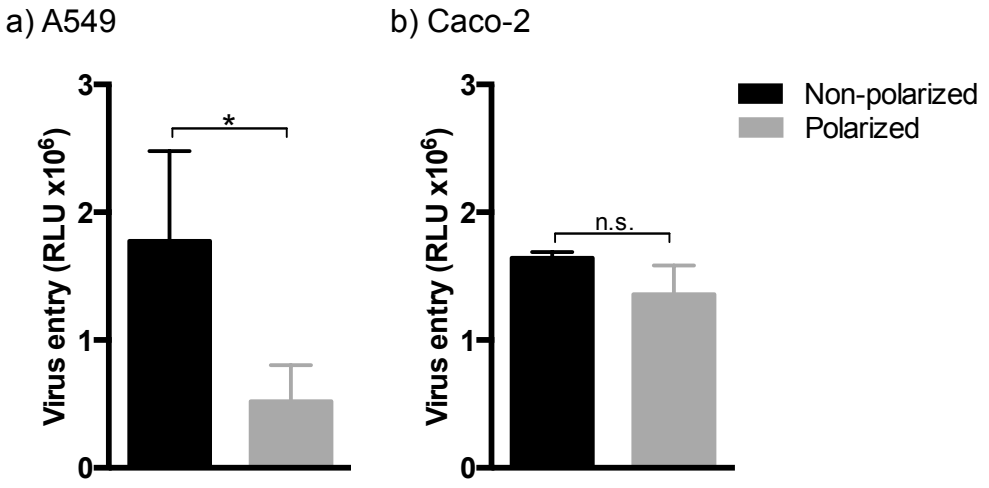

Figure 3.3 **VSV-Gpp entry is restricted into epithelial cells.**

a-b) VSV-Gpp entry into polarized cells compared to non-polarized was assessed by infecting cells with equal volumes of the same stock of VSV-Gpp and quantifying by luciferase assay at 48h. Data presented are net RLU minus RLU obtained for NEpp infection in each condition. Representative of 2 biological replicates, error bars show SD of 3 technical replicates, statistical comparison by Unpaired t test: n.s. = $P > 0.05$, * = $P \leq 0.05$.

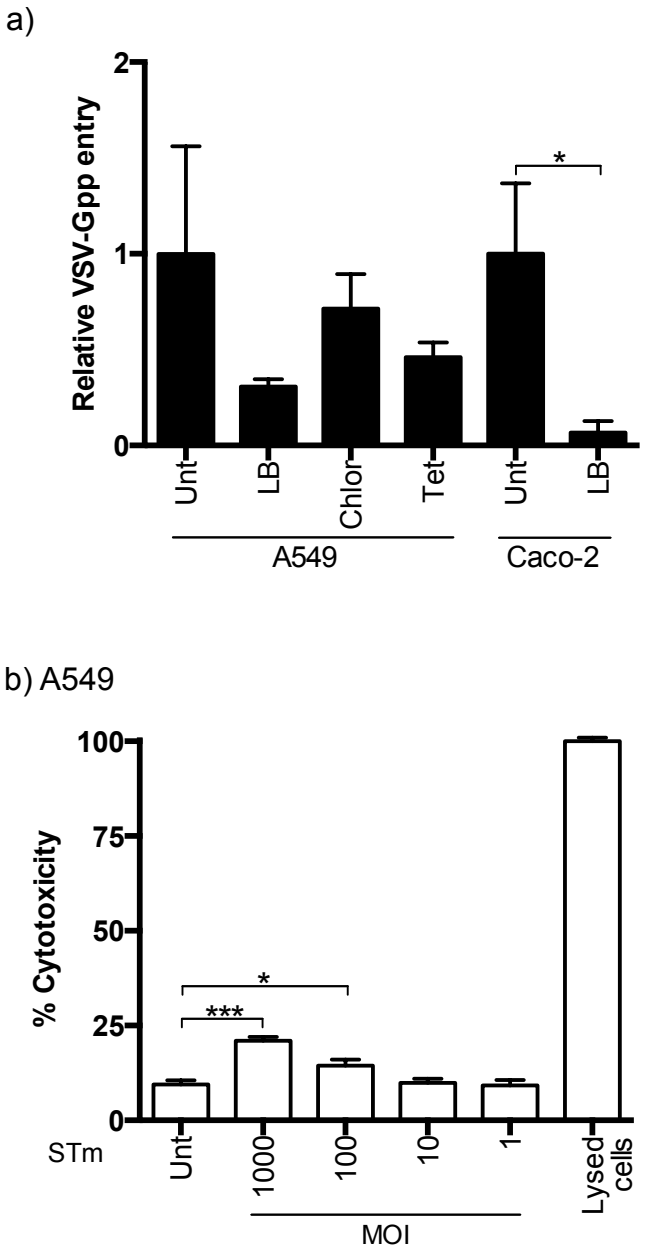

Figure 3.4 **Optimization of conditions for bacterial addition to epithelial cells.**

a) Polarized cells were treated with 1:2 vol/vol LB broth, 34 µg/mL chloramphenicol or 20 µg/mL tetracycline for 1h prior to VSV-Gpp addition and entry was quantified by luciferase assay at 48h. Data are presented as relative to VSV-Gpp entry into untreated cells. b) Polarized A549 cells were incubated with stated MOI of STm (strain SL1344) for 1h prior to addition of 34 µg/mL chloramphenicol. Supernatant was collected at 24h to determine cytotoxicity by LDH assay. Positive control supernatant was generated by 2x freeze-thaw lysis of untreated cells and used to calculate 100% cytotoxicity. Data are presented as relative to positive control. Representative of 2 biological replicates, error bars show SD of 3 technical replicates, statistical comparison by Unpaired t test: * = $P \leq 0.05$, *** = $P \leq 0.001$.

To further assess the effect of bacteria on epithelial cell viability we used the LDH cytotoxicity assay, following 1h incubation of A549 cells with STm. We tested MOIs from one to 1000 bacteria per epithelial cell and found that 10 was the highest possible MOI that could be used without affecting cell viability (**Fig.3.4b**). Levels of bacterial invasion of epithelial cells will be discussed later in this chapter.

These preliminary experiments allow us to assess the effect of short-term exposure to live STm on virus entry (**Fig.3.5a**). We included TNF, which has been previously reported to promote virus entry, as a positive control (Fletcher et al., 2014). Using this model system, we found that that STm significantly increased VSV-Gpp entry in all three epithelial cell lines tested (**Fig.3.5b-d**). We present data using pathogenic STm strain SL1344, but comparable data were observed with the attenuated STm strain, SL3261 (data not shown). These data support our hypothesis that bacteria can increase virus entry and may reveal a new mechanism for synergistic polymicrobial interactions *in vivo*.

3.4 STm promotes VSV-Gpp entry independent of epithelial cell polarization

We sought to determine whether the pro-viral effect of STm on polarized epithelial cells was mediated via bacterial alteration of cellular permeability. To assess this we used two different methods: flux of a fluorescent molecule from apical to basolateral media using epithelial cells polarized on a transwell, and TJ protein localization by immunofluorescence. Polarized A549 or Caco-2 cells were incubated with STm for

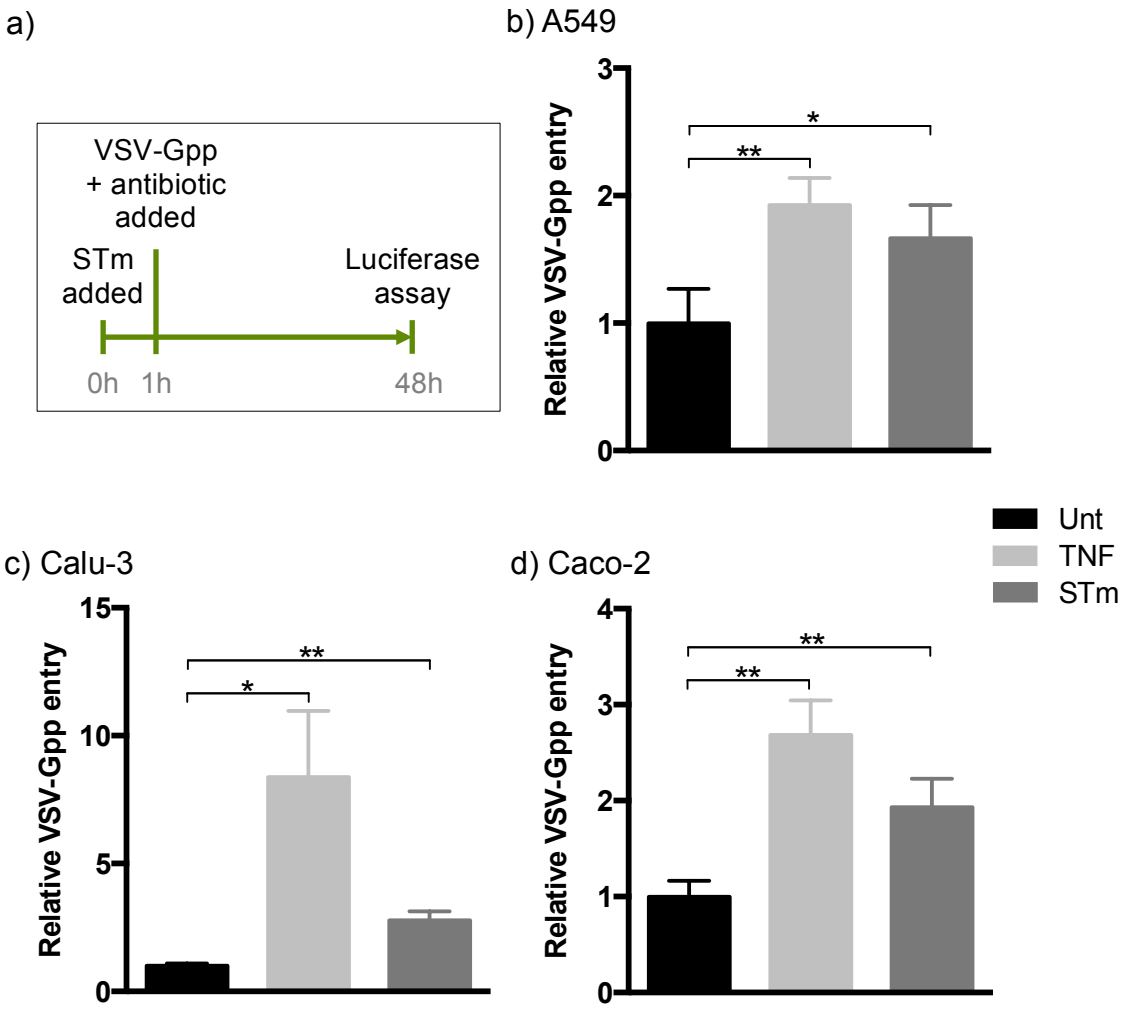

Figure 3.5 **STm increases VSV-Gpp entry into epithelial cells.**

a) Schematic diagram of experimental setup showing timing of STm addition, VSV-Gpp addition and epithelial cell lysis to determine pseudoparticle entry by measuring luciferase activity. b-d) Polarized cells were treated with STm (MOI 10) or TNF (100 ng/mL) for 1h prior to addition of VSV-Gpp and chloramphenicol (34 µg/mL) and virus entry was quantified by luciferase assay at 48h. Data are presented as relative to VSV-Gpp entry into untreated cells. Representative of 3 biological replicates, error bars show SD of 3 technical replicates, statistical comparison by Unpaired t test: * = $P \leq 0.05$, ** = $P \leq 0.01$.

1h and 70 kDa FITC-dextran administered apically. We observed a minimal effect of STm on paracellular permeability (**Fig.3.6a**).

We then stained for localization of TJ proteins ZO-1 and occludin, using cells fixed after 1h incubation with or without STm, and saw no changes in junctional patterns (**Fig.3.6b**). Caco-2 TJs showed a characteristic web-like pattern (Boyle et al., 2006) whereas TJs were less defined between A549 cells, as previously reported (Törmäkangas et al., 2010), suggesting no change in TJ integrity. Together these results indicate that that STm does not increase viral entry by altering epithelial cell permeability and we therefore designed experiments to explore the mechanism underlying STm pro-viral activity.

3.5 STm increases entry of pseudoparticles with diverse viral glycoproteins

Firstly, we determined whether the pro-viral activity of STm would be present in non-polarized cells, since epithelial cell permeability was not affected by the presence of bacteria. Secondly, we investigated the impact of culturing STm in LB broth or cell culture media (DMEM) prior to adding bacteria to epithelial cells. It has been reported that STm grown in different media have varying phenotypes, due to altered transcription patterns (Blair et al., 2013). There was no difference between the bacteria grown in different media, but remarkably there was a much greater increase in virus entry into non-polarized A549 cells, around five-fold (**Fig.3.7a**), compared to two-fold for polarized A549 cells (**Fig.3.5b**). Using non-polarized Caco-2 cells there was a comparable boost in VSV-Gpp entry using DMEM grown STm, but no significant increase in entry using LB grown STm (**Fig.3.7b**).

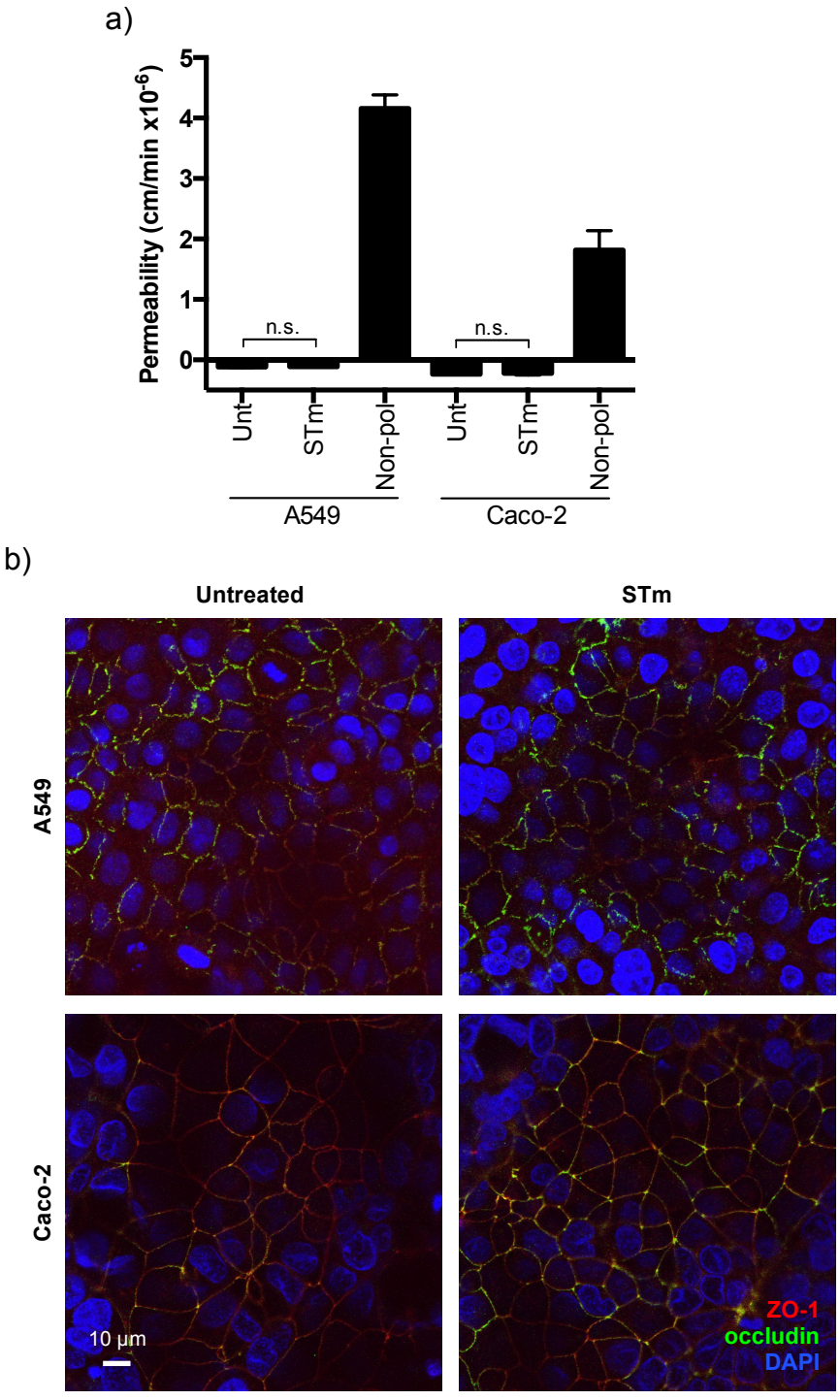

Figure 3.6 **The pro-viral effect of STm is not occurring through altered barrier integrity.**

Figure 3.6 **cont.**

a) Cells were cultured on transwells. Polarized cells were incubated with STm (MOI 10) for 1h and movement of 70 kDa FITC-dextran from the apical to basolateral medium was monitored to determine the rate over 30 min. Data are presented as the permeability coefficient. Representative of 2 biological replicates, error bars show SD of 2 technical replicates. b) Cells were polarized on coverslips, incubated with STm (MOI 10) for 1h and fixed to visualize TJ proteins ZO-1 and occludin by immunofluorescence; nuclei were stained with DAPI. Cells were imaged using a Zeiss 510 Meta confocal microscope with 63x objective and LSM software. Scale bar indicates 10 μm. Images are representative of 2 biological replicate experiments.

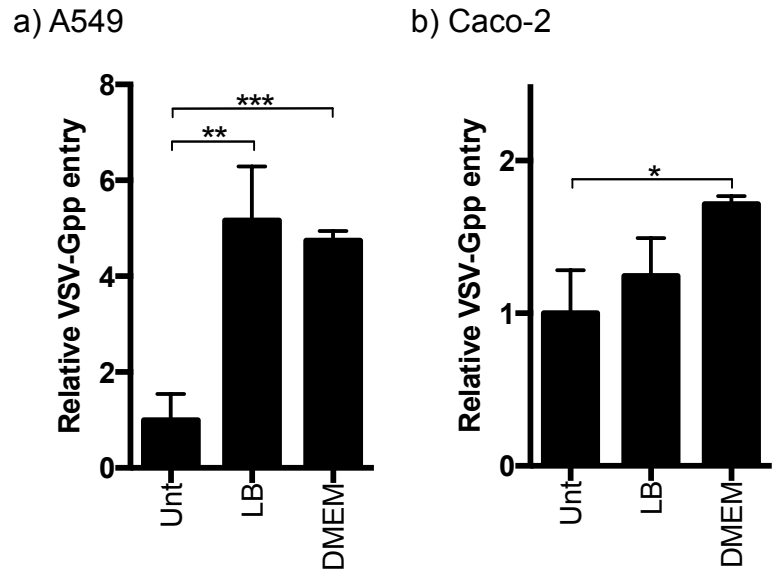

Figure 3.7 **STm increases VSV-Gpp entry into non-polarized cells.**

a-b) Non-polarized cells were treated with STm grown in bacterial culture broth and resuspended in DMEM (LB), or STm grown in cell culture medium (DMEM), both at MOI 10, for 1h prior to VSV-Gpp and chloramphenicol addition. Entry was quantified by luciferase assay at 48h. Data are presented as relative to VSV-Gpp entry into untreated cells. Representative of 2 biological replicates, error bars show SD of 3 technical replicates, statistical comparison by Unpaired t test: * = $P \leq 0.05$, ** = $P \leq 0.01$, *** = $P \leq 0.001$.

There was a greater pro-viral effect using STm on non-polarized A549 cells compared to polarized cells, but no difference for Caco-2 cells. We investigated whether there was a difference in the response to STm in non-polarized cells compared to polarized cells by measuring IL-8 secretion, as a marker of an innate immune response (Eckmann et al., 1993). We found that in all conditions the epithelial cells secreted IL-8 following STm stimulation, although there was not a significant increase for polarized A549 cells (**Fig.3.8**).

Additionally, we looked at the effect changing the antibiotic; comparing chloramphenicol to gentamicin. This antibiotic kills extracellular bacteria but cannot enter the epithelial cell to affect intracellular bacteria, allowing them to continue replicating within the cell (Elsinghorst, 1994). There was no difference in the pro-viral activity of STm depending on the type of antibiotic, and consequently the viability of bacteria within epithelial cells (**Fig.3.9a-b**).

We next determined the MOI necessary for STm to promote VSV entry. As demonstrated in **Fig.3.3b** a high MOI of 100 had a detrimental effect on the cells, this led to a decreased effect of STm on VSV-Gpp (**Fig.3.10**). The initial MOI, 10, showed the greatest effect on VSV-Gpp entry with a dose-response effect indicating that one bacterium per 100 epithelial cells would be sufficient to increase virus entry.

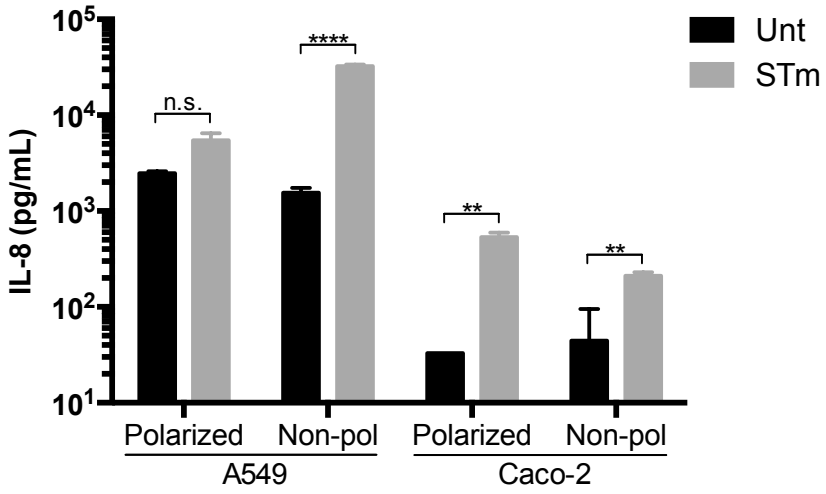

Figure 3.8 **Increased IL-8 secretion from epithelial cells exposed to STm.**

Cells were incubated with STm (MOI 10) for 1h prior to the addition of chloramphenicol. Supernatant was collected at 24h to measure IL-8 secretion by ELISA. Representative of 2 biological replicates, error bars show SD of 3 technical replicates, statistical comparison by Unpaired t test: ** = $P \leq 0.01$, **** = $P \leq 0.0001$.

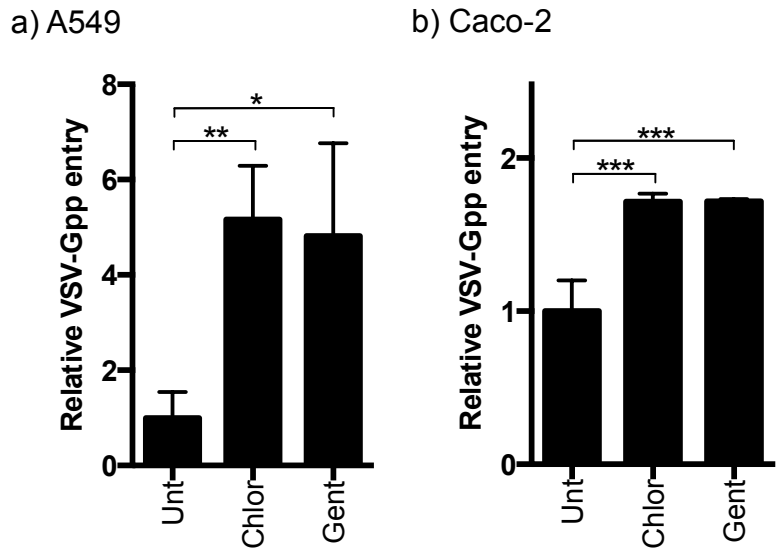

Figure 3.9 **Antibiotics with different modes of action allow STm to have comparable pro-viral effect.**

a-b) Non-polarized cells were incubated with STm (MOI 10) for 1h, prior to addition of VSV-Gpp and chloramphenicol and incubation for 48h, or to addition of VSV-Gpp and gentamicin (50 µg/mL) for 30 min, 1x wash with DMEM, addition of DMEM with gentamicin (5 µg/mL) and incubation for 48h. Entry was quantified by luciferase assay and data are represented as relative to VSV-Gpp entry into untreated cells. Representative of 2 biological replicates, error bars show SD of 3 technical replicates, statistical comparison by Unpaired t test: * = $P \leq 0.05$, ** = $P \leq 0.01$, *** = $P \leq 0.001$.

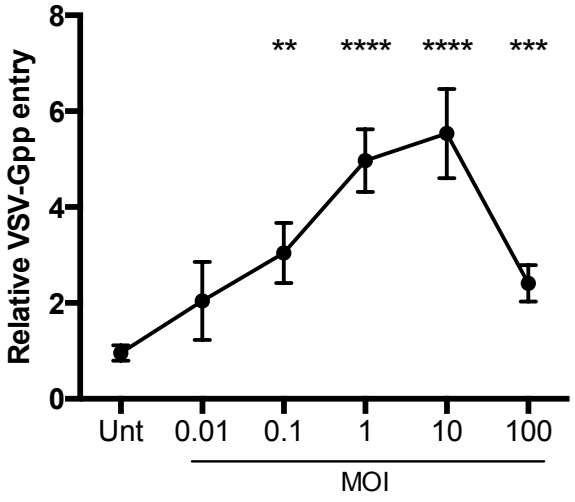

Figure 3.10 **STm pre-exposure has a dose response relationship on VSV-Gpp entry into epithelial cells.**

Non-polarized A549 cells were incubated with stated MOI of STm for 1h prior to addition of VSV-Gpp and 34 μg/mL chloramphenicol. Entry was quantified by luciferase assay at 48h. Data are presented as relative to VSV-Gpp entry into untreated cells. Representative of 2 biological replicates, error bars show SD of 3 technical replicates, statistical comparison to untreated by Unpaired t test: ** = P ≤ 0.01, **** = P ≤ 0.0001.

We then assessed whether STm would have comparable pro-viral activity using other cell lines. Detroit 562 cells are respiratory tract epithelial cells like A549 and Calu-3 cells. However, they were isolated from the pharynx, therefore higher up in the respiratory tract than the lung. There was an increase in virus entry after STm infection of these cells of around two-fold (**Fig.3.11a**), as seen with the other epithelial cell lines. Hepatocytes in the liver represent another polarized epithelial cell within the body; we tested the hepatoma cell line Huh7 with STm and VSV-G but did not see a significant increase in virus entry (**Fig.3.11b**).

Next, we assessed the entry of viral pseudoparticles bearing glycoproteins from Ebola, influenza, Lassa or MeV. These viruses enter cells using different host cell receptors, through a variety of pathways (**Table 3.1**). Remarkably, after STm treatment, A549 cells supported a four- to six-fold increase in entry for all pseudoparticles tested (**Fig.3.12a**) and Caco-2 cells a two-fold increase (**Fig.3.12b**). This suggests that the pro-viral activity of STm is broad and not specific to VSV-G. MeV does not readily infect A549 cells (Noyce et al., 2011). To assess the effect of STm on MeVpp entry into lung cells, we used A549 cells stably transfected to express the viral receptor SLAMF1. Overexpressing this protein did not affect the pro-viral activity of STm seen previously with VSV-Gpp and allowed MeVpp entry. STm pre-treatment increased MeVpp entry into A549-SLAMF1 cells three-fold (**Fig.3.12c**); comparable levels to the other pseudoparticles tested in A549 cells. Considering this data showing STm boosting virus entry through multiple pathways, and previous results ruling out the effect of STm requiring alteration of cell

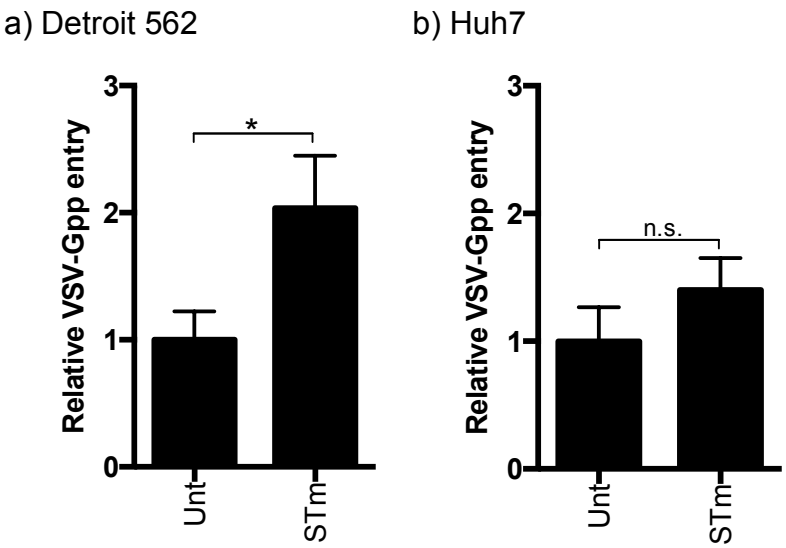

Figure 3.11 **STm has a variable effect on VSV-Gpp entry into other epithelial cell lines.**

a-b) Non-polarized lung (Detroit 562) and liver (Huh7) epithelial cells were incubated with STm (MOI 10) for 1h prior to addition of VSV-Gpp and chloramphenicol. Entry was quantified by luciferase assay at 48h. Data are presented as relative to VSV-Gpp entry into untreated cells. Representative of 3 biological replicates, error bars show SD of 3 technical replicates, statistical comparison by Unpaired t test: ns = $P > 0.05$, * = $P \leq 0.05$.

Virus	Receptor(s)	Entry pathway
VSV	LDL receptor and family[1]	Clathrin-mediated endocytosis[2]
Ebola	C-type lectins, PtdSer receptors, NPC1[3]	Macropinocytosis[3]
Influenza	Sialic acids[4]	Clathrin dependent and independent endocytosis[2]
Lassa	α-dystroglycan[5]	Multivesicular bodies[2]
MeV	SLAMF1/Nectin-4/CD46[6]	Plasma membrane fusion[7]

Table 3.1 **Summary of entry pathways and receptors used by the viral glycoproteins assessed in this study.**

Each viral pseudoparticle assessed in this study enters epithelial cells using a different receptor(s) and uptake pathway(s). [1](Finkelshtein et al., 2013; Cossart and Helenius, 2014; Moller-Tank and Maury, 2015; Skehel and Wiley, 2000; Cao et al., 1998; Noyce et al., 2011; Palgen et al., 2015)

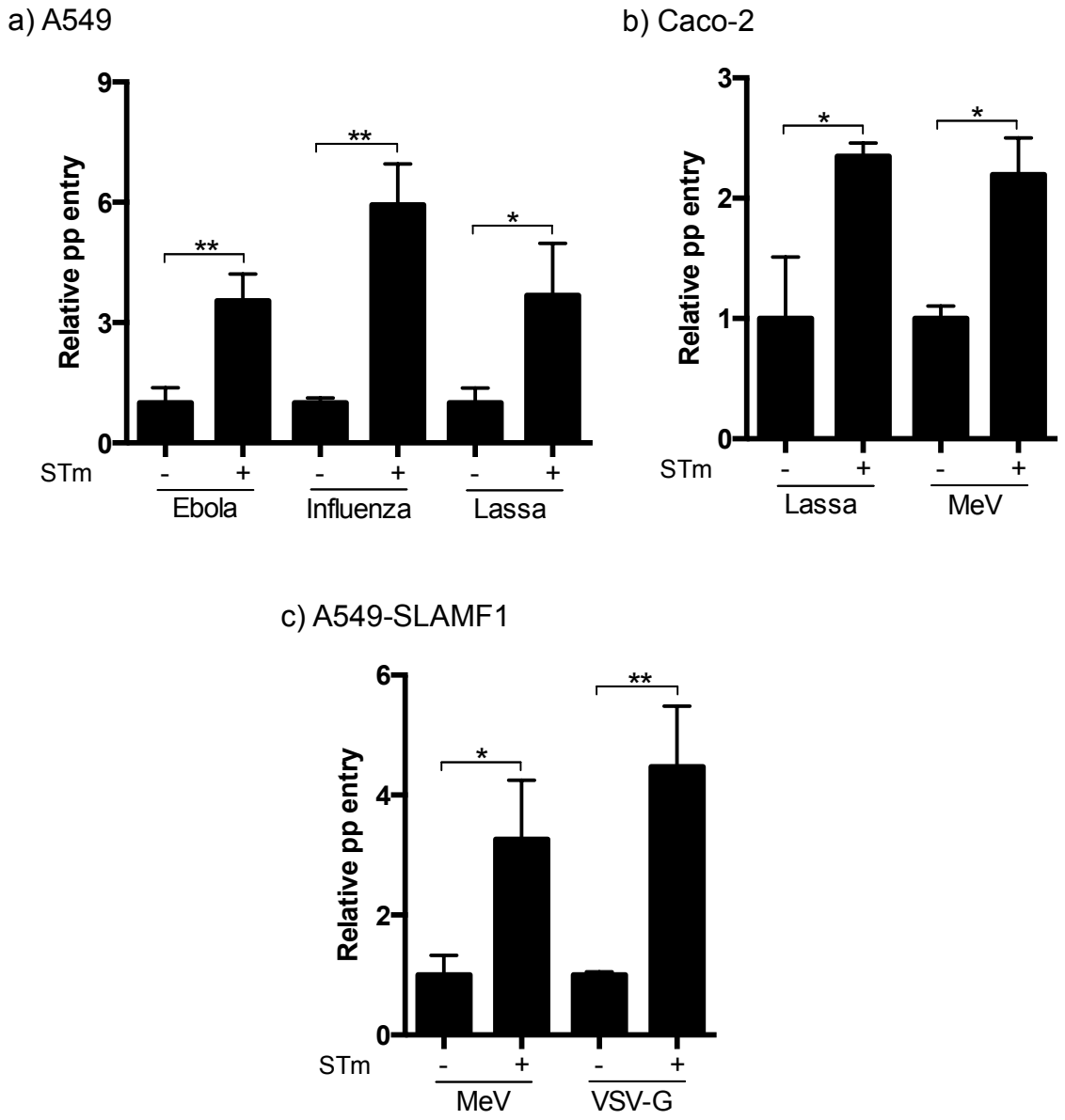

Figure 3.12 **STm increases entry of diverse viral pseudoparticles.**

a-c) Cells were incubated with STm (MOI 10) for 1h prior to addition of pseudoparticles as stated and chloramphenicol. Entry was quantified by luciferase assay at 48h. Data are presented as relative to entry of each pseudoparticle into untreated cells. Representative of 3 biological replicates, error bars show SD of 3 technical replicates, statistical comparison by Unpaired t test: * = $P \leq 0.05$, ** = $P \leq 0.01$.

permeability, we sought to investigate the mechanisms through which this was mediated.

3.6 STm specifically increases viral glycoprotein-dependent particle uptake

One potential pathway, other than glycoprotein-mediated entry, that could increase the luciferase production used to quantify virus entry by pseudoparticles would be a direct effect of STm on luciferase transcription or translation. To address this, we transfected cells with the plasmid used for pseudoparticle generation: pNL4.3env$^-$rev$^-$ luciferase, which encodes the HIV virus core competent for a single round of infection and the firefly luciferase gene. We used three different protocols to deliver the luciferase construct into cells without viral glycoprotein involvement. Firstly, A549 cells were transfected 24h prior to the addition of STm for 1h, antibiotic treatment and 24h incubation (**Fig.3.13a**). Using this method there was no difference in luciferase activity between STm-treated and untreated cells (**Fig.3.14a**). Secondly, STm was added to cells prior to transfection (**Fig.3.13b**), to imitate the pseudoparticle assay design in **Fig.3.5a**. This also showed a minimal difference in luciferase activity between untreated cells or STm treated cells (**Fig.3.14b**).

Finally, when infecting cells with pseudoparticles, it is important to include a control virus that lacks any glycoproteins and is classified as NEpp (**Fig.3.1**). These particles may be non-specifically endocytosed by the target cell and provide a background luciferase signal. Viral glycoprotein-carrying pseudoparticles are often normalised to NEpp values, which can vary between cell types. We tested the effect of STm on NEpp to determine whether the presence of bacteria could increase baseline levels

a)

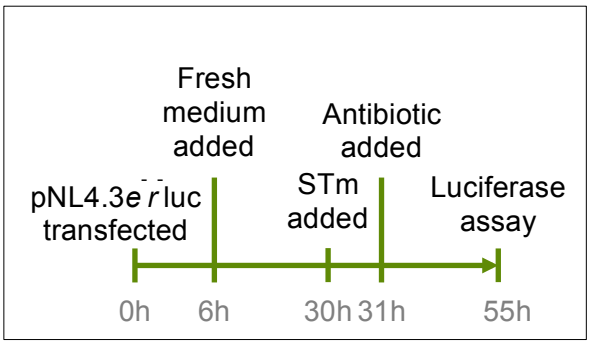

b)

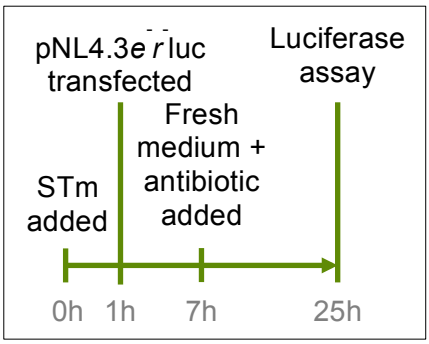

Figure 3.13 **Methods to assess the effect of STm on luciferase production.**

a-b) Schematic diagrams of two different experimental protocols used, showing timing of STm addition to and pNL4.3env-rev-luciferase transfection of epithelial cells. Transfection reagents were removed after 6h and fresh medium added to prevent cell death during the incubation time needed for luciferase production. Following 24h incubation, epithelial cells were lysed to quantify luciferase activity.

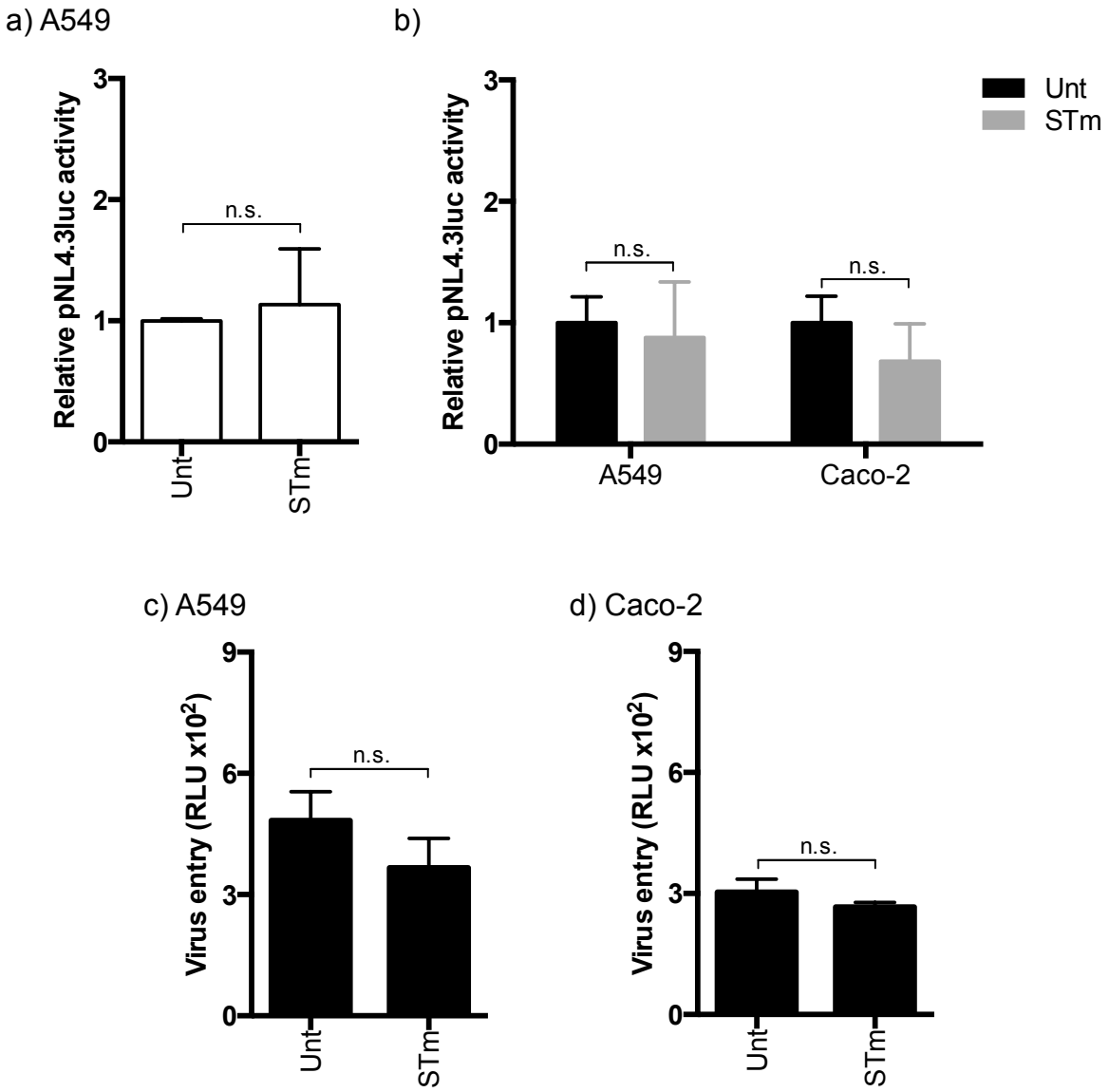

Figure 3.14 **STm has no effect on luciferase production or non-specific particle uptake.**

a) Cells were transfected with pNL4.3env⁻rev⁻luc 24h prior to incubation with STm (MOI 10) for 1h, as described in Fig.3.13a. b) Cells were incubated with STm (MOI 10) for 1h prior to transfection with pNL4.3env⁻rev⁻luc for 6h, as described in Fig.3.13b. pNL4.3env⁻rev⁻luc activity was determined by luciferase assay and data are presented as relative to untreated, transfected cells. c-d) Cells were incubated with STm (MOI 10) for 1h prior to addition of NEpp and chloramphenicol. Entry was quantified by luciferase assay at 48h. Data are presented as relative to NEpp entry into untreated cells. Representative of 3 biological replicates, error bars show SD of 3 technical replicates, statistical comparison by Unpaired t test: ns = P > 0.05.

of endocytosis. There was no increase in NEpp entry after STm in either cell line (**Fig.3.14c-d**). Together, these results support that STm promotes viral glycoprotein-mediated entry.

3.7 STm enhances the magnitude and kinetics of viral entry

We were interested to define whether STm increased the number of virus infected cells or the number of virus particles entering each cell. We determined the rate of virus entry, by washing away unbound virus at specific time points after inoculation (**Fig.3.15a**), and found that 1h pre-treatment with STm significantly increased the rate of VSV-Gpp entry into both A549 and Caco-2 epithelial cells (**Fig.3.15b-c**). Another method to investigate virus infection is to use pseudoparticles expressing a fluorescent reporter in place of luciferase, allowing visualisation of infected cells. We used VSV-Gpp encoding GFP to measure infected A549 cells by flow cytometry. With STm pre-treatment there was a clear increase in the number of infected cells (**Fig.3.15d**) and an increased mean fluorescence in the GFP+ cell population (**Table 3.2**). These results suggest that exposure of epithelial cells to STm increases their permissivity to virus entry, allowing more virus particles to bind per cell, and increases the rate of particle internalization. Furthermore, the effect of STm on the cell is long lasting. These experiments showed an increase in VSV-Gpp entry into A549 cells up to 4h post-STm exposure and up to 24h for Caco-2 cells (**Fig.3.16**).

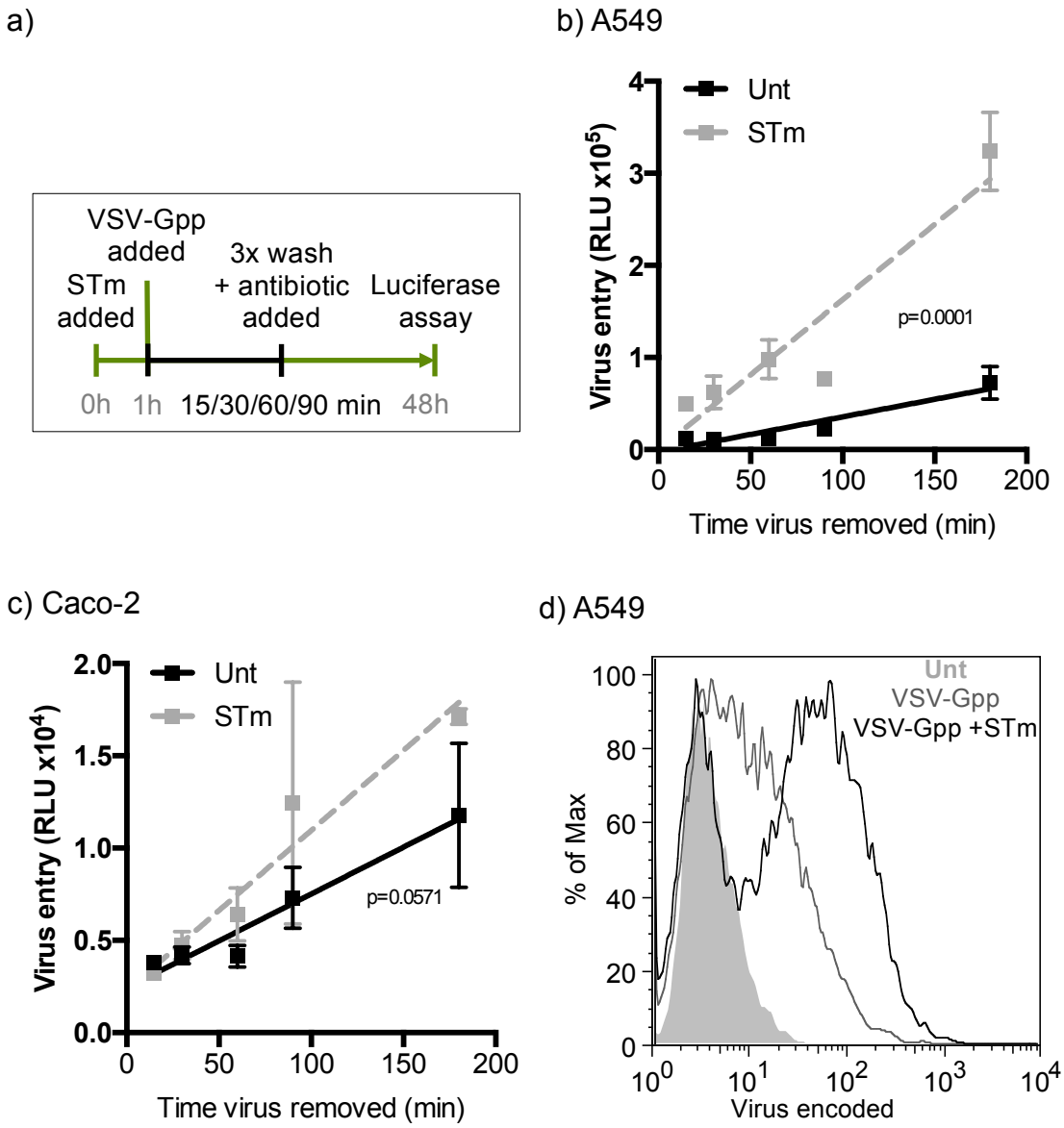

Figure 3.15 **STm increases rate and frequency of pseudoparticle entry.**

a) Schematic diagram of experimental setup showing timing of STm addition, VSV-Gpp addition and washing of epithelial cells at different time points to remove unbound pp prior to 48hr incubation. Pseudoparticle entry was measured by luciferase activity. b-c) Cells were incubated with STm (MOI 10) for 1h, VSV-Gpp was added for the specified time and the cells washed to remove unbound pp. Following washing, cells were incubated with 34 µg/mL chloramphenicol. Entry was quantified by luciferase assay at 48h. Data are presented as RLU. Representative of 3 biological replicates, error bars show SD of 3 technical replicates, statistical comparison by linear regression. c) Cells were incubated with STm (MOI 10) for 1h prior to addition of VSV-Gpp containing a GFP reporter gene and chloramphenicol. Cells were fixed at 48 hours and assessed by flow cytometry. The results are gated on live cells and presented as intensity of GFP expression versus number of events (% of max).

	Freq. of Parent	Mean
Untreated	3.1	20.8
VSV-Gpp	33.8	49.5
VSV-Gpp +STm	60.5	101

Table 3.2 **STm increases virus infection per cell.**

Cells were incubated with STm (MOI 10) for 1h prior to addition of VSV-Gpp containing a GFP reporter gene and chloramphenicol. Cells were fixed at 48 hours and assessed by flow cytometry. The results are gated on live cells, then GFP+ cells, to determine the frequency of GFP+ cells in the live cell population and the mean fluorescence intensity of the GFP+ population.

a)

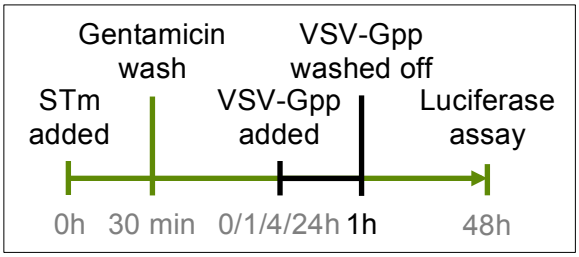

b)

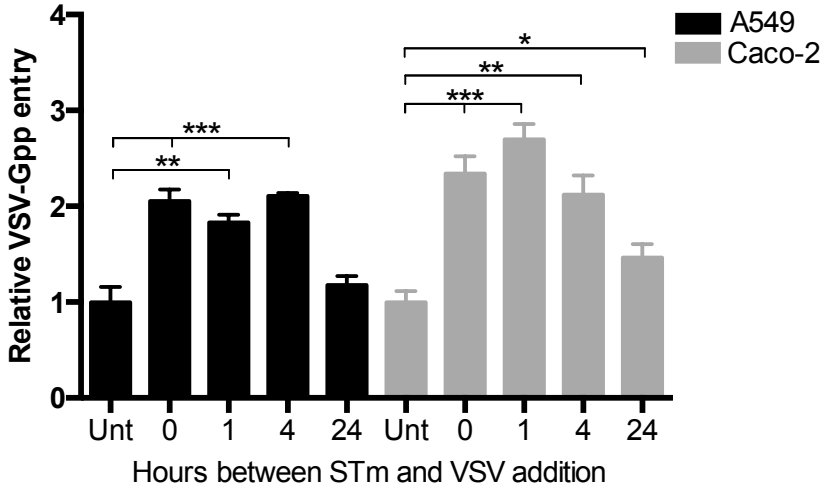

Figure 3.16 **STm increases VSV-Gpp entry for a prolonged time.**

a) Schematic diagram of experimental setup showing timing of VSV-Gpp addition during or after STm addition and subsequent high concentration gentamicin wash to kill extracellular bacteria. Gentamicin at a lower concentration was maintained for the remainder of the assay to prevent intracellular bacteria exiting epithelial cells and infecting new cells. VSV-Gpp was added for 1h and washed off to prevent new infections occurring throughout the incubation time. b) Cells were incubated with STm (MOI 10) for 30 min, washed and incubated with gentamicin (50 µg/mL) for 30 min, washed and incubated with gentamicin (5 µg/mL). VSV-Gpp was added at the time indicated post-STm addition for 1h and washed off. Entry was quantified by luciferase assay at 48h. Data are presented as relative to VSV-Gpp entry into untreated cells. Representative of 3 biological replicates, error bars show SD of 3 technical replicates, statistical comparison by Unpaired t test: * = $P \leq 0.05$, ** = $P \leq 0.01$, *** = $P \leq 0.001$.

3.8 STm invades A549 cells

STm can enter intestinal epithelial cells to facilitate intracellular replication in SCV (Steele-Mortimer, 2008) and has been reported to invade Caco-2 cells via the apical surface and escape from the basolateral surface within 2h (Finlay and Falkow, 1990). We were interested to determine whether STm invaded A549 cells. Bacterial invasion into A549 and Caco-2 cells can be quantified by lysing the epithelial cells with the detergent triton X-100, serially diluting the lysate and plating on LB agar to determine CFU/mL. This method demonstrated that, while significantly more bacteria adhered to Caco-2 cells than A549 cells, comparable numbers of bacteria invaded both cell types (**Fig.3.17**).

To determine whether cells infected with STm were more likely to be infected with VSV-Gpp, pseudoparticles were generated containing GFP as a reporter. Representative images of untreated and STm treated A549 cells infected with VSV-Gpp expressing GFP are shown in **Fig.3.18a**. While there are virus-infected cells containing STm, an example of which is shown in **Fig.3.18b**, the majority of virus-infected cells do not contain bacteria. This suggests that STm invasion is not required for its pro-viral effect.

3.9 Bacterial invasion and pathogenicity islands are not required to promote virus entry

STm has many effects on epithelial cells, including through the expression of MAMPs that can interact with cells. Nevertheless, the majority of effectors are encoded by two secretion systems located on genetic pathogenicity islands. SPI-1 facilitates

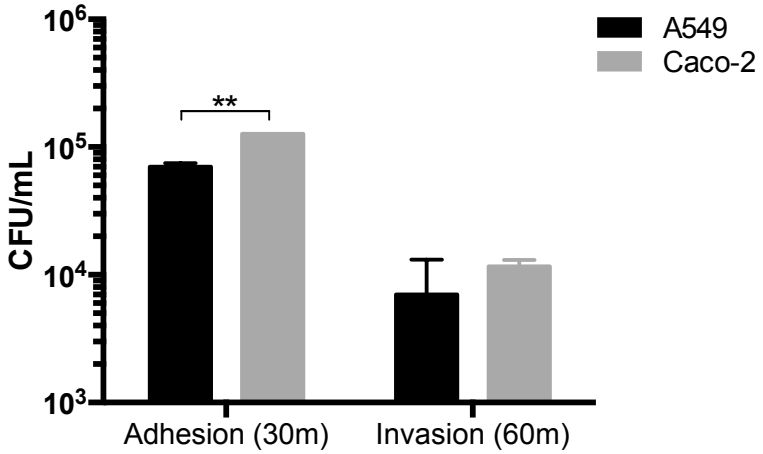

Figure 3.17 **STm is internalized by epithelial cells.**

Epithelial cells were treated with STm (MOI 10) for 1h and lysed using Triton X-100, or washed and treated with gentamicin (50 µg/mL) for 30 min to kill extracellular bacteria then lysed. Cell lysates were plated on LB agar overnight and colonies counted to determine colony forming units (CFU) able to adhere to and invade cells. Invasion was calculated by removing number of adhered bacteria from total number of bacteria in whole cell lysate. Representative of 2 biological replicates, error bars show SD of 2 technical replicates, statistical comparison by Unpaired t test: ** = $P \leq 0.01$.

a)

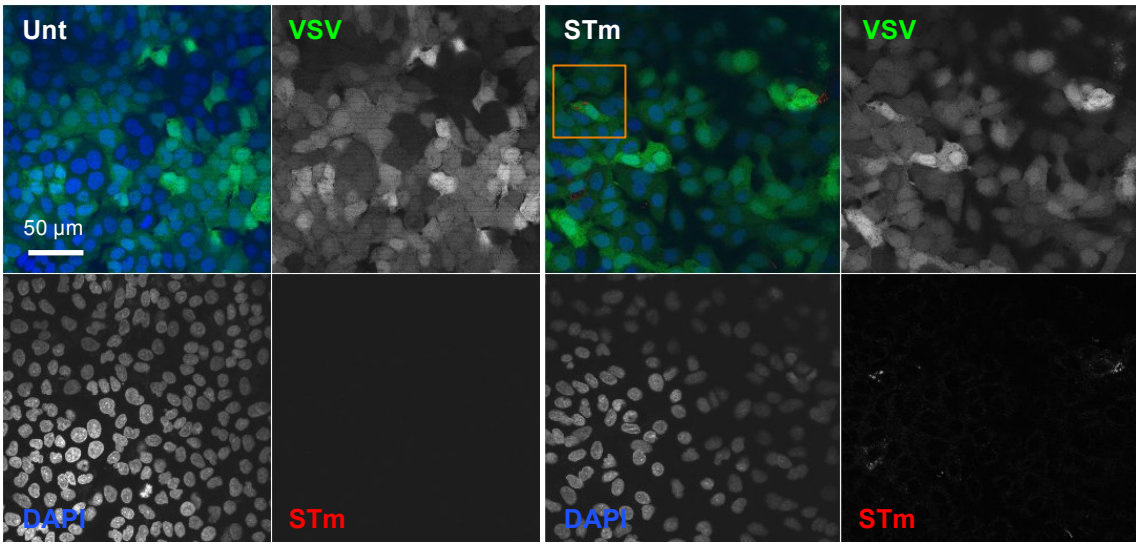

b) zoom

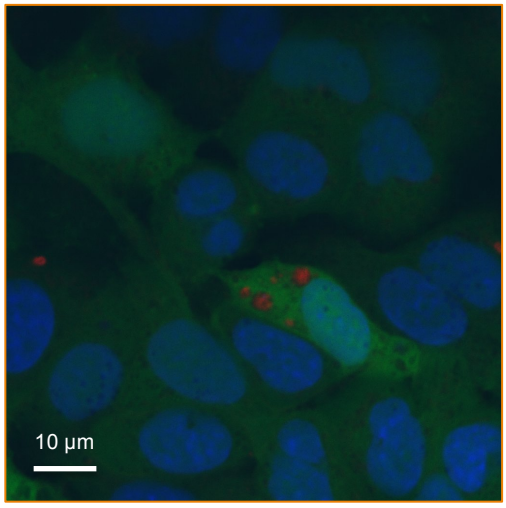

Figure 3.18 **VSV-Gpp and STm localization in A549 cells.**

a) A549 cells were incubated with STM (MOI 10) for 1h prior to addition of VSV-Gpp containing a GFP reporter gene and chloramphenicol. At 48h, cells were fixed to determine levels of STm LPS by immunofluorescence; nuclei were stained with DAPI. Cells were imaged using a Zeiss 510 Meta confocal microscope with 40x objective and LSM software. There was no clear association between STm infected cells and VSV-Gpp infected cells. Scale bar indicates 50 µm. b) Zoom of orange box in top right hand image showing an example of a STm and VSV-Gpp infected cell, surrounded by solely VSV-Gpp infected cells. Scale bar indicates 10 µm.

invasion of host cells and can have effects such as altering TJ integrity (Boyle et al., 2006; McGhie et al., 2009). As established in **Fig.3.6,** there was no effect on cell permeability or TJs during the 1h STm incubation prior to viral infection. However, SPI-1 effectors can have other effects. We assessed whether bacterial invasion was necessary for the pro-viral effect using an SPI-1 mutant strain of STm unable to secrete some of the effectors used for invasion. This mutant strain showed a comparable level of adhesion to epithelial cells as wild type STm, but reduced invasion (**Fig.3.19**). STm ΔSPI-1 increased VSV-Gpp entry into A549 cells with comparable levels to the wild type. However, it had slightly less pro-viral activity in Caco-2 cells (**Fig.3.20a**). SPI-2 effectors are released in the SCV to facilitate intracellular survival and can also affect actin dynamics (McGhie et al., 2009). We tested a SPI-2 mutant strain and saw no difference compared to the wild type strain in adhesion and invasion assays (**Fig.3.19**). Furthermore, there was comparable pro-viral activity in A549 cells, although slightly lower than wild type in Caco-2 cells (**Fig.3.20a**). These data suggest that SPI-1 and SPI-2 effectors are not necessary to increase VSV-Gpp entry in A549 cells and may play a role in STm pro-viral activity in Caco-2 cells.

Considering that invasion is not essential for STm to promote virus entry, we assessed whether live bacteria were required. STm was killed by heating to 100°C for 20 minutes and plated on agar to ensure no bacterial growth. Unexpectedly, heat-killed bacteria promoted VSV-Gpp entry with comparable levels to live bacteria in both cell lines (**Fig.3.20b**). These results suggest that STm does not need to invade

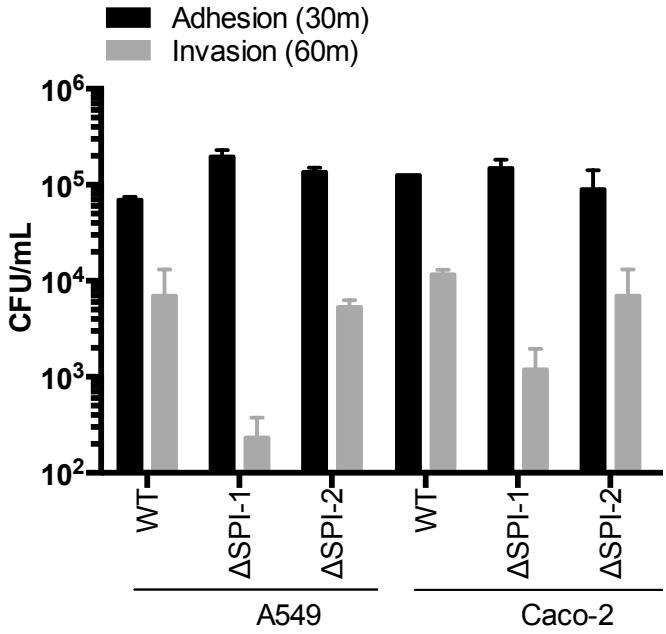

Figure 3.19 **Adhesion and invasion of mutant bacterial strains tested.**

Epithelial cells were treated with WT STm, STm ΔSPI-1 or STm ΔSPI-2 (MOI 10) for 1h and lysed using Triton X-100, or washed and treated with gentamicin (50 μg/mL) for 30 min to kill extracellular bacteria then lysed. Cell lysates were plated on LB agar overnight and colonies counted to determine colony forming units (CFU) able to adhere to and invade cells. Invasion was calculated by removing number of adhered bacteria from total number of bacteria in whole cell lysate. STm ΔSPI-1 has comparable adhesion to but reduced invasion of epithelial cells. Representative of 2 biological replicates

a)

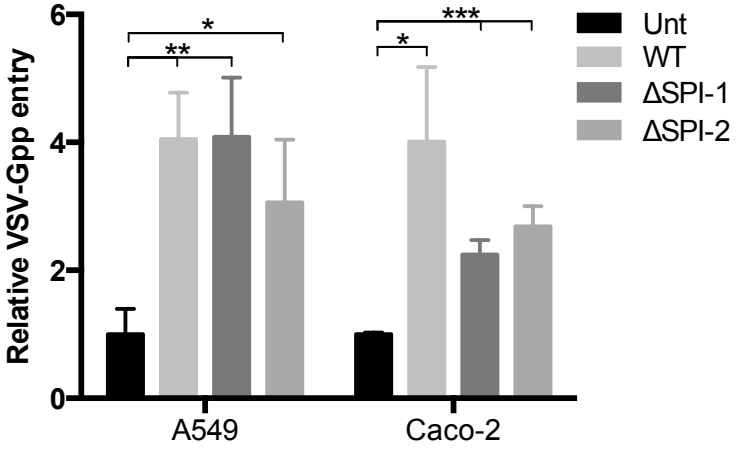

b)

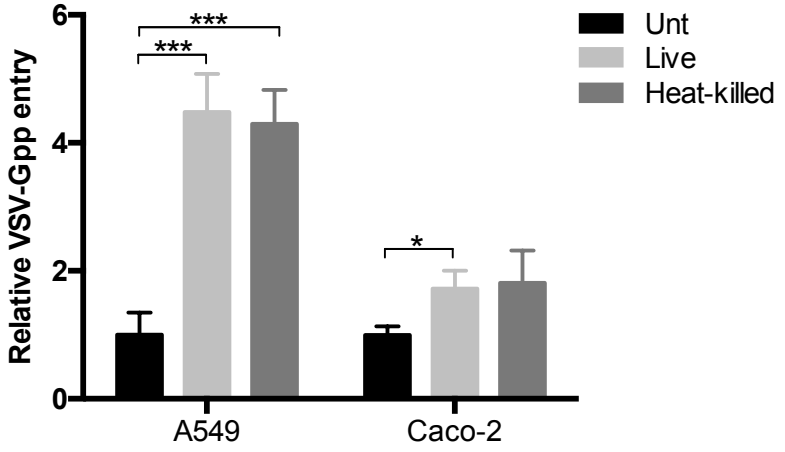

Figure 3.20 **The effect of STm does not require invasive, live bacteria.**

a) Cells were treated with WT STm, STm ΔSPI-1 or STm ΔSPI-2 (MOI 10) for 1h prior to addition of VSV-Gpp and chloramphenicol. Entry was quantified by luciferase assay at 48h. Data are presented as relative to VSV-Gpp entry into untreated cells. b) Cells were treated with live STm or heat-killed STm (100 °C for 20 min; MOI 10) for 1h prior to addition of VSV-Gpp and chloramphenicol. Entry was quantified by luciferase assay at 48h. Data are presented as relative to VSV-Gpp entry into untreated cells. Representative of 3 biological replicates, error bars show SD of 3 technical replicates, statistical comparison by Unpaired t test: * = $P \leq 0.05$, ** = $P \leq 0.01$, *** = $P \leq 0.001$.

cells or utilise any active processes, such as secretion of effectors that may alter the host cell TJs or cytoskeleton, to increase virus entry.

3.10 Discussion

We aimed to develop a model system to investigate the influence of bacterial exposure on virus infection of epithelial cells. The epithelial surfaces in the body are known to be colonised by bacteria, even the lung which was previously reported to be sterile (Dickson and Huffnagle, 2015). This suggests that an epithelial cell targeted for infection by a virus is likely to have bacterial cells, or their products, in close proximity. It has been reported that viral entry into polarized cells can be restricted (Walters et al., 2001; Mee et al., 2008) and that altering the monolayer permeability with cytokines counters this effect (Fletcher et al., 2014). We hypothesised that bacteria would increase virus entry because many bacterial species, and their effector molecules, have been shown to increase epithelial cell permeability (Boyle et al., 2006; Caron et al., 2015; Freedman et al., 2016).

We established this model system using polarized cell lines (**Fig.3.2**) and observed that, when polarized, the cells supported lower levels of viral entry (**Fig.3.3**). We identified the highest bacterial MOI, added with an antibiotic, suitable to maintain viable epithelial cells during the course of the assay (**Fig.3.4**). Then, using this model, we saw that STm could increase viral entry into multiple epithelial cell types. Furthermore, this pro-viral activity was not limited by viral glycoprotein type or entry pathway (**Fig.3.12**). Interestingly, following STm pre-treatment, Huh7 hepatocyte-derived cells did not support increased VSV-Gpp entry (**Fig.3.11b**). It is hard to

determine why this cell line would respond differently without knowing the mechanism of the bacterial effect, which will be explored in subsequent chapters.

It was important to determine that the STm-induced increase in reporter activity was dependent on viral glycoprotein-mediated entry, rather than transcription or translation of the luciferase reporter. To do this we transfected cells with the luciferase reporter plasmid used to produce pseudoparticles and saw no increase after STm treatment (**Fig.3.14**). We also tested the effect of STm on control pseudoparticles without a viral glycoprotein and saw no increase in background particle uptake in either A549 or Caco-2 cells, confirming that a glycoprotein-receptor interaction is necessary. A general increase in non-specific uptake might have been an interesting mechanism for increased viral entry, considering that different viral entry pathways are increased.

To reject our hypothesis that the effect of STm on virus entry would be through altered epithelial cell permeability we have collected data using different experimental methods. Initially, we assessed the effect of STm on the paracellular permeability of cells cultured on a transwell using a fluorescent dextran molecule. This technique showed no effect of STm treatment (**Fig.3.6a**) although it has previously been reported to show altered Caco-2 cell permeability after EGTA treatment to deplete calcium (Mee et al., 2008). We also imaged TJ proteins 1h after STm was added and saw no difference compared to untreated cells (**Fig.3.6b**). This result is in contrast to previous reports; Boyle et al. (2006) fixed the cells 4h after STm treatment using a MOI of 50, whereas we are using a MOI of 10 for 1h. It may be that we are not using

sufficient bacteria or allowing them enough time to target TJ proteins. However, it is remarkable that one bacterium per 10 epithelial cells can significantly increase virus entry.

Further data supporting this conclusion are the results showing that STm increases viral entry into non-polarized cells (**Fig.3.7**) and the ability of STm ΔSPI-1 to increase VSV-Gpp entry (**Fig.3.20a**), given that the effect of STm on epithelial cell polarization is mediated by SPI-1 effectors (Boyle et al., 2006). The observation that growth medium does not alter the effect of bacteria on virus entry (**Fig.3.7**) may have predicted the finding that SPI-1 and SPI-2 are not necessary for the pro-viral effect, as it has been reported that growth media can affect SPI transcription (Blair et al., 2013). Furthermore, heat-killed STm are as effective as live bacteria, supporting the conclusion that invasive bacteria are not required.

Another possible mechanism for increased virus entry could have been through secondary messengers, secreted in response to STm and having an autocrine or paracrine effect on virus entry. The cytokines TNF and IL-1β have been reported to increase using many of these pseudoparticles (Fletcher et al., 2014). Analysis of epithelial cell supernatant after STm treatment by ELISA suggested that neither A549 nor Caco-2 cells were secreting either cytokine (data not shown), ruling out this hypothesis for currently known cytokine mediators.

It has been published that a non-typeable *H. influenzae* strain can increase rhinovirus entry by upregulating the virus receptor ICAM-1 (Sajjan et al., 2006). Interestingly, it

appears that the determining factor for how much STm boosts virus entry under these conditions is the cell line, rather than the virus type or pathway of entry. There was an approximate five-fold increase in virus entry into non-polarized A549 cells, however, only a two-fold increase into Caco-2 cells. Since these viruses use different cellular receptors and uptake pathways it is unlikely that STm would regulate all of these receptors. Alternatively, STm may target a host pathway downstream of receptors, allowing multiple receptor-mediated interactions to be regulated and the next step would be to look at internalization pathways. We will examine cellular signalling pathways more in the next chapter, but it is a fairly long-lived response, as determined in **Fig.3.16**.

3.11 Summary

We present results showing that epithelial cell exposure to STm, whether live or heat-killed, increases host cell permissivity to allow more virus entry, faster, and using viral glycoproteins that enter the cell via multiple pathways. In the next chapter we will focus on how STm achieves this, given that it is not through altered host cell TJs or actin remodelling by SPI effectors.

4. IDENTIFICATION OF FLAGELLIN AS THE PRO-VIRAL FACTOR

4.1 Introduction

In the previous chapter we determined that short-term exposure to STm augments the ability of epithelial cells to support virus entry. To determine the mechanism(s) behind this pro-viral activity, since heat-killed bacteria gave comparable results to live, we were interested in secreted factors that may interact with epithelial cells. Bacteria can alter host cell biology through a number of distinct mechanisms, such as the release of virulence factors, toxins and outer membrane vesicles (OMVs; (Lee and Schneewind, 2001; Kaparakis-Liaskos and Ferrero, 2015). Many of these factors are recognized by the innate immune system, as indicated in **Table 4.1**. These include LPS, flagellin and outer membrane protein (Omp) porins that may be recognized by TLRs (McClure and Massari, 2014).

LPS is composed of three regions: lipid A, core and O antigen (**Fig.4.1a**, (Maldonado et al., 2016) and is one of the most abundant bacterial molecules found on Gram-negative bacteria. Lipid A is recognized by TLR4, using the accessory molecules lipid binding protein (LBP) and lipid A binding protein (CD14; (Miller et al., 2005). TLR4 signaling leads to a potent pro-inflammatory response, which can aid in bacterial clearance and modulate host cell responses. However, elevated LPS levels can overwhelm the host and cause sepsis (Opal, 2007). On lung and gut epithelial surfaces, TLR4 may be expressed basolaterally or intracellularly

Ligand	Receptor(s)
CpG DNA	TLR9
Flagellin	NAIP/NIrc4 TLR5
Gram-negative PGN	NOD1
Gram-positive PGN	NOD2
Lipoproteins, cell wall components e.g. porins, PGN	TLR2 (in complex with TLR1/TLR6)
LPS	TLR4

Table 4.1 **Bacterial factors recognized by host cell receptors.**

Ligands found in bacterial cells, including peptidoglycan (PGN) and lipopolysaccharide (LPS), can be detected by host cells such as epithelial cells through toll-like receptors (TLR) and nucleotide-binding oligomerization domain (NOD)-like receptors.

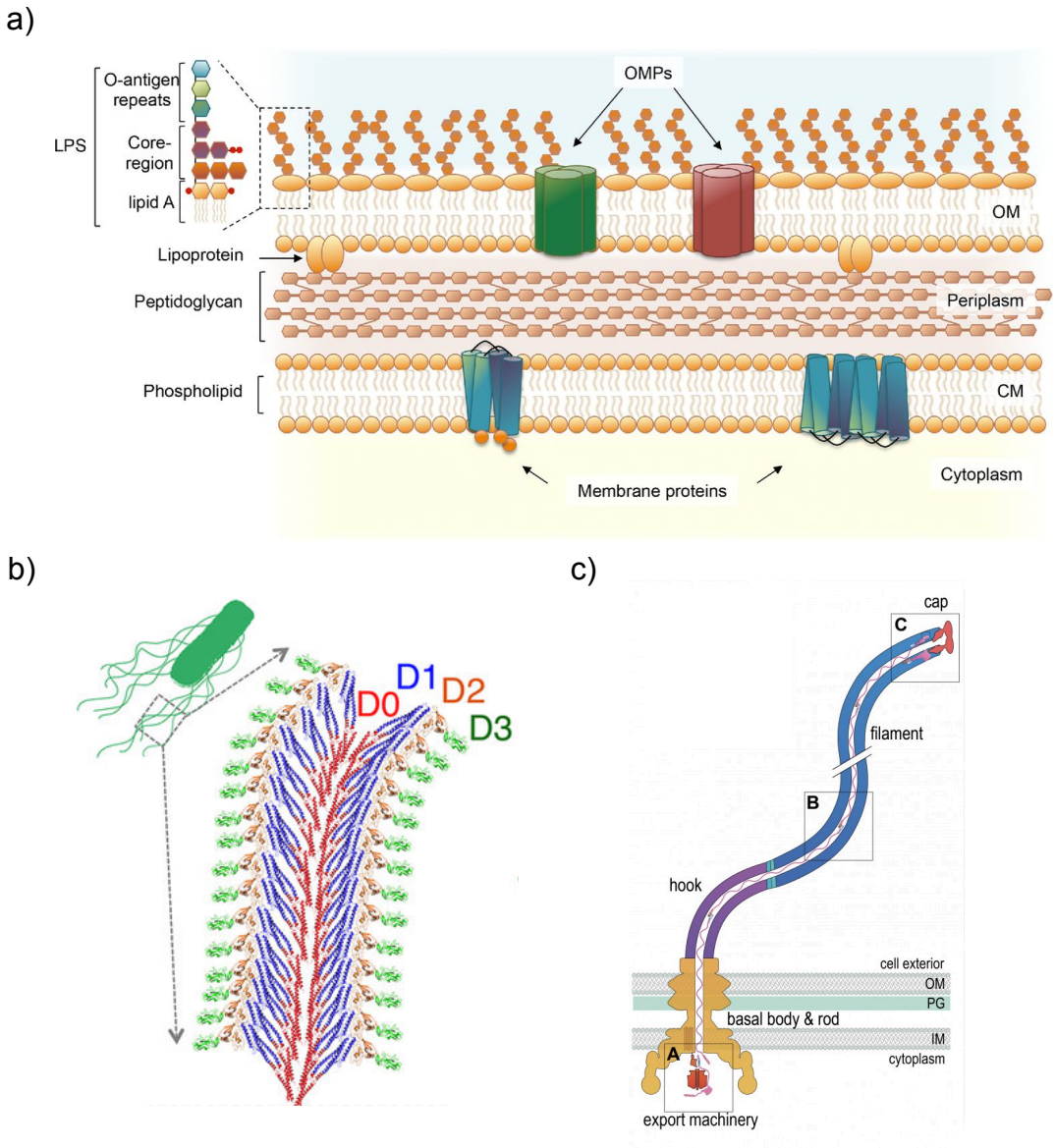

Figure 4.1 **Components of the Gram-negative outer membrane.**

a) The structure of the outer membrane, from Maldonado et al., 2016. LPS is comprised of O-antigen repeats, the core region and lipid A, and forms the outer leaflet of the outer membrane (OM). Outer membrane proteins (OMP) such as porins can span the OM. Peptidoglycan and lipoproteins are found in the periplasm. Membrane proteins can also span the cytoplasmic membrane (CM). b) The structure of polymerized flagellin forming flagellar filaments, adapted from (Lu and Swartz, 2016) Flagellin contains four domains and each domain (D0-D3) is labeled by colour to demonstrate that D0 and D1 are inaccessible to host cell receptors when flagellin is polymerized. c) The flagellum is composed of three substructures, adapted from (Evans et al., 2014). A. The basal body and rod substructure spans the inner and outer membranes (IM, OM) and contains export machinery to move unfolded flagellin subunits through a channel in the flagellum. B. The main body of the flagellum is the filament, which can be up to 20 µm and is attached to the basal body via the hook section. C. Transported subunits are able to fold and incorporate into the tip, below the cap.

(McClure and Massari, 2014). This could avoid hyper-responsiveness due to constant exposure of epithelial cells to LPS during bacterial colonization of these sites.

STm flagellin is a ~50 kDa protein that comprises the main structure of bacterial flagella, which enable bacterial cells to propel themselves and adhere to host cells (**Fig.4.1b-c**). Flagella can extend far from the bacterial surface and can be shed as monomeric flagellin during assembly (Lu and Swartz, 2016). The monomers can be recognized by TLR5, specifically in the D1 region of flagellin, and also by NLR apoptosis-inhibitory protein (NAIP), which is part of the NAIP/Nlrc4-inflammasome, in the D0 region (Rossez et al., 2015). TLR5 is expressed predominantly on the basolateral surface of intestinal epithelial cells to prevent hyper-responsiveness to commensal bacteria, but enables detection of bacteria escaping through a breach in barrier permeability (Vijay-Kumar and Gewirtz, 2009). Both Gram-positive and Gram-negative bacteria can express flagellin. STm expresses two forms of flagellin, phase 1: FliC and phase 2: FljB. Each bacterial cell alternates between the expression of these antigenically distinct proteins, a mechanism called flagellar phase variation, to escape immune recognition (Yamamoto and Kutsukake, 2006).

Omps are trimeric proteins that form a pore through the outer membrane to allow nutrient transport into the periplasm (**Fig.4.1a**; (Galdiero et al., 2012). They can be recognized by TLR2/TLR6 (McClure and Massari, 2014). OmpC and OmpF can also be detected by the host via SLAM family members, leading to phagolysosomal

maturation and bacterial killing (Berger et al., 2010). However, these receptors are usually found on hematopoietic cells.

PGN, found in both Gram-positive and Gram-negative cell walls, can be recognized by nucleotide-binding oligomerization domain-containing protein (NOD)1 and NOD2 (**Table.4.1;** (Motta et al., 2015). PGN is composed of glycan strands, peptide subunits and interpeptide bridges and forms a layer around the bacterium to maintain its shape and protect from the environment (Bertsche et al., 2015). While Gram-negative bacteria have a thin layer between the inner and outer membranes, Gram-positive bacteria have a much thicker layer that comprises the outermost coating (**Fig.4.1a**). Both types of bacteria can shed PGN and Gram-negative PGN is detected by NOD1, whereas Gram-positive PGN is detected by NOD2 (Motta et al., 2015).

In the previous chapter we showed that STm can promote viral entry. We were interested in determining whether the pro-viral activity of STm is specific to this bacterial species, as we have already found that the effect is not through SPI-1 or SPI-2 (**Fig.3.20a**). We aimed to determine whether one bacterial factor is responsible for the pro-viral activity and if so could this factor be present on other species, or potentially specific to Gram-negative bacteria, as there are many common MAMPs that are recognized by host cells.

4.2 STm conditioned medium increases VSV entry

After finding that heat-killed STm increase VSV-Gpp entry into epithelial cells to comparable levels seen with live bacteria (**Fig.3.20b**) and low multiplicities of infection are sufficient to stimulate viral entry (**Fig.3.10**), we hypothesized that secreted bacterial factors promote epithelial permissivity. To investigate this possibility, we evaluated the effect of conditioned media (CM) from STm cultures in mid-log phase for their effect on VSV-Gpp infection of A549 cells (**Fig.4.2a**). One hour pre-treatment of A549 cells with the CM increased VSV-Gpp entry in a dose responsive manner (**Fig.4.2b**). However, the CM had no effect on VSV-Gpp infection of Caco-2 cells. This result suggests a difference between lung and gut epithelial cell responses to bacterial products. It also highlights that bacterial cell presence is not necessary for secreted factors to influence host cell processes.

4.3 Discovery of the secreted pro-viral factor

During STm growth in high glucose media the pH can fall from pH 7 to as low as pH 5 (Walker et al., 1997). Since mammalian cells can be reversibly altered by short-term exposure to low pH (Taylor, 1962), and many cellular processes are pH-dependent, we evaluated the pH of the CM. Using pH test strips we determined that STm CM had no significant effect on the pH of the media (**Fig.4.3**), allowing us to test for the presence of secreted bacterial pro-viral factors in the CM.

To elucidate the composition of the secreted factor(s) in CM able to increase virus entry, the CM was boiled for 20 minutes to denature heat sensitive factors, or

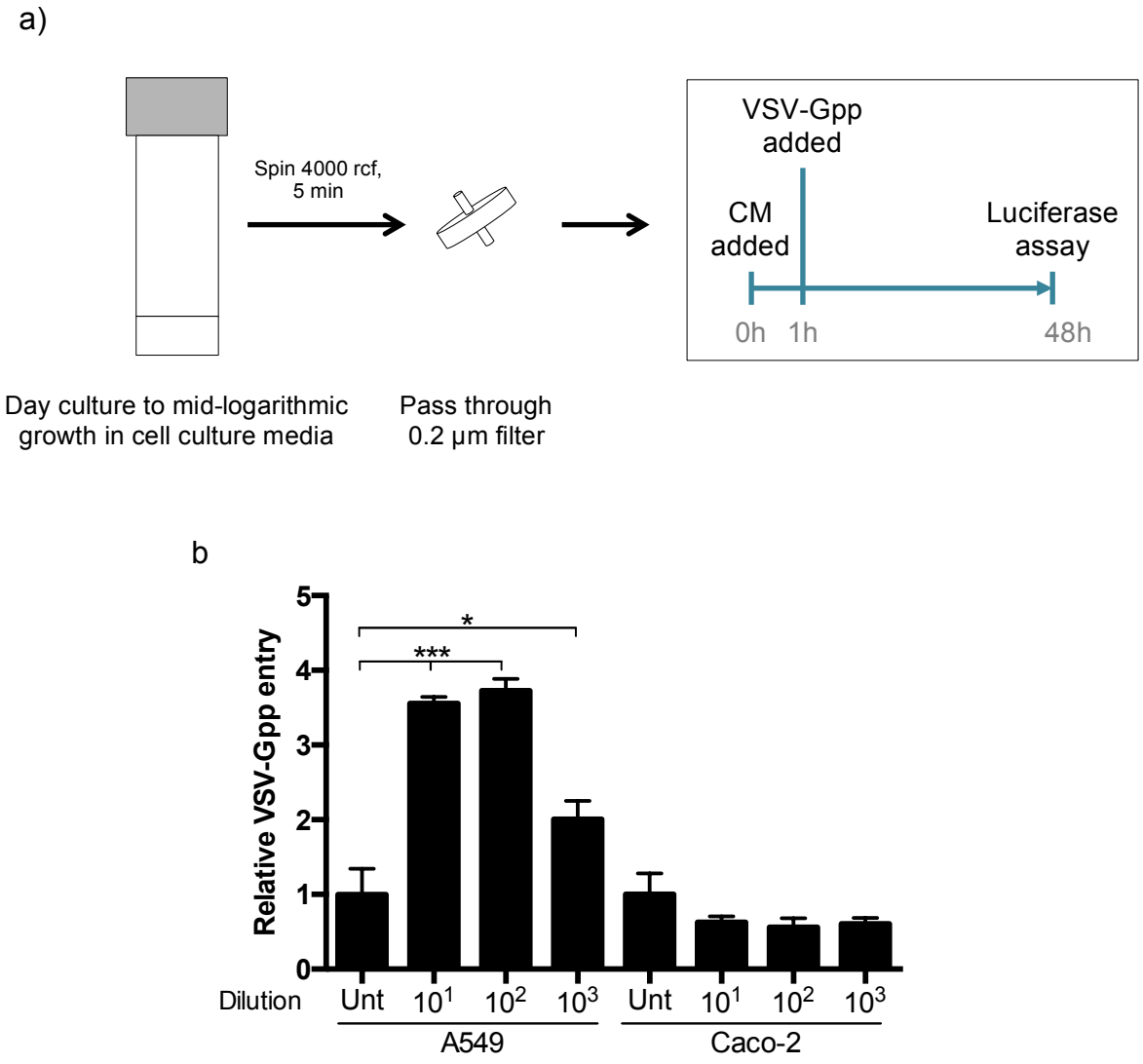

Figure 4.2 **VSV-Gpp entry can be increased using STm CM.**

a) Schematic diagram of experimental setup showing production of STm conditioned media (CM) and addition to epithelial cells. STm cultures were spin clarified and filtered to allow stimulation of epithelial cells with secreted bacterial products without the presence of whole bacteria, prior to pseudoparticle infection. b) A549 or Caco-2 cells were treated with wild type STm CM diluted from 1 in 10 to 1 in 1000 for 1h and infected with VSV-Gpp. Entry was quantified by luciferase assay at 48h. Data are presented as relative to VSV-Gpp entry into untreated cells. Representative of 3 biological replicates, error bars show SD of 3 technical replicates, statistical comparison by Unpaired t test: * = $P \leq 0.05$, *** = $P \leq 0.001$.

Figure 4.3 **CM does not have an altered pH.**

Top panel of image: pH indicator paper strips were tested for efficacy with standard solution controls at pH 10, 7 and 4. Bottom panel of image: STm CM from strains SL1344 (top row) and SL3261 (middle row) cultured in DMEM were pH tested at indicated dilutions from neat to 1 in 1000. Control DMEM without bacterial culture was also pH tested (bottom row).

sonicated to disrupt OMVs. Sonication of cellular membranes is can be a harsh method and the CM was incubated on ice before, during and after sonication to prevent temperature rises leading to protein denaturation. Neither treatment method reduced the efficacy of CM to increase viral entry (**Fig.4.4a**), suggesting that the pro-viral factor(s) are heat resistant and do not require intact OMV membranes to alter host cell permissivity.

LPS is an abundant heat-stable component of the bacterial outer membrane that can induce cytokine expression at subnanogram quantities (Majde, 1993). Epithelial cells recognize LPS through TLR4 and activate downstream signaling pathways. We tested purified whether STm LPS could modulate VSV-Gpp infectivity and observed no detectable increase in host cell permissivity (**Fig.4.4b**).

Given that LPS did not replicate results with STm or CM, we tested whether the heat resistant factor was proteinaceous by digesting the CM with proteinase K (PrK) for 30 minutes, then heat inactivating the enzyme prior to treating A549 cells. This treatment abolished the pro-viral activity of the CM compared to control CM that was treated with PrK buffer and heated for the same amount of time (**Fig.4.4c**). Therefore, the factor is PrK sensitive, which makes it unlikely to be LPS or PGN.

To characterise the STm-encoded proteins present in the CM we separated them using SDS-PAGE. CM was concentrated 300x using TCA and Coomassie staining of the gel showed two bands of around 50 kDa and less than 11 kDa (**Fig.4.5a**). To determine which band contained the pro-viral factor we used size fractionation.

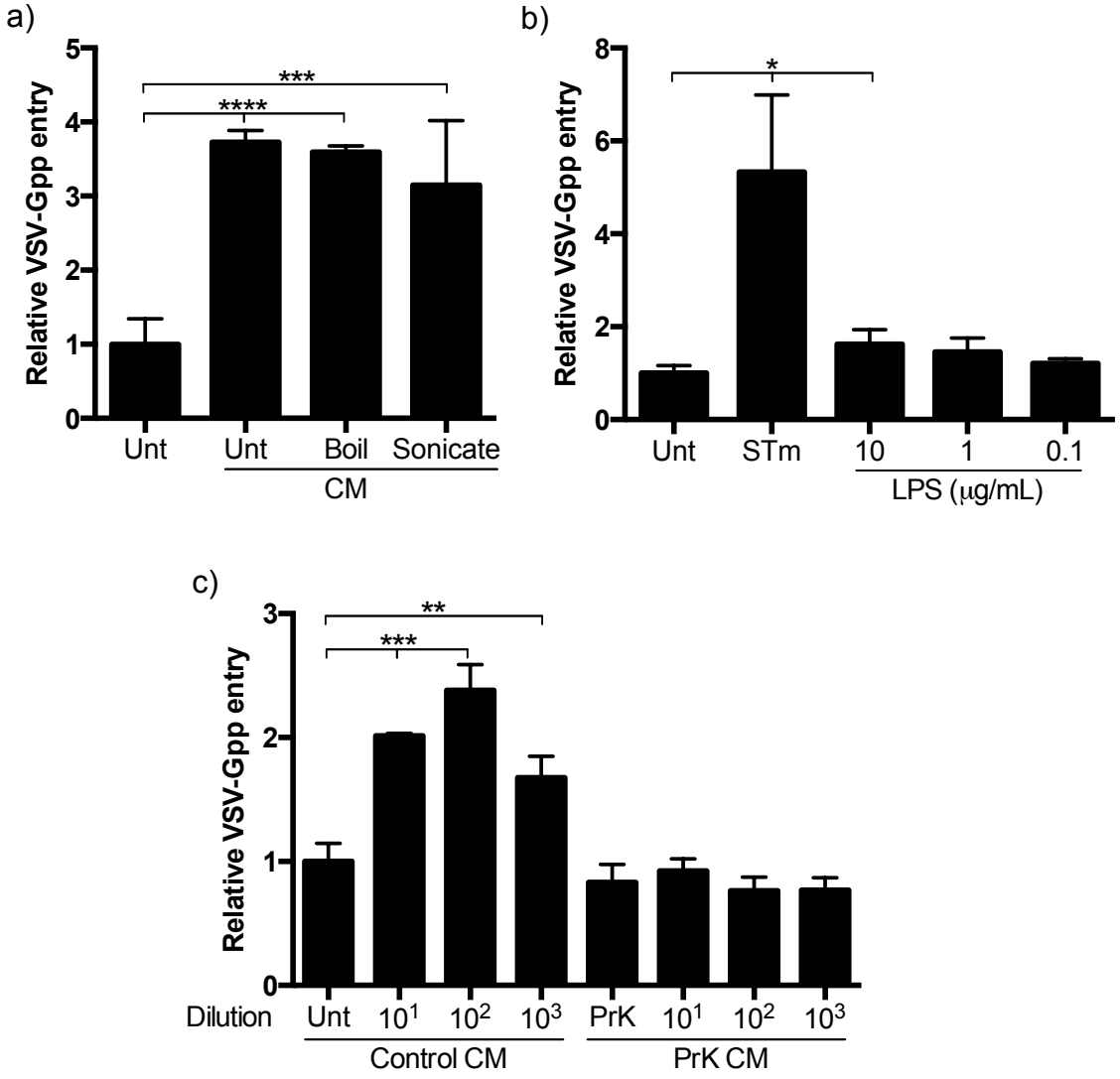

Figure 4.4 **The pro-viral factor(s) in CM are heat-stable proteins.**

A549 cells were treated with; (a) STm CM untreated, heated at 100 °C for 20 min or sonicated; (b) STm (MOI 10) or purified LPS from STm at indicated concentrations; (c) CM untreated or incubated with PrK for 30 min and heated to inactivate PrK at indicated dilutions. Each treatment was added for 1h prior to VSV-Gpp infection and entry was quantified by luciferase assay at 48h. Data are presented as relative to VSV-Gpp entry into untreated cells. Representative of 3 biological replicates, error bars show SD of 3 technical replicates, statistical comparison by Unpaired t test: * = $P \leq 0.05$, ** = $P \leq 0.01$, *** = $P \leq 0.001$, **** = $P \leq 0.0001$.

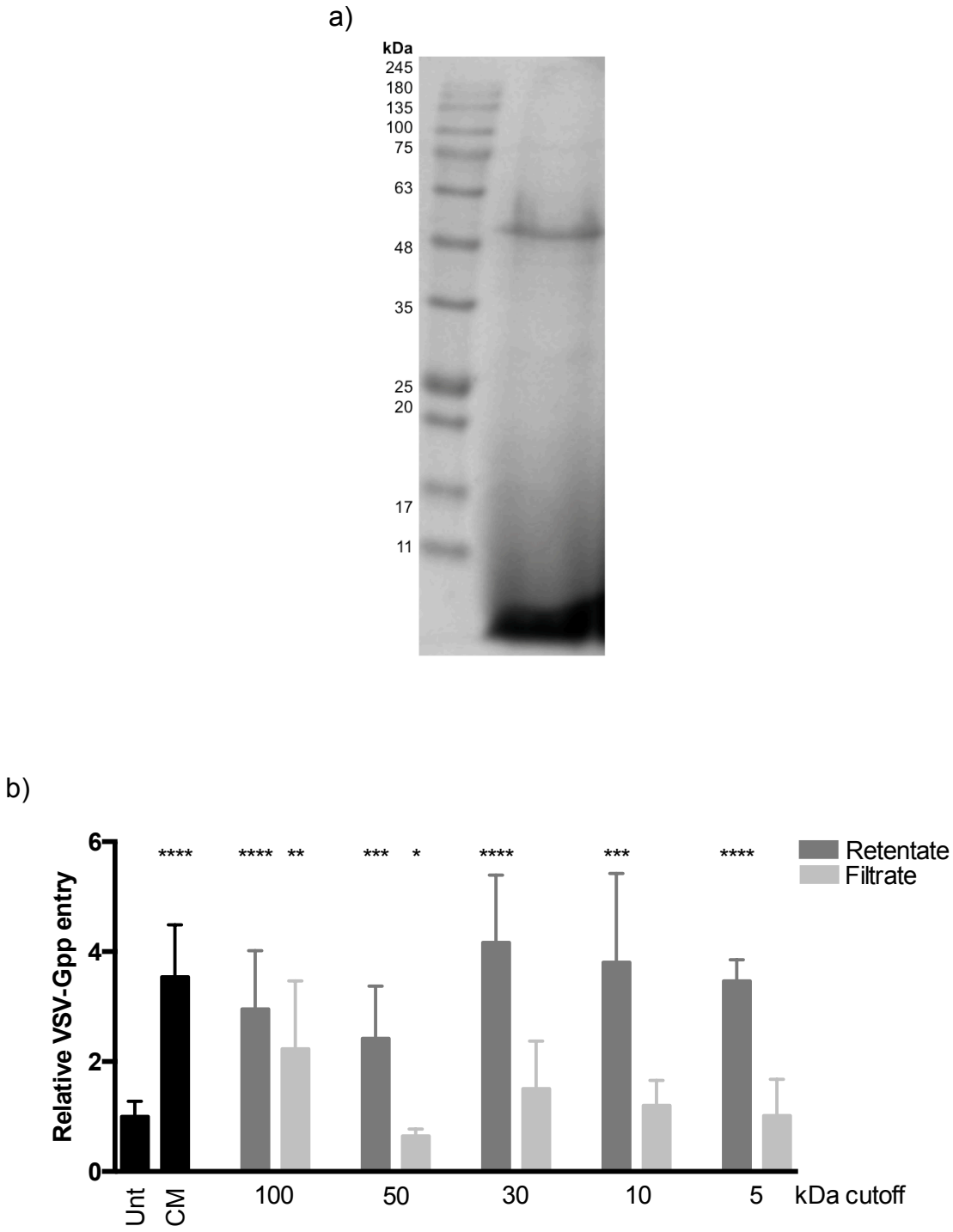

Figure 4.5 **Size determination of pro-viral CM factor.**

Figure 4.5 **cont.**

a) STm CM was concentrated by TCA precipitation and loaded into a 12% SDS gel for electrophoresis and Coomassie staining, identify two protein bands of ~50 and <10 kDa. b) CM was spin fractionated using molecular weight cut off columns of indicated sizes. Retentate and filtrate were collected from each column and added to A549 cells for 1h prior to VSV-Gpp infection and entry was quantified by luciferase assay at 48h. Data are presented as relative to VSV-Gpp entry into untreated cells. Filtrate >50 kDa shows reduced pro-viral activity. Collated results of 3 biological replicates, each with 3 technical replicates. Error bars show SD, statistical comparison to untreated by Unpaired t test: * = $P \leq 0.05$, ** = $P \leq 0.01$, *** = $P \leq 0.001$, **** = $P \leq 0.0001$.

CM was passed through molecular weight cut-off columns of varying sizes and the resulting fractions assessed for their effect on VSV-Gpp infection of A549 cells. There was a loss of pro-viral activity in filtrates containing proteins smaller than 50 kDa (**Fig.4.5b**). However, all of the retentates that contained proteins greater than 100 kDa increased virus entry, although there were no bands larger than 50 kDa detected by SDS-PAGE.

To identify candidate proteins in CM we performed mass spectrometric analysis of the CM fraction greater than 100 kDa. This semi-quantitative technique identified over 50 proteins in the CM for each independent run, the first 10 of which are shown in **Table 4.2**. Fragments of the protein flagellin, the major component of bacterial flagella, were highly represented in both runs. Another protein found in both samples was a membrane protein that we identified as siiE. This is a non-fimbrial adhesin protein secreted by a SPI-4 encoded type I secretion system that is reported to be necessary for STm invasion of polarized cells (Barlag and Hensel, 2015). It is a giant protein of 595 kDa, allowing it to protrude from the outer membrane and interact with the host cell, so did not fit the 50–100 kDa profile of our pro-viral factor. However, flagellin is approximately 50 kDa and polymerizes, but migrates through SDS gels as a monomer, which fits the profile (Smith et al., 2003).

4.4 Flagellin increases VSV-Gpp entry

Purified flagellin (phase I FliC) isolated from STm (Flores-Langarica et al., 2015) was assessed using the same pseudoparticle infection protocol developed for STm and CM. We observed an approximate two-fold increase in VSV-Gpp entry at all

Run 1	Accession	Description	Score	Coverage	# Proteins
1	Q9R4Q8	**Flagellin** OS=Salmonella typhimurium PE=4 SV=1 - [Q9R4Q8_SALTM]	224.45	71.60	23
2	P06179	**Flagellin** OS=Salmonella typhimurium (strain LT2 / SGSC1412 / ATCC 700720) GN=fliC PE=1 SV=4 - [FLIC_SALTY]	204.27	66.67	72
3	A0A023SY02	Membrane protein OS=Salmonella typhimurium GN=CY43_22240 PE=4 SV=1 - [A0A023SY02_SALTM]	155.47	7.90	39
4	T5JUR5	**Flagellin** (Fragment) OS=Salmonella enterica subsp. enterica serovar Typhimurium str. STm5 GN=B581_33465 PE=4 SV=1 - [T5JUR5_SALTM]	153.80	48.88	37
5	F2FXD3	Large repetitive protein OS=Salmonella enterica subsp. enterica serovar Gallinarum str. SG9 GN=SG9_4189 PE=4 SV=1 - [F2FXD3_SALGL]	125.68	6.89	11
6	P0A1D3	60 kDa chaperonin OS=Salmonella typhimurium (strain LT2 / SGSC1412 / ATCC 700720) GN=groL PE=3 SV=2 - [CH60_SALTY]	113.09	35.77	6
7	T5K407	Large repetitive protein (Fragment) OS=Salmonella enterica subsp. enterica serovar Typhimurium str. STm5 GN=B581_35875 PE=4 SV=1 - [T5K407_SALTM]	86.07	8.90	11
8	A0A038EFQ2	Capsid protein OS=Salmonella enterica subsp. enterica serovar Typhimurium str. 108402 GN=N936_24625 PE=4 SV=1 - [A0A038EFQ2_SALTM]	51.55	30.42	3
9	Q8HAA2	Sb36 OS=Salmonella phage ST64B GN=sb36 PE=4 SV=1 - [Q8HAA2_9CAUD]	41.74	39.64	6
10	F2FHV4	Enolase OS=Salmonella enterica subsp. enterica serovar Dublin str. SD3246 GN=eno PE=3 SV=1 - [F2FHV4_SALDU]	40.96	16.67	2
Run 2	**Accession**	**Description**	**Score**	**Coverage**	**# Proteins**
1	Q9R4Q7	**Flagellin** OS=Salmonella typhimurium PE=4 SV=1 - [Q9R4Q7_SALTM]	285.19	63.73	22
2	A0FLJ5	Phase I **flagellin** middle domain variant C174 OS=Salmonella typhimurium GN=fliC PE=4 SV=1 - [A0FLJ5_SALTM]	257.24	59.96	46
3	T5K278	**Flagellin** (Fragment) OS=Salmonella enterica subsp. enterica serovar Typhimurium str. STm3 GN=B573_24790 PE=4 SV=1 - [T5K278_SALTM]	193.96	37.08	32
4	A0A038EDW8	**Flagellin** (Fragment) OS=Salmonella enterica subsp. enterica serovar Typhimurium str. 108402 GN=N936_02335 PE=4 SV=1 - [A0A038EDW8_SALTM]	166.02	52.27	5
5	A0A023SY02	Membrane protein OS=Salmonella typhimurium GN=CY43_22240 PE=4 SV=1 - [A0A023SY02_SALTM]	132.33	7.38	37
6	F2FBE7	Phase-1 **flagellin** OS=Salmonella enterica subsp. enterica serovar Dublin str. SD3246 GN=SD3246_1252 PE=4 SV=1 - [F2FBE7_SALDU]	130.93	14.65	11
7	F2FIW3	Putative Ig domain protein OS=Salmonella enterica subsp. enterica serovar Dublin str. SD3246 GN=SD3246_4515 PE=4 SV=1 - [F2FIW3_SALDU]	117.63	6.62	21
8	A0A038EFQ2	Capsid protein OS=Salmonella enterica subsp. enterica serovar Typhimurium str. 108402 GN=N936_24625 PE=4 SV=1 - [A0A038EFQ2_SALTM]	73.45	31.42	3
9	P0A1D3	60 kDa chaperonin OS=Salmonella typhimurium (strain LT2 / SGSC1412 / ATCC 700720) GN=groL PE=3 SV=2 - [CH60_SALTY]	55.89	29.38	6
10	H8M1H4	Phosphoglycerate kinase OS=Salmonella enterica subsp. enterica serovar Typhimurium str. 798 GN=pgk PE=3 SV=1 - [H8M1H4_SALTM]	52.73	31.68	2

Table 4.2 **Flagellin is abundant in CM.**

The 10 most abundant proteins found in STm CM filtered through a 100 kDa molecular weight cut off column. The peptides present in CM were identified by semi-quantitative mass spectrometry and the Sequest algorithm was used to determine the score: as a measure of the quality of protein identification, coverage of each protein and the number of proteins detected. Proteins identified are ranked by score. Data from two independent runs are presented.

concentrations tested (left hand side; **Fig.4.6a**). The absence of a dose-dependent relationship prompted us to review the protocol, to identify the minimum dose of flagellin able to increase virus entry. Cells were incubated with flagellin for one hour, unbound flagellin removed and the cells infected with VSV-Gpp. We observed a dose-response relationship, as shown on the right hand side of **Fig.4.6a**, for which the maximum boost in viral entry was approximately 3.5-fold; equivalent to that of CM. However, as seen with CM (**Fig.4.2b**), there was no effect of flagellin on VSV-Gpp entry into Caco-2 cells (**Fig.4.6b**). These data highlight a new role for flagellin to increase lung epithelial cell permissivity to support virus infection.

4.5 Flagellin is the pro-viral factor in CM

To determine whether flagellin was the only pro-viral factor present in the CM, we used two methods. Firstly, we evaluated the effect of co-treating cells with CM and flagellin to identify whether they would be additive or synergistic. Using the CM and flagellin together at less than maximum doses achieved a comparable boost to either treatment alone, at their maximum dose, suggesting an additive mode of action consistent with both agents targeting the same pathway (**Fig.4.7a**). Secondly, we depleted flagellin from CM by affinity chromatography using a sepharose-anti-flagellin column (Bobat et al., 2011) and the flow-through collected and screened for its effect on VSV-Gpp infection. The pooled flow-through had a reduced effect on viral entry compared to untreated CM (**Fig.4.7b**). Together, these results point towards flagellin as the pro-viral factor in CM.

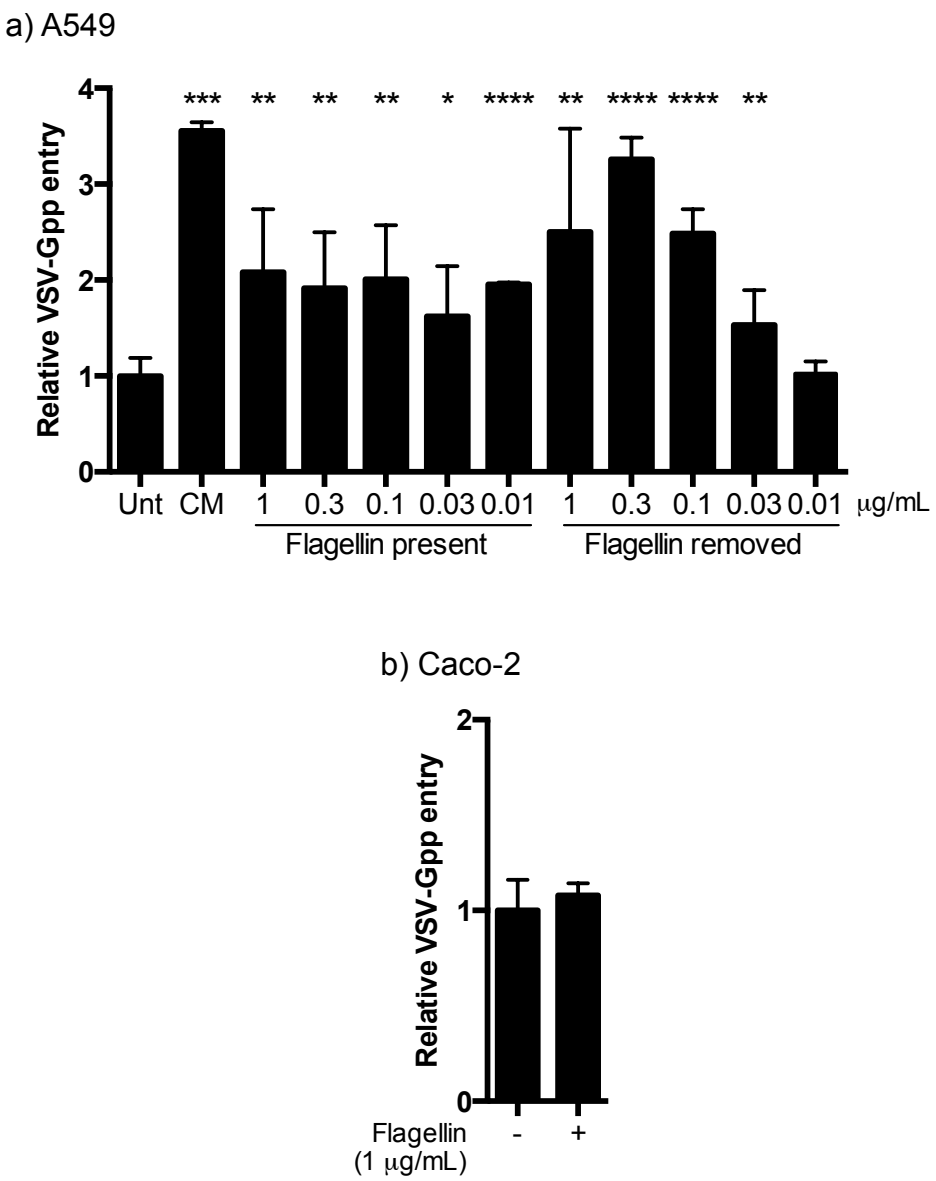

Figure 4.6 **Flagellin increases VSV-Gpp entry into A549 cells.**

a) A549 cells were treated with CM or flagellin, at indicated concentrations, for 1h and either VSV-Gpp was added on top of the treatment (left hand side) or the flagellin was removed and VSV-Gpp added (right hand side). Entry was quantified by luciferase assay at 48h. Data are presented as relative to VSV-Gpp entry into untreated cells. Representative of 3 biological replicates, error bars show SD of 3 technical replicates, statistical comparison to untreated by Unpaired t test: * = $P \leq 0.05$, ** = $P \leq 0.01$, *** = $P \leq 0.001$, **** = $P \leq 0.0001$. b) Caco-2 cells were treated with flagellin and VSV-Gpp added. Entry was quantified by luciferase assay at 48h. Data are presented as relative to VSV-Gpp entry into untreated cells. Representative of 2 biological replicates, error bars show SD of 3 technical replicates, statistical comparison by Unpaired t test was n.s. ($P > 0.05$).

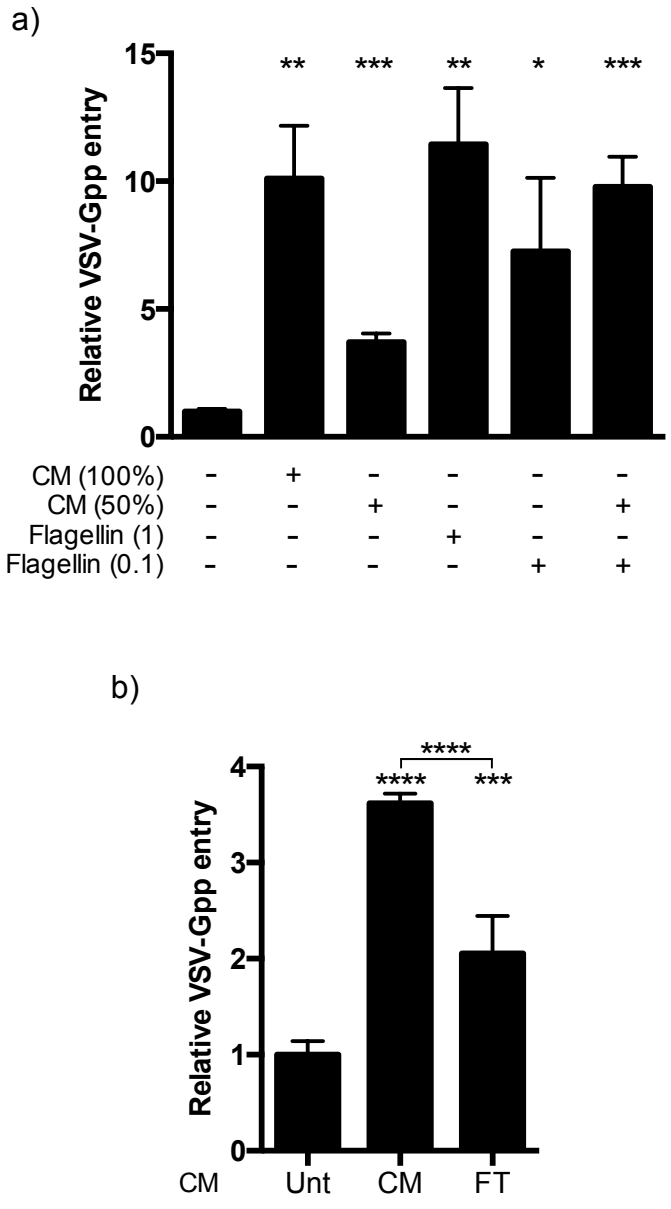

Figure 4.7 **Flagellin is the factor in CM.**

A549 cells were treated with; (a) CM at a dilution that gave a full or 50% boost in viral infection with or without flagellin at indicated concentrations (µg/mL); (b) untreated CM or pooled flow-through (FT) from affinity chromatography using an anti-flagellin monoclonal antibody to deplete flagellin; for 1h prior to VSV-Gp. Entry was quantified by luciferase assay at 48h. Data are presented as relative to VSV-Gpp entry into untreated cells. Representative of 3 biological replicates. Error bars show SD of 3 technical replicates, statistical comparison to untreated by Unpaired t test: n.s. = $P > 0.05$, * = $P \leq 0.05$, ** = $P \leq 0.01$, *** = $P \leq 0.001$, **** = $P \leq 0.0001$.

4.6 Variable epithelial responses to flagellin

One observation during these experiments was variability in the pro-viral activity of flagellin, STm or CM. To demonstrate this, **Fig.4.8** shows the results from every experiment using flagellin and VSV-Gpp, where each grey dot represents an infection value. While there was not always an increase in virus entry using 0.1 µg/mL flagellin, with 0.3-1 µg/mL flagellin we always observed a boost in infection and this could vary from two- to 14-fold. Since the same purified flagellin and VSV-Gpp preparations were used in aliquots stored at -80°C this result is likely to be attributable to variations in the epithelial cell response. We failed to observe an effect of flagellin on VSV-Gpp when using high passage A549 cells (data not shown) and used low passage cells for all experiments.

4.7 Aflagellate STm fails to modulate virus entry

STm encodes two flagellin genes that allow phase variation to avoid recognition by the host immune system (Yamamoto and Kutsukake, 2006). To determine whether flagellin is the sole factor secreted by bacterial cells to increase epithelial cell permissivity to viruses, an aflagellate STm mutant strain was produced. This *fliC*$^{-}$*fljB*$^{-}$ strain had minimal effect on VSV-Gpp entry into A549 cells; independent of whether the whole bacterium or CM was added (**Fig.4.9**). This result strengthens the findings in **Table 4.2** and **Fig.4.7** that flagellin is the pro-viral factor present in the CM and identifies flagellin as the causative agent for STm to potentiate virus entry.

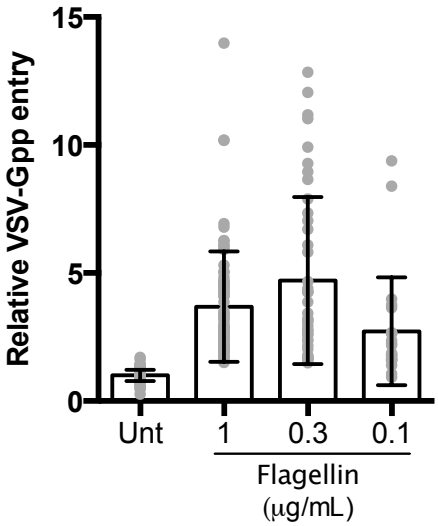

Figure 4.8 **Variable epithelial cell responses to flagellin.**

Collated results from all experiments performed exposing non-polarized A549 cells to the stated concentrations of STm flagellin and subsequent VSV-Gpp addition to determine virus entry at 48 hours by luciferase assay. Data are presented as relative to VSV-Gpp entry into untreated cells. Error bars show SD, statistical comparison by Unpaired t test was **** ($P \leq 0.0001$) for each flagellin-treated condition compared to untreated.

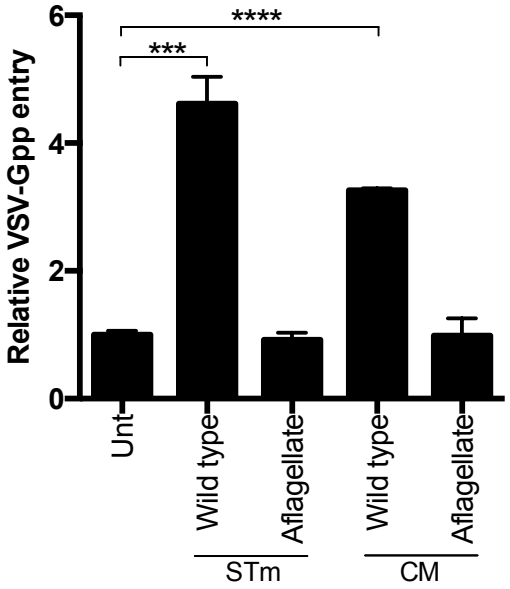

Figure 4.9 **Aflagellate STm fails to modulate VSV-Gpp entry.**

A549 cells were treated with wild type or *fliC*$^{-}$*fljB*$^{-}$ strains of STm (MOI 10), or CM produced from these strains, for 1h prior to VSV-Gpp addition. Entry was quantified by luciferase assay at 48h. Data are presented as relative to VSV-Gpp entry into untreated cells. Representative of 2 biological replicates, error bars show SD of 3 technical replicates, statistical comparison by Unpaired t test: *** = $P \leq 0.001$, **** = $P \leq 0.0001$.

4.8 Other species of bacteria can increase VSV-Gpp entry

Many species of bacteria express flagellin and we were interested to compare a panel of bacterial species, both Gram-negative and Gram-positive, to determine their effect on virus entry (**Table 4.3**). Interestingly, we found that all species of bacteria tested, except for *S. aureus*, increased VSV-Gpp infection of A549 and Caco-2 cells (**Fig.4.10a & c**). We also assessed CM from bacteria showing pro-viral activity and noted that CM from flagellated species increased virus entry (**Fig.4.10b**). As seen previously using STm (**Fig.3.7**), there was a greater pro-viral activity in A549 cells than Caco-2 cells, with the exception being *K. pneumoniae*. These results suggest that the pro-viral activity of STm is not a species-specific mechanism and flagellin is the major factor driving increased A549 cell permissivity to virus infection.

4.9 *P. aeruginosa* flagellin can increase virus entry

To determine whether flagellin from a different bacterial species could increase virus entry, we assessed the effect of *P. aeruginosa* and its flagellin on virus uptake. Comparison of wild type and aflagellate strains confirmed that *fliC* expression was necessary for *P. aeruginosa* to increase VSV-Gpp infection (**Fig.4.11a**). Furthermore, purified *P. aeruginosa* flagellin increased virus entry in a dose-responsive manner (**Fig.4.11b**), as seen with STm flagellin (**Fig.4.6a**). These data demonstrate that the effect of STm flagellin on VSV-Gpp entry is not bacterial species specific.

To determine whether flagellin from *P. aeruginosa* would also enhance entry of viruses other than VSV, A549 cells were pre-treated with flagellin and infected with influenza pseudoparticles. Influenza infection has previously been reported to

Bacterial species	Gram stain	Flagellum
B. subtilis	Positive	Yes
EP *E. coli*	Negative	Yes
K. pneumoniae	Negative	No
P. aeruginosa	Negative	Yes
STm	Negative	Yes
S. aureus	Positive	No

Table 4.3 **Characteristics of the bacterial species used in this study.**

The panel of bacteria assessed for pro-viral activity in this study contains both Gram negative and Gram positive species, with and without endogenous flagella.

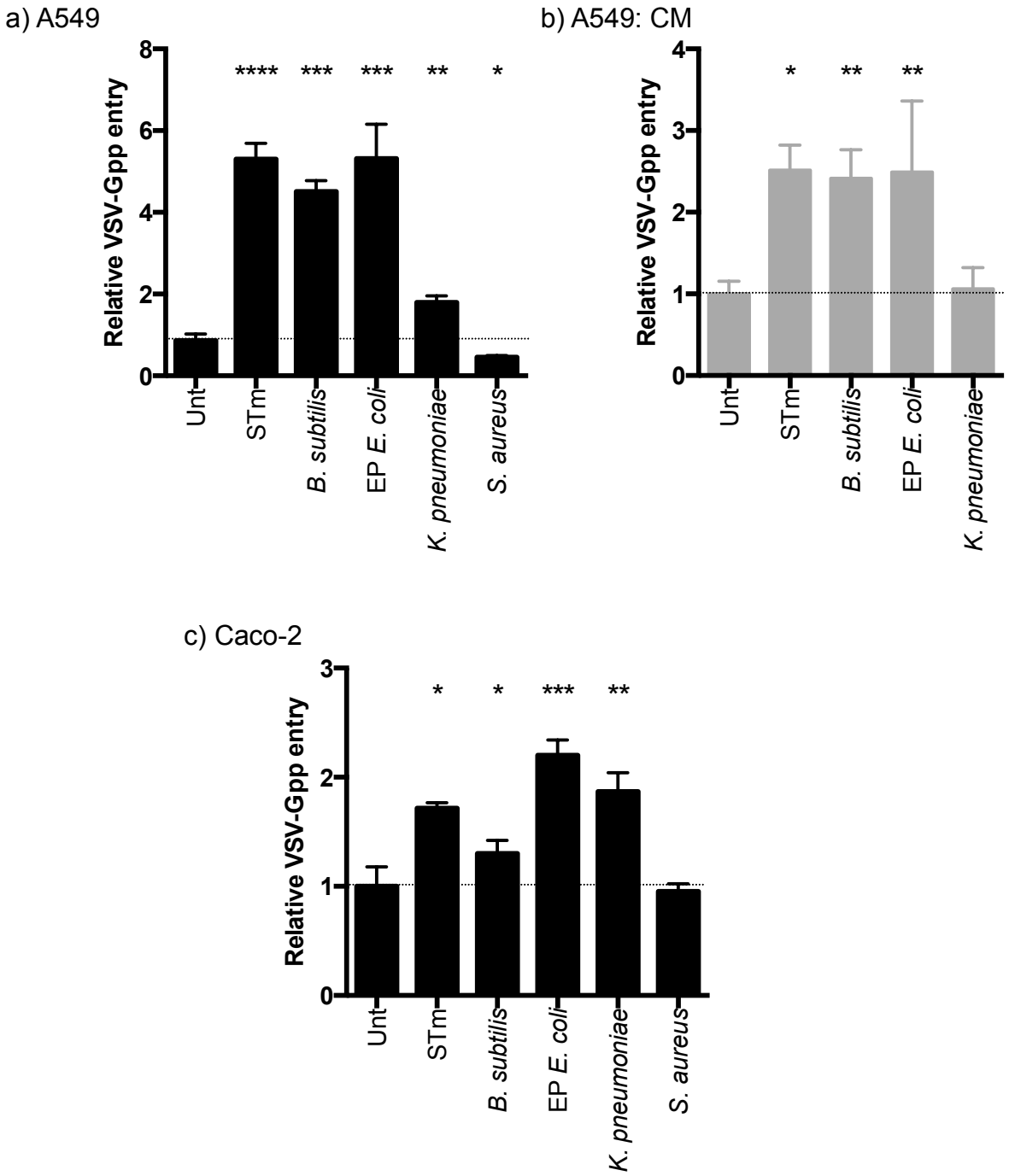

Figure 4.10 **Other species of bacteria can increase VSV-Gpp entry.**

(a) A549 or (c) Caco-2 cells were treated with the bacterial species stated (MOI 10) for 1h prior to VSV-Gpp and chloramphenicol addition. Entry was quantified by luciferase assay at 48h. Data are presented as relative to VSV-Gpp entry into untreated cells. b) A549 cells were treated with CM from bacteria species stated for 1h prior to VSV-Gpp addition. Entry was quantified by luciferase assay at 48h. Data are presented as relative to VSV-Gpp entry into untreated cells. Representative of 2 biological replicates, error bars show SD of 3 technical replicates, statistical comparison to untreated by Unpaired t test: * = $P \leq 0.05$, ** = $P \leq 0.01$, *** = $P \leq 0.001$, **** = $P \leq 0.0001$.

increase the chance of secondary bacterial infection, including *P. aeruginosa* (Renk et al., 2014; Lee et al., 2015). We report that the inverse of this relationship may also be true, as flagellin pre-treatment increased influenza entry (**Fig.4.11c**).

4.10 Polyclonal antibody to flagellin has a negligible effect on the pro-viral activity of flagellin

Flagellin elicits a humoral immune response in the host and anti-flagellin responses in serum are frequently used as a marker for bacterial translocation across the gut (Svärd et al., 2015). However, the role of anti-flagellin antibodies is unclear. While flagellin is an effective carrier antigen that increases the immune response to other antigens (Cunningham et al., 2004; Simon and Levine, 2012; Kim et al., 2015), antibody produced in response to flagellin does not necessarily control bacterial numbers (Bobat et al., 2011).

We were interested to know whether the presence of anti-flagellin antibodies would modulate the pro-viral activity of flagellin on epithelial cells. To assess this, serum samples from four STm FliC or mock immunized mice were pooled and heat inactivated. We confirmed the presence of anti-flagellin antibodies by ELISA (**Fig.4.12a**). Flagellin was incubated with the pooled sera for 30 minutes incubated with A549 cells for one hour prior to infecting with VSV-Gpp. Incubating flagellin with sera had minimal effects on its pro-viral activity (**Fig.4.12b**), despite the high level of anti-flagellin antibodies present.

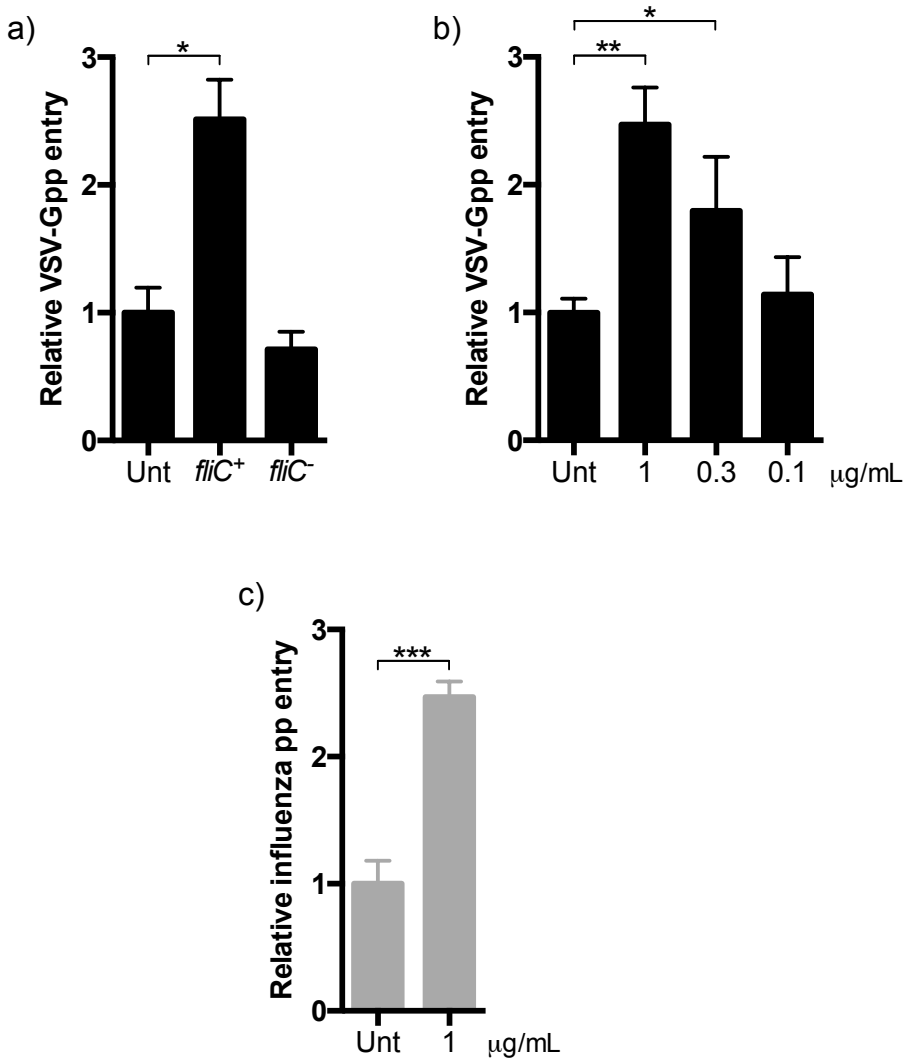

Figure 4.11 ***P. aeruginosa* flagellin is able to increase virus entry.**

A549 cells were treated with; (a) wild type or aflagellate *P. aeruginosa* strains (MOI 10) or (b) purified *P. aeruginosa* flagellin at indicated concentrations, for 1h prior to VSV-Gpp addition. Entry was quantified by luciferase assay at 48h. Data are presented as relative to VSV-Gpp entry into untreated cells. Representative of 3 biological replicates. c) A549 cells were treated with purified *P. aeruginosa* flagellin for one hour prior to influenza (H7N1) pseudoparticle addition. Entry was quantified by luciferase assay at 48h. Data are presented as relative to VSV-Gpp entry into untreated cells. Error bars show SD of 3 technical replicates, statistical comparison by Unpaired t test: * = $P \leq 0.05$, ** = $P \leq 0.01$, *** = $P \leq 0.001$.

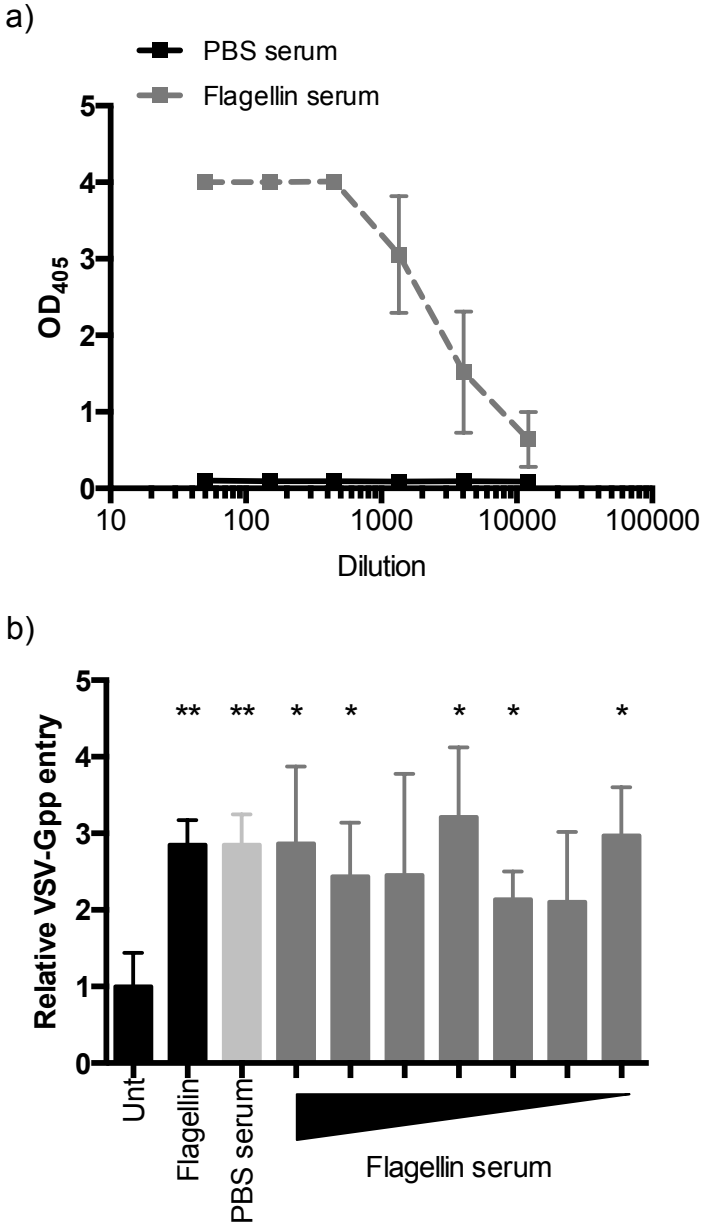

Figure 4.12 **The effect of flagellin is not blocked by antibody.**

a) Mouse sera from four PBS-immunized and four STm FliC-immunized mice were analyzed by ELISA using a flagellin coated plate and OD_{405} measured to determine the presence of anti-flagellin antibodies. Data produced by Dr. Adriana Flores-Langarica. b) Mouse serum samples were pooled, heat inactivated and incubated with flagellin (0.3 µg/mL) at 37°C for 30 min prior to treating A549 cells for 1h. VSV-Gpp was added and entry was quantified by luciferase assay at 48h. Data are presented as relative to VSV-Gpp entry into untreated cells. Representative of 3 biological replicates, error bars show SD of 3 technical replicates, statistical comparison to untreated by Unpaired t test: * = $P \leq 0.05$, ** = $P \leq 0.01$.

4.11 Discussion

We were interested to define the bacterial component facilitating STm-mediated increase in viral entry and whether this effect was mediated by STm-specific secreted factors. We demonstrate that flagellin secreted by STm (**Fig.4.6a**) and other bacterial species such as *P. aeruginosa* (**Fig.4.11**) increases epithelial cell permeability to virus infection (**Fig.4.13c**) and this activity is not perturbed by anti-flagellin antibodies (**Fig.4.12b**).

We found that neither CM nor flagellin alone was sufficient to increase virus entry into Caco-2 cells, but heat-killed STm potentiated infection (**Fig.3.20b**). It may be that more than one MAMP is necessary to prime a pro-inflammatory response in intestinal epithelial cells that can become tolerized through continuous bacterial exposure. Invasion of Caco-2 cells by STm, or uptake of heat-killed bacteria, may deliver flagellin to intracellular TLR5, where individual molecules may not be internalized. It would be interesting to test the effect of basolaterally-administered flagellin on virus entry, adding the virus to either apical or basolateral membranes.

The immunostimulatory potential of secreted flagellin in bacterially conditioned medium has been reported elsewhere. Two independent studies used similar techniques to identify flagellin as the secreted factor from *E. coli* and STm. Both studies report stability following heat treatment, a proteinaceous molecule around 50 kDa and minimal effect of aflagellate mutant strains (Gewirtz et al., 2001b; Schlee et al., 2007). Importantly, Gewirtz et al., 2001b, reported that their 50 kDa band purified by anion exchange column contained amino acid sequences from FliC and FljB,

suggesting that our STm CM may contain both isoforms. Strains deficient in either FliC or FljB induced IL-8 activity, however FljB expression was less stimulatory.

One method to establish whether that flagellin was the sole pro-viral component in CM was to evaluate their combined mode of activity: to assess whether they would interact additively or synergistically. If two treatments target the same pathway then their combined activity will equal the sum of their individual activities. Whereas if the treatments work synergistically, their combined activity will be greater than the sum due to activation of multiple pathways (Singh et al., 2000a). In our assay, a 50% dilution of CM gave a three-fold increase in virus entry and 0.1 µg/mL flagellin gave a seven-fold increase. Combined they reached 10-fold, indicating an additive interaction and that flagellin is most likely the pro-viral factor in CM (**Fig.4.7a**).

Interestingly, we observed a greater increase in viral entry when flagellin was added to A549 cells for a limited one hour period (**Fig.4.6a**). This could be due to negative feedback loops induced by flagellin stimulation. Flagellin signaling through TLR5 uses myeloid differentiation factor 88 (MyD88) to activate the NF-κB pathway, but also the mitogen-activated protein kinase (MAPK) pathway (Yu et al., 2003; McClure and Massari, 2014). Yu et al. (2006) reported that flagellin-induced IL-8 was increased when cells were treated with the phosphoinositide 3-kinase (PI3K) inhibitor, wortmannin, through increased MAPK signaling. This was verified using PI3K deficient mice, which displayed increased KC expression (the murine equivalent of IL-8) after flagellin treatment compared to wild type (Yu et al., 2006). Interestingly, the level of KC in mouse serum peaked at the first time point of collection, two hours,

and declined by six hours, which is comparable to the pattern of flagellin-induced pro-viral activity in our results (**Fig.3.16**). Prolonged expression of pro-inflammatory markers can be harmful to the host, leading to negative feedback mechanisms and this may explain why an excess of flagellin did not increase virus entry to comparable levels as a one hour exposure.

Focusing on the flagellated bacterial species and their pro-viral activity, we found that exposure of A549 cells to STm or *B. subtilis* bacteria or their CM increased virus entry (**Fig.4.10a-b**). Previous reports suggest that, when using the same concentration, STm flagellin can induce A549 cells to express higher levels of IL-8 than *B. subtilis* flagellin (Im et al., 2009). However, expression of monomeric flagellin by different bacterial species *in vitro* may vary, accounting for the comparable effect seen in our experiments. Furthermore, although the D0 (NAIP recognition) and D1 (TLR5 recognition) domains are highly conserved between species, the D2 and D3 regions can vary in sequence and glycosylation, which has been reported to affect their pro-inflammatory activity (Verma et al., 2005; Rossez et al., 2015).

E. coli and STm are the most closely related bacterial species tested, so it could be predicted that they would boost virus entry to comparable levels, as observed with A549 cells (**Fig.4.10a-b**). Flagellin from EP *E. coli* strains, as used in this study, has been reported to play a role in adherence to intestinal epithelial cells (Rossez et al., 2015), which may explain the increased pro-viral activity with EP *E. coli* compared to STm in Caco-2 cells (**Fig.4.10c**). Interestingly, using Caco-2 cells we observed a greater pro-viral effect with *K. pneumoniae* than *B. subtilis*, suggesting that there may

be more potentiation by Gram-negative bacteria than Gram-positive and minimal association for flagellate vs. aflagellate strains. Considering that the CM did not increase VSV-Gpp entry into Caco-2 cells, the effect of LPS or other factors was not tested. However, the concentration of LPS in CM was not measured and it may be informative to test LPS for pro-viral activity with Caco-2 cells. Additionally, there were no correlations between increased pro-viral activity using lung and gut pathogens on the cell type they would interact with in he host.

P. aeruginosa increased virus entry into A549 cells to a lesser extent than other flagellated bacteria (**Fig.4.11a**). However, purified *P. aeruginosa* flagellin showed comparable activity to STm flagellin (**Fig.4.11b**). This could be explained by variable expression of flagella by different bacterial species. STm, *B. subtilis* and EP *E. coli* are peritrichous, meaning they can be covered in multiple flagella, whereas *P. aeruginosa* has a single flagellum (Guttenplan et al., 2013; Pfaller et al., 2015). It is known that the TLR5 binding site is hidden by the structure of flagella, so monomeric units of flagellin are necessary for host cell recognition (Eaves-Pyles et al., 2001). To avoid this, *P. aeruginosa* has been reported to degrade the monomeric flagellin it produces. (Bardoel et al., 2011) found that an alkaline protease, AprA, secreted by bacteria could prevent TLR5-mediated signaling, when administered to cells with flagellin, by cleaving the free flagellin monomers. However, it did not cleave flagellin within flagellar structures. A second, similar mechanism using an elastase to degrade flagellin has also been found in *P. aeruginosa* (Casilag et al., 2016). The presence of this immune evasion mechanism may also explain why CM from *P. aeruginosa* had a minimal effect on virus entry in our experiments (data not shown). AprA-mutant *P.*

aeruginosa, and CM produced for their study, induced TLR5 signaling over 100-fold higher than wild type *P. aeruginosa* (Bardoel et al., 2011). It would be interesting to test the activity of this strain or its CM on virus entry.

While AprA-mutant *P. aeruginosa* could activate TLR5 signalling and promote virus entry, there are species of bacteria with flagellin that is not detected by TLR5: *H. pylori* and *Campylobacter jejuni*. These species still require flagellar motion for pathogenesis, but they can evade TLR5-mediated immune responses. This is achieved by alterations in a seven amino acid stretch of the D1 domain containing the area facilitating TLR5 recognition (Andersen-Nissen et al., 2005). Testing these flagellin monomers would determine whether the pro-viral effect requires TLR5 or can be mediated by NAIP signaling or a novel mechanism. Interestingly, the authors note that altering this region in STm FliC to prevent TLR5 activation reduced bacterial motility and compensatory mutations were necessary to restore polymerization.

The role of flagellin-specific antibodies during STm infection is unclear. We report that polyclonal flagellin-specific sera had a negligible effect on flagellin pro-viral activity. This could be due to anti-FliC antibody recognizing the external domains of flagellin that are exposed when flagella are formed (Salazar-Gonzalez and McSorley, 2005), therefore unable to block the TLR5 and NAIP recognition domains that are only accessible on monomers (**Fig.4.1b**). These results suggest that the effect of flagellin on host cell permissivity may be effective in environments that are naïve or pre-exposed to flagellated bacteria.

4.12 Summary

In this chapter we have identified the pro-viral factor secreted by STm that increases lung epithelial cell permissivity to virus entry as flagellin. Furthermore this effect is not specific to STm, *Pseudomonas aeruginosa* flagellin increased influenza pseudoparticle entry. *Pseudomonas aeruginosa* colonization has been highlighted as a risk factor for increased susceptibility to influenza infection in individuals with CF (Renk et al., 2014). Our next aim was to determine the mechanism of flagellin activity.

5. DISSECTING THE PRO-VIRAL ACTIVITY OF FLAGELLIN AT A CELLULAR LEVEL

5.1 Introduction

In the previous chapter, we identified that bacterially encoded flagellin can increase virus entry into lung epithelial cells. Flagellin is abundantly expressed by a wide variety of bacterial species, making it a prominent target for recognition by host cells (Zhao and Shao, 2015). Extracellular flagellin can be bound by TLR5, leading to MyD88-dependent activation of NF-κB and AP-1, to induce cytokine, chemokine and IFN expression (**Fig.5.1**). This pro-inflammatory response recruits immune cells to sites of bacterial colonization to aid immune clearance (McClure and Massari, 2014). Flagellin is also detected by the NAIP/Nlrc4-inflammasome in the cytosol (**Fig.5.2**; (Khameneh and Mortellaro, 2014), which leads to caspase-dependent IL-1β production and cell death (Zhao and Shao, 2015).

Flagellated bacteria in the lung have been reported to promote pulmonary fibrosis. (Kondo et al., 2012), found that flagellin increased NF-κB activity in A549 cells in a dose-responsive manner and the activity peaked between four and eight hours. The mechanism was reported to be via TLR5, based on the addition of purified flagellin extracellularly. In contrast, detection of flagellin by NAIP requires intact bacterial cells and can lead to host cell death (Sun et al., 2007). We therefore hypothesized that flagellin binding to TLR5 and signaling through NF-κB facilitated pro-viral activity.

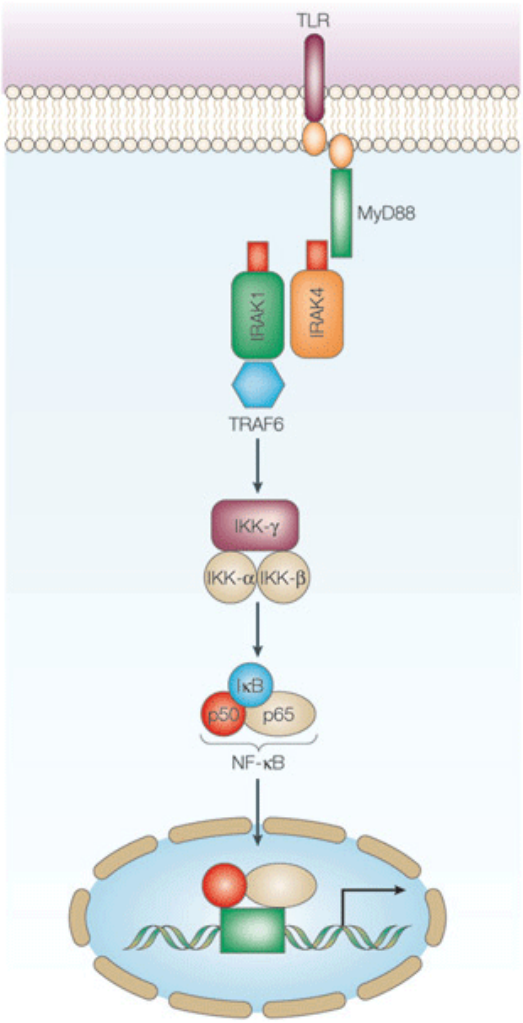

Figure 5.1 **TLR signaling activates NF-κB.**

From (Miller et al., 2005) Host cells can detect microbe associated molecular patterns (MAMP) through toll-like receptors (TLR). These are membrane-spanning proteins that, upon binding a ligand, recruit sequentially MyD88, interleukin-1 receptor-associated kinase (IRAK) 1 and 4 and TNF-receptor-associated factor (TRAF) 6. This leads to phosphorylation of the IκB kinase (IKK) complex, which phosphorylates IκB. IκB phosphorylation releases it from the NF-κB subunits p50 and p65, allowing them to translocate to the nucleus and act as a transcription factor for a wide range of genes that regulate the immune response.

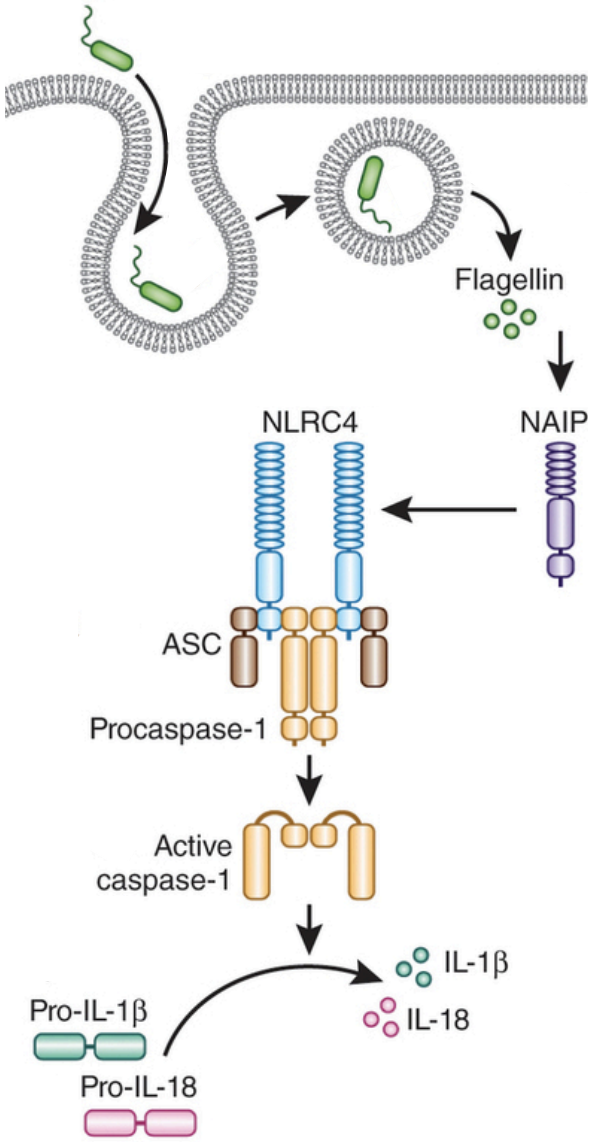

Figure 5.2 **NAIP/Nlrc4-inflammasome activation by flagellin.**

Adapted from (Khameneh and Mortellaro, 2014) Flagellated bacteria that enter host cells and secrete flagellin into the cytoplasm can be detected by NLR apoptosis-inhibitory protein (NAIP). NAIP interacts with NOD-like receptor (NLR)C4 and ASC to form an inflammasome that activates caspase-1. Caspase-1 converts pro-interleukins (IL)-1β and -18 into cytokines IL-1β and IL-18, inducing an inflammatory response.

H. influenzae can potentiate rhinovirus infection of primary airway epithelial cells by increasing their cell surface expression of ICAM-1, enabling more virus to attach to the host cell (Sajjan et al., 2006). One route for flagellin to increase the entry of VSV, influenza, MeV, Ebola and Lassa is by upregulating host cell receptors. However, given the diversity of receptors used by these different viral glycoproteins (**Table 3.1**), this seems unlikely. Moreover, the observation that STm promotes MeV entry into A549 cells engineered to overexpress the viral receptor SLAMF1 (**Fig.3.12**) suggests that receptor modulation is an unlikely explanation for the pro-viral activity.

To increase the entry of viruses using different pathways, flagellin may be potentiating multiple host cell processes and altering each virus pathway independently, or inducing diverse virus entry through the upregulation of one pathway. This could help all viruses to gain access into the host cell. For example, most cell types express heparin sulphate proteoglycans (HSPGs) that contain long polysaccharide chains, these bind viruses through electrostatic interactions and aid virus entry (Bishop et al., 2007). The upregulation of HSPGs on host cell membranes could augment virus entry using a variety of pathways (Zhang et al., 2016). Interestingly, influenza can enter cells via clathrin-dependent and independent pathways, and this can vary by cell type (Edinger et al., 2014). Conversely, an IFN-stimulated gene has been identified, called ADAP2, that encodes a protein to restrict virus entry, including VSV, by altering the entry pathway to macropinocytosis and likely facilitating degradation of the particles (Shu et al., 2015). This suggests that innate immune signaling can modulate virus entry pathways. In this chapter, we will

design experiments to examine the mechanism underlying the pro-viral activity of flagellin.

5.2 Lentiviral pseudoparticles do not directly bind flagellin

Although LPS had a modest ability to increase virus entry in this model system, it is known to bind to poliovirus particles, which can augment virus attachment to host cells (Robinson et al., 2014). LPS has also been reported to enhance transmission of MMTV *in vivo* by binding to virus particles (Wilks et al., 2015). It was important to determine whether flagellin increases pseudoparticle entry by direct binding to the viral particle.

The recombinant STm flagellin used in these experiments contains a poly-histidine tag, to facilitate affinity purification using a nickel column (Bobat et al., 2011). VSVpp or NEpp were incubated with flagellin for one hour at 37°C, mixed with Ni-NTA agarose beads for one hour and allowed to settle in a column. The flow through was collected and the beads washed with PBS to remove unbound virus. Flagellin was then eluted using imidazole and the eluates collected to quantify viral particles.

Lentiviral pseudoparticles were quantified using the PERT assay (**Fig.5.3**); which detects particle associated RTase that generates cDNA from exogenous, synthetic MS2 RNA (Pizzato et al., 2009; Vermeire et al., 2012). Although viral particles were eluted from the nickel beads by imidazole, we observed comparable levels of VSV or NE particles independent of pre-incubating with flagellin (**Fig.5.4a-b**). This result suggests that the pro-viral activity of flagellin is not mediated through direct association with virus particles, but through interactions with the epithelial cell or via a ternary complex with virus and cells.

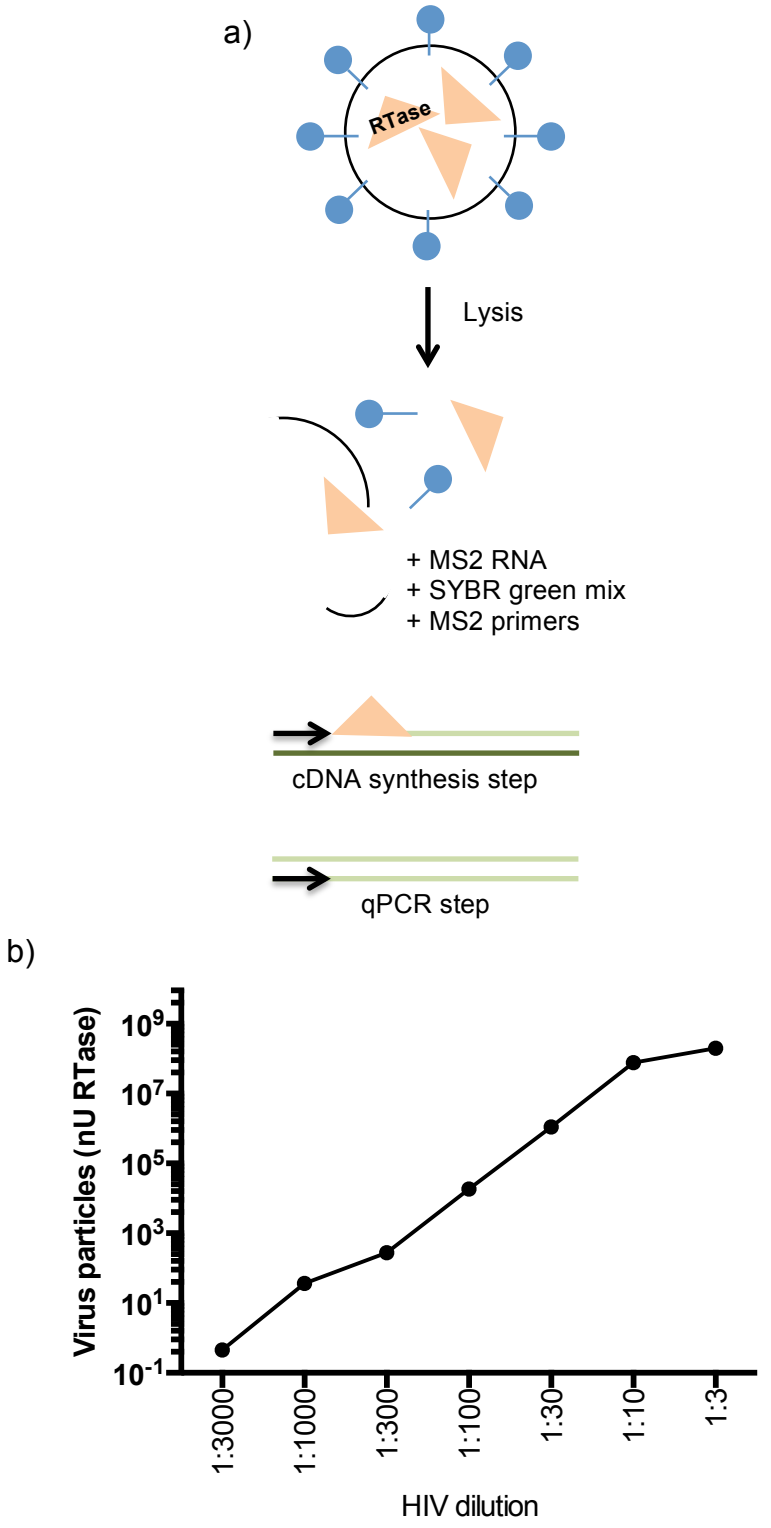

Figure 5.3 **Detection of virus particles by PERT assay.**

Figure 5.3 **cont.**

a) Schematic diagram of the product enhanced reverse transcriptase (PERT) assay used to detect reverse transcriptase (RTase) in virus particles. Following lysis of the particles, reagents are added to facilitate RTase-dependent generation of cDNA, which can be quantified by PCR. A standard curve can be produced using a 10-fold dilution series of recombinant HIV-1 RTase to determine units of RTase (Vermeire et al., 2012). b) A serial dilution of HIV-1 assessed by PERT assay. Data presented are viral particles as determined by units of RTase.

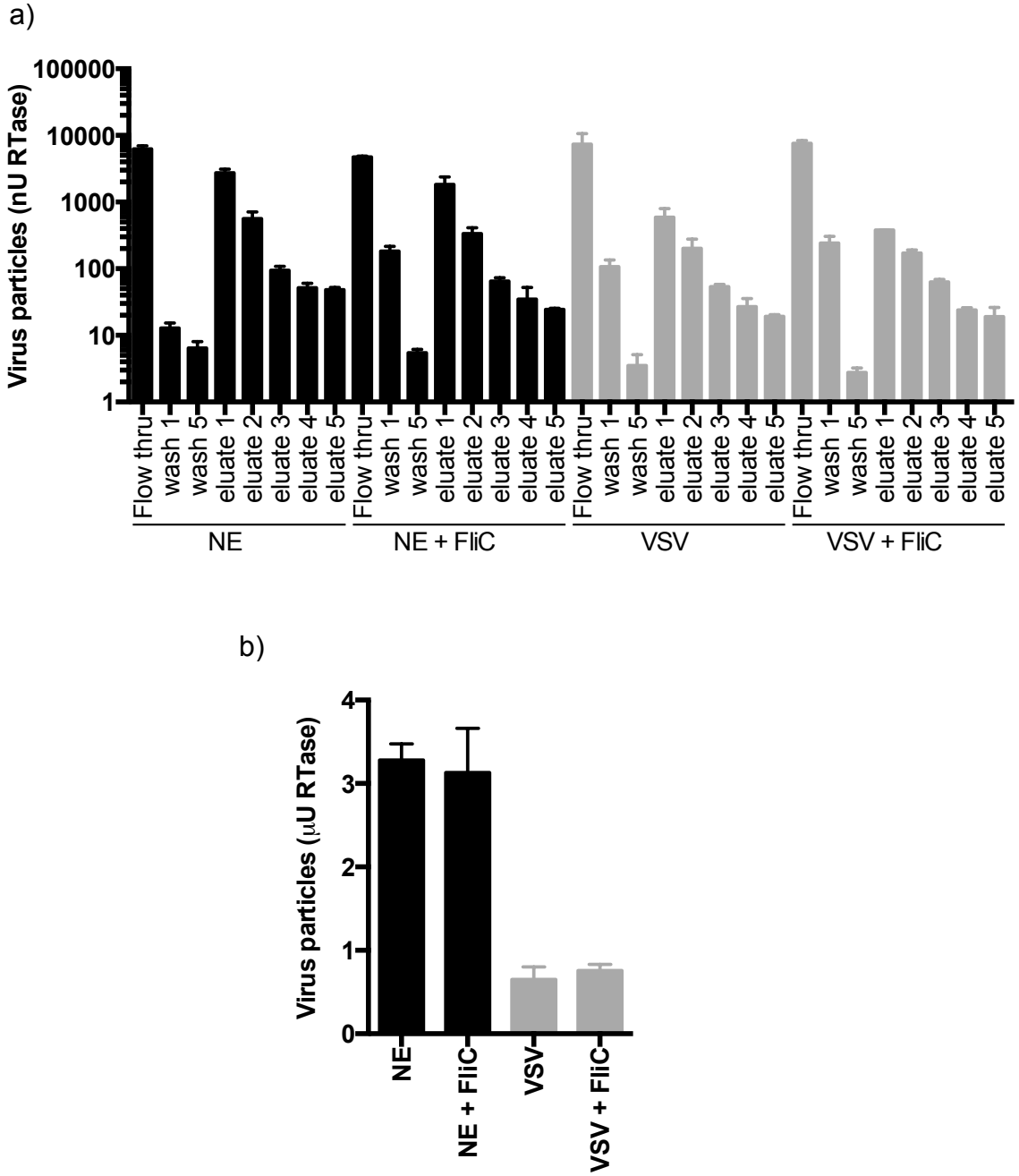

Figure 5.4 **Pseudoparticles do not directly bind flagellin.**

a) Pseudoparticles were incubated with 0.3 μg/mL STm flagellin at 37°C for 1h prior to addition of Ni-NTA agarose beads for 1h at room temperature on a rotary mixer. The beads were loaded onto a column, flow through was collected and the beads were washed 5x with PBS. Flagellin was eluted by washing 5x with PBS containing 100mM imidazole. Viral particles in all fractions were quantified by PERT assay. Data presented are viral particles as determined by units of RTase. b) The total number of viral particles eluted for each condition in (a). Representative of 2 biological replicates, error bars show SEM of 2-4 technical replicates, statistical comparison by Unpaired t test was n.s. ($P > 0.05$).

5.3 Flagellin does not modulate viral attachment to cells

Since many of the viral pseudotypes we have studied can engage HSPGs as the first step in low affinity attachment we investigated the effect of flagellin on pseudoparticle attachment. Virus internalization can be prevented by cooling the cells to 4°C, which renders endocytosis or membrane fusion ineffective (Guyader et al., 2002).

The PERT assay was used to assess the binding of VSV-Gpp at 4°C compared to 37°C in the presence of flagellin. At 4°C, flagellin treatment had a modest effect on the number of bound virus particles, but it significantly increased the number of virus particles present in cells infected at 37°C **(Fig.5.5**). These data suggest that the pro-viral activity of flagellin occurs after virus binding. To further examine this, the effect of flagellin treatment one hour prior to VSV-Gpp addition was compared to flagellin treatment one hour after VSV-Gpp addition at 4°C, with a washing step to remove any unbound virus particles. Although there was decreased virus entry at 4°C compared to 37°C, the effect of flagellin was comparable whether added before or after the virus (left-hand side; **Fig.5.6**). That the pro-viral activity of flagellin still occurs after virus binding has taken place suggests that this effect happens at a later step in the virus entry pathway.

To assess internalization, we compared the effect of flagellin added before or after virus infection at 37°C. Again, the effect of flagellin was comparable whether added before or after virus pseudoparticles (right-hand side; **Fig.5.6**), suggesting that flagellin does not increase internalization but acts at a later stage of entry. Interestingly, the boost in virus entry with flagellin treatment was around five-fold at

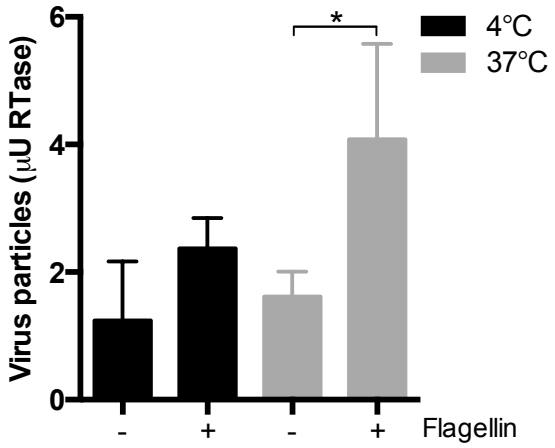

Figure 5.5 **Flagellin increases virus internalization at 37°C.**

Flagellin (0.3 µg/mL; removed after 1h) was added to non-polarized A549 cells before VSV-Gpp was added for 1h at 4°C or 37°C and the cells were lysed for quantification by PERT assay. Data presented are viral particles as determined by units of RTase, with background RTase activity in untreated cells removed. Representative of 2 biological replicates, error bars show SD of 4 technical replicates, statistical comparison by Unpaired t test: * = P ≤ 0.05, ** = P ≤ 0.01.

a)

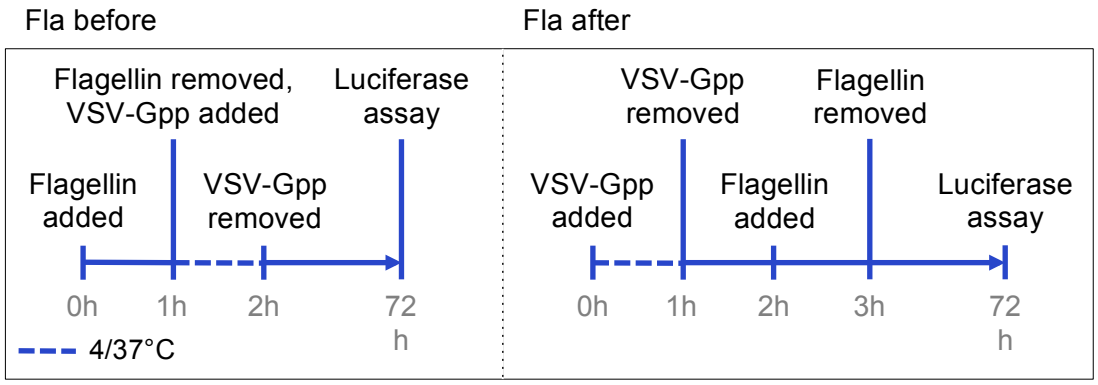

b)

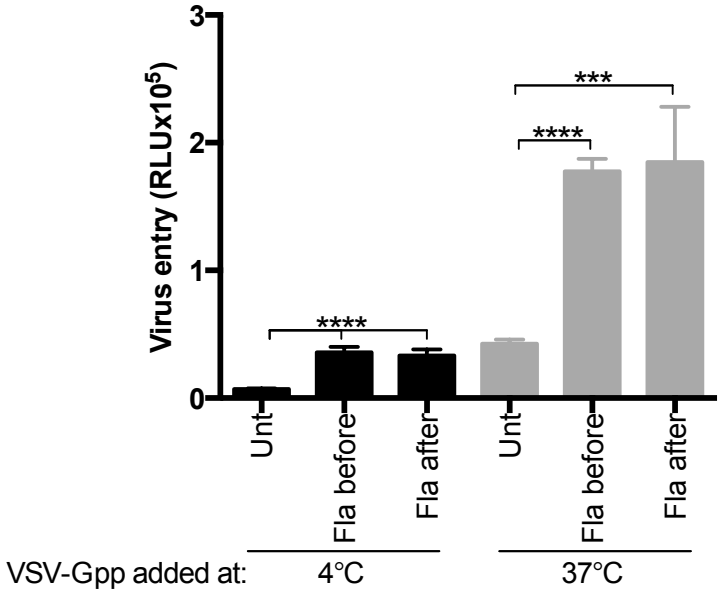

Figure 5.6 **The pro-viral activity of flagellin is post-binding.**

a) Schematic diagram of experimental setup showing timing of flagellin (fla) addition, VSV-Gpp addition and epithelial cell lysis to determine pseudoparticle entry by measuring luciferase activity. b) Flagellin (0.3 µg/mL) was added to non-polarized A549 cells 1h before or immediately after VSV-Gpp was added for 1h at 4°C or 37°C and the cells were washed 3x with DMEM to remove unbound virus. Entry was quantified by luciferase assay at 72h. Data are presented as relative luciferase units (RLU). Representative of 2 biological replicates, error bars show SD of 4 technical replicates, statistical comparison by Unpaired t test: *** = P ≤ 0.001, **** = P ≤ 0.0001.

both temperatures. Together, these data indicate that the pro-viral activity of flagellin occurs after virus binding and may be post-internalization.

5.4 Inhibition of common virus entry pathways

STm had a pro-viral effect on a wide range of virus entry pathways (**Fig.3.12**). We were interested to determine whether flagellin altered the route of virus internalization and evaluated a well-characterized panel of inhibitors that target actin polymerization, clathrin-mediated endocytosis and macropinocytosis. A549 cells were pre-treated with each drug for 30 min prior to incubating with flagellin for one hour and infecting with VSV-Gpp for a defined period of one hour. All of the treatments reduced untreated VSV-Gpp entry and bafilomycin A1 prevented infection (**Fig.5.7a**), consistent with reports that VSV infects cells via clathrin-mediated endocytosis. Importantly, flagellin treatment still boosted virus infection of drug-treated cells over to comparable levels as untreated virus, with the exception of the actin inhibitor, jasplakinolide (**Fig.5.7b**). As a control to examine the potential off-target effects of the inhibitors to modify flagellin signaling, we measured IL-8 expression at 48 hours. We noted a significant reduction in IL-8 expression following jasplakinolide treatment (**Fig.5.7c**), suggesting that this drug may affect IL-8 secretion or reduce NF-κB activation, rather than specifically affecting virus entry. None of the other treatments had any significant effect on flagellin-boosted VSV-Gpp entry or IL-8 secretion.

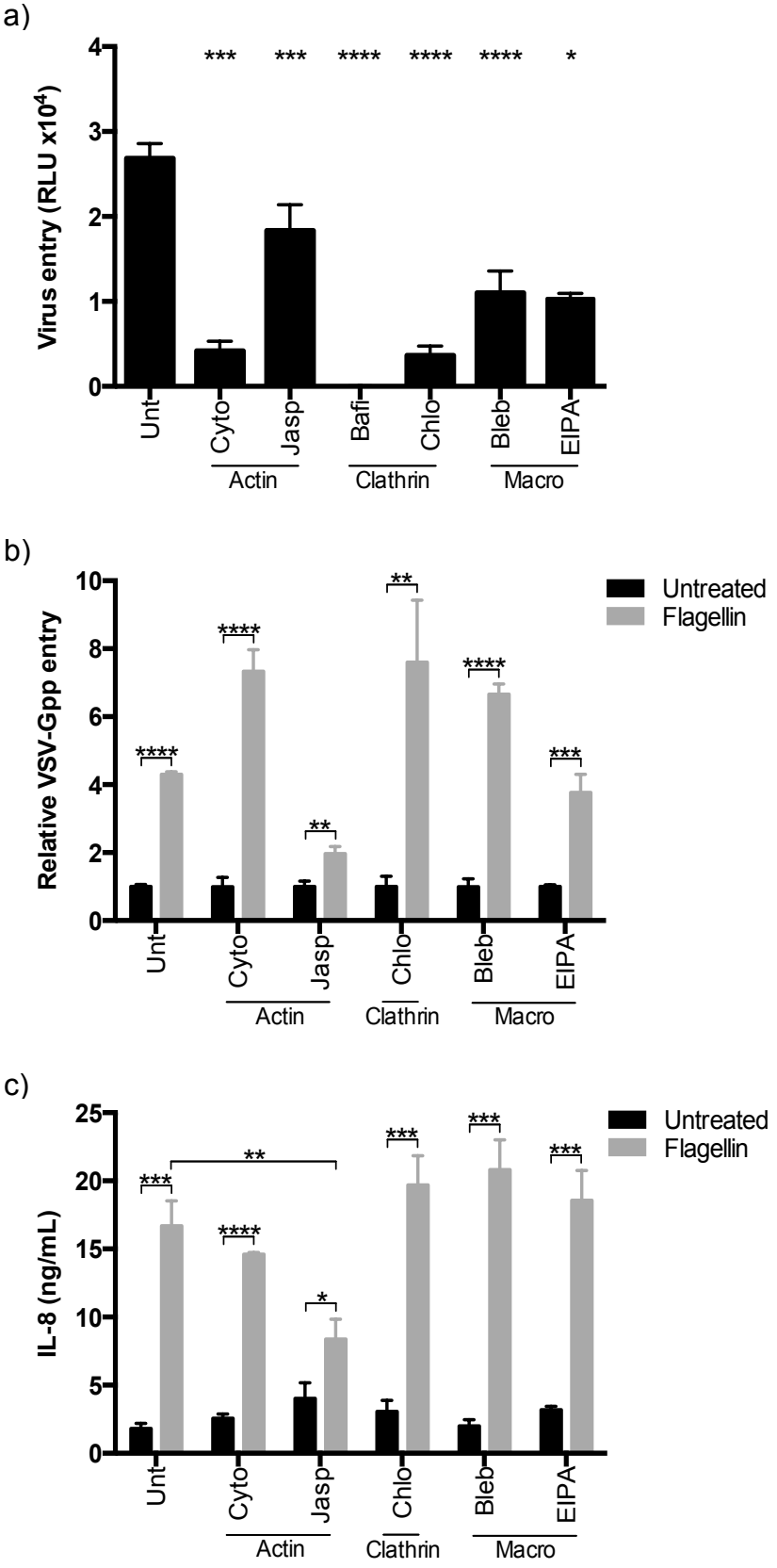

Figure 5.7 **The effect of cell entry inhibitors.**

Figure 5.7 **cont.**

Non-polarized A549 cells were treated with inhibitors as stated for 30 minutes, for concentrations see methods. a) VSV-Gpp was added and entry was quantified by luciferase assay at 48h. Data are presented as relative luciferase units (RLU). b) Flagellin (0.3 µg/mL; removed prior to virus addition) was added for one hour prior to VSV-Gpp. Entry was quantified by luciferase assay at 48h. Data are presented as relative to VSV-Gpp entry into inhibitor treated cells without flagellin stimulation. c) Supernatant from (b) was collected at 48h to measure IL-8 secretion by ELISA. Error bars show SD of 3 technical replicates, statistical comparison by Unpaired t test: * = $P \leq 0.05$, ** = $P \leq 0.01$, *** = $P \leq 0.001$, **** = $P \leq 0.0001$.

5.5 Flagellin does not affect clathrin-mediated endocytic uptake of transferrin

To investigate further whether flagellin increased the cellular uptake of ligands that utilize the clathrin-mediated endocytic pathway, we tested the well-characterized ligand transferrin. A549 cells were pre-treated with flagellin and incubated at 37°C with fluorescently labeled transferrin, which binds the transferrin receptor and is the archetypal cargo for clathrin-mediated endocytosis (Le Roy and Wrana, 2005). Cells were fixed at defined time points and uptake assessed by flow cytometry. As a control, cells were incubated at 4°C to determine background levels of transferrin binding to the host cell, since ligand uptake is temperature-dependent. To confirm that fluorescence detected after incubation at 37°C was due to intracellular transferrin; cells were fixed and co-stained for the plasma membrane located protein CD81 (**Fig.5.8a**), demonstrating intracellular transferrin localization.

Representative flow cytometry plots are shown in **Fig.5.8b** and the kinetic results are collated in **Fig.5.8c**. While the background fluorescence at 4°C did not change over time, there was a peak in transferrin uptake at 15 minutes, which slowly declined. Treatment with flagellin did not affect either binding at 4°C or its uptake at 37°C (**Fig.5.8c**). These results, together with the result using an inhibitor of clathrin-mediated endocytosis, chloroquine (**Fig.5.7b**), suggest that flagellin does not modulate this uptake pathway.

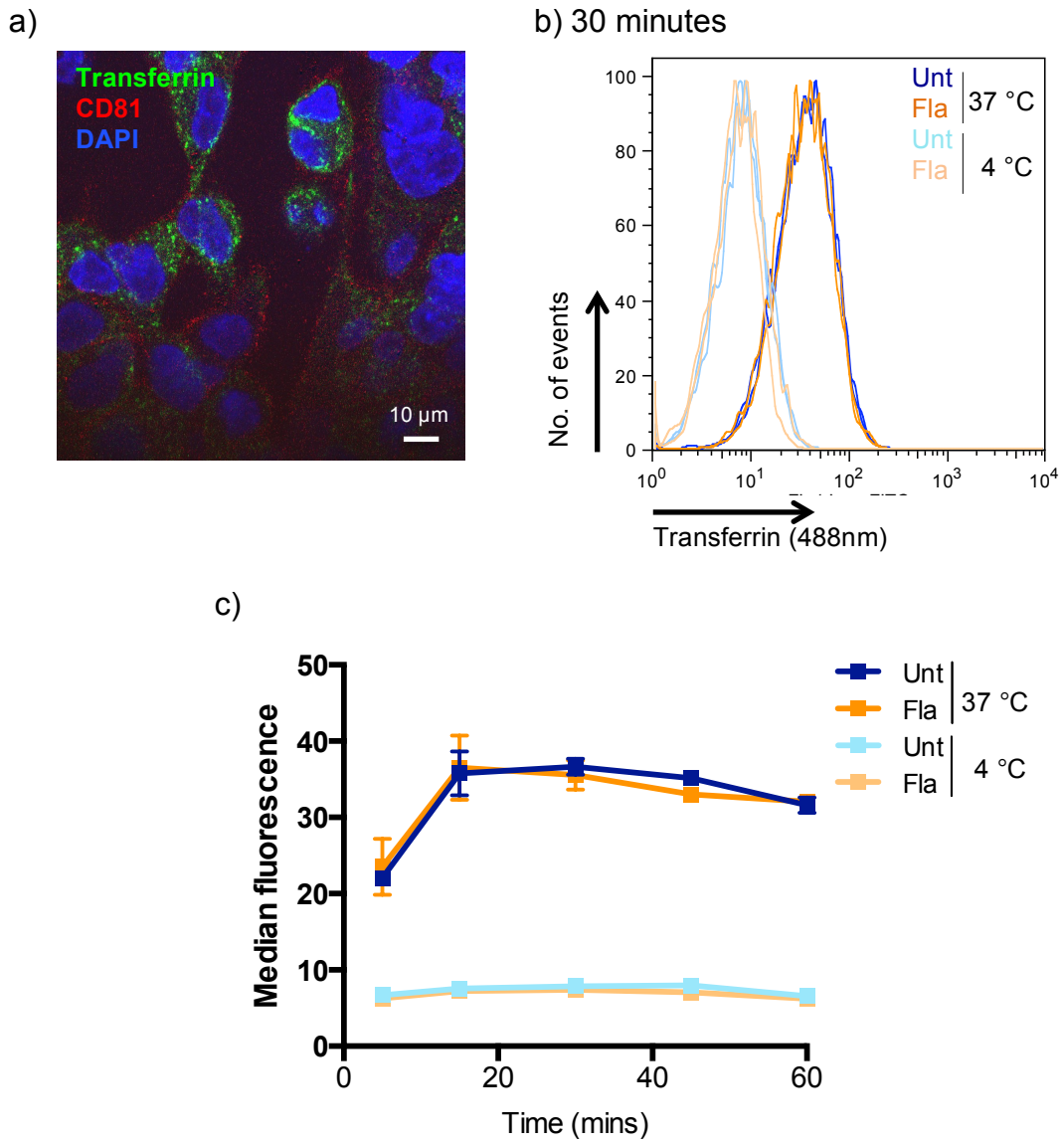

Figure 5.8 **Flagellin does not have an effect on clathrin-mediated endocytosis.**

a) Non-polarized A549 cells were grown on coverslips, incubated with transferrin Alexa Fluor 488 (Tf; 10 µg/mL) for 1h and fixed to visualise CD81 by immunofluorescence; nuclei were stained with DAPI. Cells were imaged using a Zeiss 510 Meta confocal microscope with 10x objective and LSM software. Scale bar indicates 10 µm. (b) and (c) Non-polarized A549 cells were treated with flagellin (1 µg/mL; removed prior to Tf addition) for 1h prior to Tf addition and incubated at 37°C or 4°C. Cells were fixed at stated time points and analyzed by flow cytometry. The results are gated on live cells and presented as intensity of fluorescent Tf uptake versus number of events (% of max), or median fluorescence of the population over time. Representative of 3 biological replicates, error bars show SD of 2 technical replicates.

5.6 Flagellin does not affect macropinocytic uptake

Macropinocytosis, also known as ‘cell drinking’, is a ligand-induced process allowing non-specific uptake of extracellular fluid and has emerged as another pathway for virus entry (Mercer and Helenius, 2012). Although the inhibitors blebbistatin and EIPA were unable to prevent the pro-viral effect of flagellin (**Fig.5.7b**), we assessed the effect of flagellin in a functional macropinocytosis assay using fluorescently labeled dextran and flow cytometry. To ensure that the fluorescence detected was intracellular and not bound on the surface of the cell, a bleach buffer that quenches extracellular fluorescence was used, as previously described (Aleksandrowicz et al., 2011), and CD81 co-staining confirmed this (**Fig.5.9a**).

Representative flow cytometry plots are shown in **Fig.5.9b** and the results collated in **Fig.5.9c**. PMA was used as a positive control to induce macropinocytosis (Aleksandrowicz et al., 2011). While PMA showed a steady increase in the uptake of the fluorescent dextran, there was no change following flagellin treatment (**Fig.5.9c**), confirming the results seen previously with inhibitors of macropinocytosis that this is not the mechanism for increased virus entry.

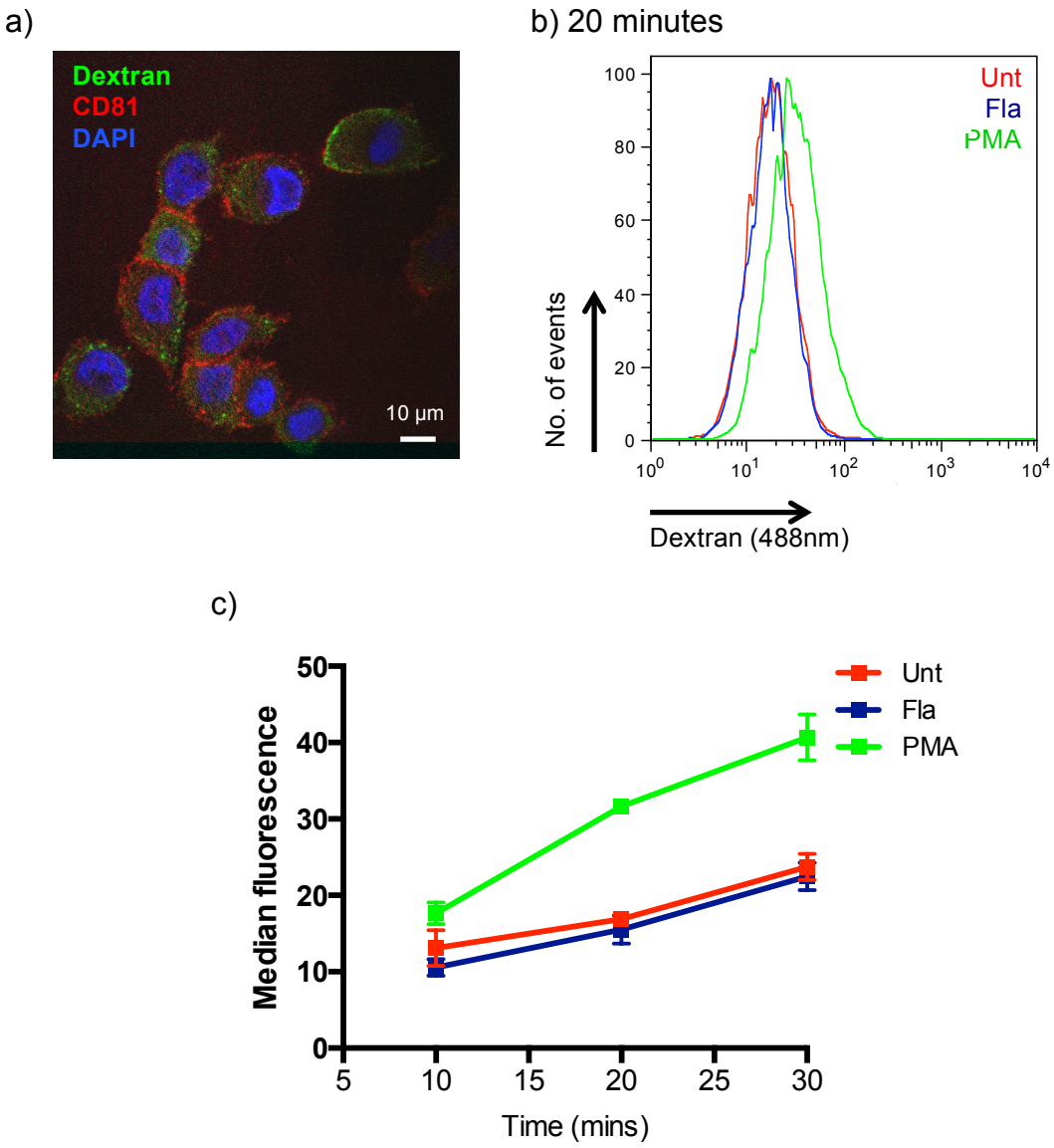

Figure 5.9 **Flagellin does not have an effect on macropinocytosis.**

a) Non-polarized A549 cells were grown on coverslips, incubated with Oregon green 10 kDa dextran (100 µg/mL) for 1h and fixed to visualise CD81 by immunofluorescence; nuclei were stained with DAPI. Cells were imaged using a Zeiss 510 Meta confocal microscope with 10x objective and LSM software. Scale bar indicates 10 µm. (b) and (c) Non-polarized A549 cells were treated with flagellin (1 µg/mL; removed prior to dextran addition) for 1h prior to dextran addition and incubated at 37°C. Cells were washed with bleach buffer, fixed at stated time points and analyzed by flow cytometry. The results are gated on live cells and presented as intensity of fluorescent dextran uptake versus number of events (% of max), or median fluorescence of the population over time. Representative of 3 biological replicates, error bars show SD of 3 technical replicates.

5.7 The pro-viral activity of flagellin is NF-κB dependent

To determine whether NF-κB activation contributes to the effect of flagellin on virus entry, we evaluated a small molecule inhibitor MLN4924. MLN4924 was designed as an anti-cancer treatment and has been reported to inhibit the RelA (p65) component of NF-κB translocating to the nucleus, thereby preventing activation (Milhollen et al., 2010). This compound was reported to inhibit LPS-induced cytokine secretion by macrophages (Chang et al., 2012). Of note, MLN4924 was recently reported to have a negligible effect on VSV infection of HeLa epithelial cells, in line with our results (Song et al., 2016).

Initially, we determined the concentration of MLN4924 required to prevent STm activation of NF-κB using the pConA reporter plasmid. This plasmid contains a luciferase reporter under the control of multiple NF-κB binding sites. STm induced a six-fold increase in NF-κB activity that was reduced by pretreating the cells with MLN4924 in a dose-dependent manner (**Fig.5.10a**).

We assessed the effect of pre-treating cells with MLN4924 on STm, CM or flagellin priming of VSV-Gpp infection, as previously described. The drug was present throughout. This protocol blocked the effect of bacteria or secreted flagellin on virus entry (**Fig.5.10b**). We measured IL-8 expression using the supernatant from this experiment, demonstrating that MLN4924 significantly decreased the amount of IL-8 released after STm stimulation (**Fig.5.10c**). Together these results identify NF-κB

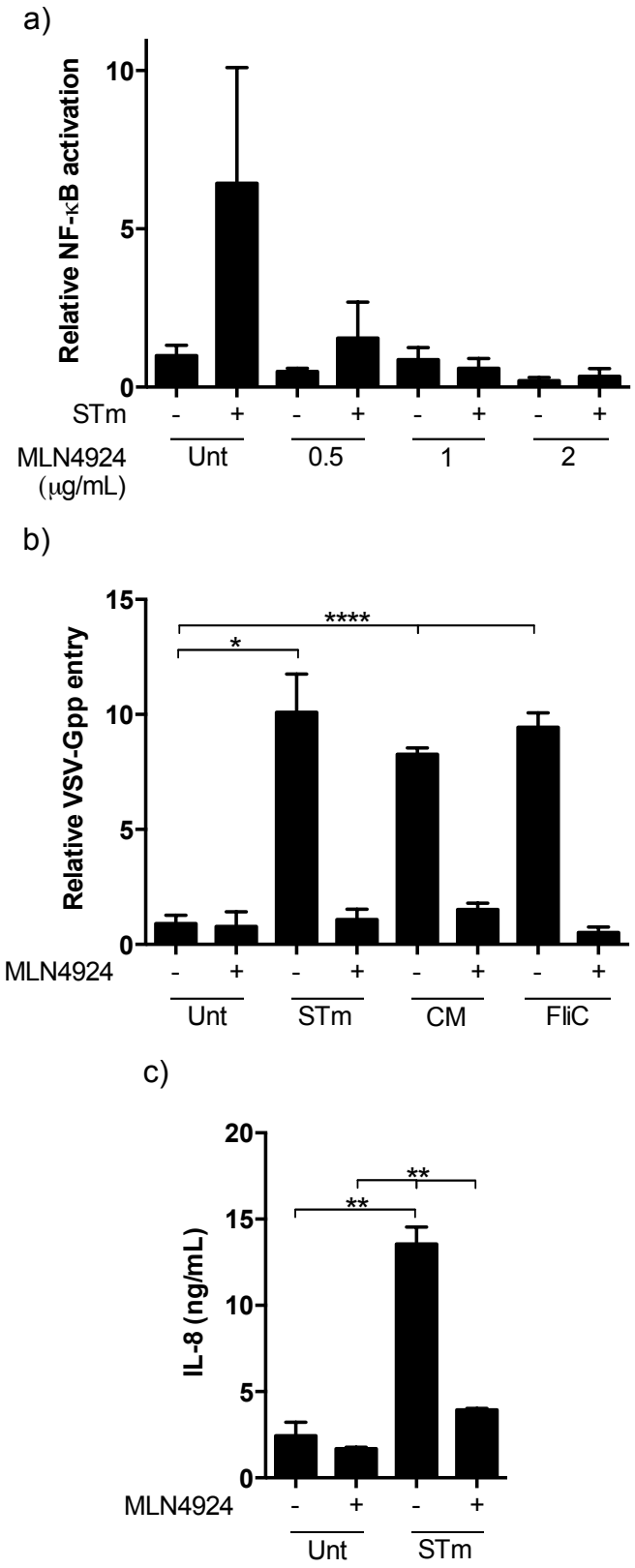

Figure 5.10 **MLN4924 prevents the effect of flagellin on VSV entry.**

Figure 5.10 **cont.**

a) A549 cells were transfected with the NF-κB reporter plasmid pConA-luciferase, incubated for 24 hours and pre-treated for 15 mins with MLN4924 at indicated concentrations. STm (MOI 10) was added for 1 hour prior to chloramphenicol addition. NF-κB activation was quantified by luciferase assay at 48h. Data are presented as relative to NF-κB activation in untreated cells. Representative of 3 biological replicates, error bars show the standard error of the mean (SEM) of 3 technical replicates, statistical comparison by Unpaired t test was n.s. ($P > 0.05$). b) Non-polarized A549 cells were pre-treated with MLN4924 (1 μM) for 15 mins. STm (MOI 10), CM or flagellin (0.3 μg/mL; removed prior to virus addition) were added for one hour prior to VSV-Gpp addition. Entry was quantified by luciferase assay at 48h. Data are presented as relative to VSV-Gpp entry into untreated cells. c) Supernatant from (b) was collected at 24h to measure IL-8 secretion by ELISA. Representative of 3 biological replicates, error bars show SD of 2-6 technical replicates, statistical comparison by Unpaired t test: * = $P \leq 0.05$, ** = $P \leq 0.01$, **** = $P \leq 0.0001$.

activation as a key pathway to facilitate the pro-viral activity of STm flagellin, or the whole bacterium, for lung epithelial cells.

5.8 The pro-viral effect of flagellin through NF-κB signaling is TLR5 dependent

To independently confirm a role for NF-κB in the pro-viral activity of flagellin, we used siRNA to silence RelA (**Fig.5.11a**) and observed a significant decrease in the effect of flagellin on VSV-Gpp infection (**Fig.5.11c**). Flagellin can be detected in epithelial cells by TLR5, leading to NF-κB activation, or NAIP, leading to inflammasome activation (López-Yglesias et al., 2014). To determine which was mediating the pro-viral effect of flagellin, we evaluated the effect of siRNA silencing TLR5. Cells transfected with TLR5 siRNA were not as permissive to the pro-viral activity of flagellin (**Fig.5.11c**), suggesting a role for TLR5. However, given the limited availability of antibodies to detect TLR5 we were unable to validate the effect of the siRNA on protein expression levels and quantified TLR5 mRNA levels by RT-PCR (**Fig.5.11b**). There was a no significant effect on TLR5 mRNA levels in cells transfected with siRNA targeting TLR5. However, given there was a phenotypic difference compared to the control, it could be that the primer used detects a different isoform and is unsuitable for this assay. Earlier results showed that neither CM nor flagellin was able to increase VSV-Gpp entry into Caco-2 cells (**Fig.4.2b**, **Fig.4.6b**). We were interested to quantify TLR5 mRNA levels relative to A549 cells (**Fig.5.12**). We observed significantly higher levels of TLR5 mRNA in Caco-2 cells, suggesting that mRNA levels are not able to predict protein expression, or that the TLR5 produced is not available for or responsive to flagellin stimulation.

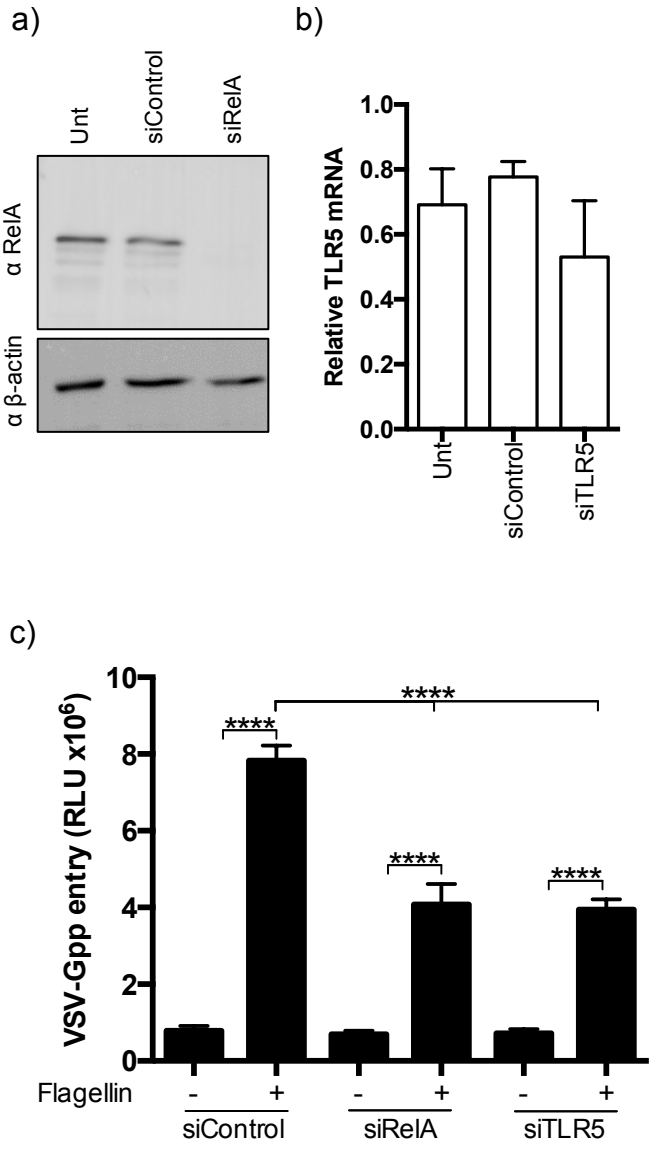

Figure 5.11 **The pro-viral effect of flagellin signals through TLR5.**

A549 cells were transfected with siRNA to target RelA, TLR5, or a control, and cultured for 24 hours. a) Cells were lysed to determine RelA or control β-actin expression by SDS-PAGE and western blotting b) Cells were lysed to determine TLR5 expression relative to control GAPDH by qRT-PCR. c) Flagellin (0.3 μg/mL; removed prior to virus addition) was added for 1h prior to VSV-Gpp addition. Entry was quantified by luciferase assay at 48h. Data are presented as relative luciferase units (RLU). Representative of 3 biological replicates, error bars show SD of 3-4 technical replicates, statistical comparison by Unpaired t test: **** = P ≤ 0.0001.

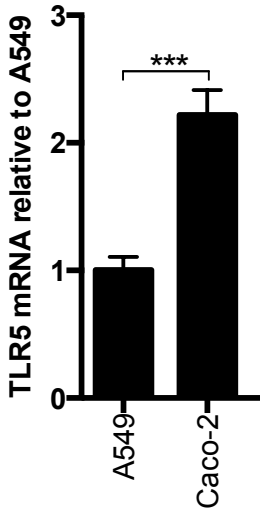

Figure 5.12 **TLR5 mRNA levels.**

A549 and Caco-2 cells were lysed to determine TLR5 mRNA relative to control GAPDH mRNA by qRT-PCR. Data are presented as relative to TLR5 mRNA levels in A549 cells. Error bars show SD of 3 technical replicates, statistical comparison by Unpaired t test: *** = $P \leq 0.001$.

5.9 Discussion

Our experiments to determine the mechanism of flagellin priming virus uptake into A549 cells showed that MLN4924, a small molecule inhibitor of NF-κB activation, reversed the pro-viral activity (**Fig.5.10b**). MLN4924 targets and inhibits the NEDD8-activating enzyme to regulate the activity of cullin-ring ligases. These ligases are involved in the proteasomal degradation of many intracellular proteins (Soucy et al., 2009). Given the broad activity of MLN4924, although it has been reported to hold RelA in the cytoplasm of cells (Milhollen et al., 2010), we confirmed that RelA was involved in the pro-viral activity of flagellin with siRNA silencing. The reduced pro-viral activity of flagellin (**Fig.5.11c**), could be explained by incomplete silencing of RelA, or suggest a role for cullin-ring ligase targets in the pro-viral activity of flagellin.

To further assess the effect of MLN4924 in A549 cells, cell supernatant was collected and showed decreased IL-8 secretion (**Fig.5.10c**). This is one downstream effect of NF-κB signaling by STm (Tallant et al., 2004) and strengthens the conclusion that MLN4924 is preventing NF-κB activation to block the activity of flagellin on virus entry. The observation that flagellin is sufficient to increase virus entry implies that epithelial barriers in the body that are sparsely colonized by flagellated bacteria may be affected, through a bystander effect. Interestingly, this phenotype was not observed with gut-derived Caco-2 cells, suggesting cell type selectivity.

Flagellin can be recognized in host cells by TLR5 and NAIP (López-Yglesias et al., 2014). We found that siRNA silencing of TLR5 decreased the effect of flagellin on VSV-Gpp entry, but did not abrogate the effect. This could be because the silencing

of TLR5 was not complete, as PCR results were inconclusive, or because the pro-viral effect is also mediated by NAIP/Nlrc4-inflammasome signaling within the cell. It may be important to assess the whether inflammasome signaling can occur in A549 cells, as they are reported to express low levels of NAIP (Vinzing et al., 2008). An alternative approach to determine the role of TLR5 signaling would be to evaluate mutant TLR5 proteins lacking either the extracellular binding region or the intracellular signaling region, or test mutant flagellin proteins unable to bind TLR5 for their effect on viral pseudoparticle uptake (Eaves-Pyles et al., 2001; Gewirtz et al., 2001a).

We assessed the possibility of his-tagged flagellin binding to the virus, using the PERT assay to detect virus particles, with a nickel affinity column. Interestingly, virus particles were eluted upon imidazole addition, although this was not increased in the presence of flagellin (**Fig.5.4**). HIV particles are derived from host cell membranes and are negatively charged (Lai et al., 2009), this could allow weak binding to positively charged nickel ions that would be disrupted by the addition of imidazole. Previous studies identifying that LPS binds to MMTV assessed this by ELISA, using both anti-envelope glycoprotein antibodies and biotinylated LPS (Wilks et al., 2015). A similar method could be used to eliminate the background signal of non-specific virus binding to nickel.

We defined the role of flagellin in virus binding and internalization by studying pseudoparticle attachment at 4°C and quantifying virus particles bound or internalized after a one hour incubation. VSV-Gpp entry into A549 cells is reduced at

4°C (**Fig.5.6**). This is likely due to a disruption in the recycling of endocytic receptors to the plasma membrane when cells are at a low temperature (Maxfield and McGraw, 2004), allowing less availability of receptors for virus particles to bind to. Interestingly, a previous study has reported that after binding host cells at 4°C, around one third of VSV particles are internalized and this happens within five minutes of increasing the temperature to 37°C. The pH-dependent fusion step occurs within 30 minutes for the majority of internalized particles (Johannsdottir et al., 2009). We found that flagellin was able to increase virus entry when added after a one hour infection at 37°C (**Fig.5.6**), during which the majority of virus particles should have internalized and fused. One limitation to this finding is that we are using retroviral pseudoparticles rather than full-length VSV, as used by Johannsdottir et al., 2009, and this could be altering virus entry kinetics.

It would be informative to assess the effect of flagellin on VSV-Gpp entry expressing a GFP reporter while using NH_4Cl to prevent endosomal acidification. Comparing the results to the kinetic profile reported by Johannsdottir et al., 2009, could determine whether flagellin promotes virus fusion in the endosome. It is also reported that three times more VSV binds to the cell surface than is internalized, when cells are untreated (Johannsdottir et al., 2009). Flagellin could be affecting this stage of the viral entry process to allow a higher proportion of virus into the cell. The PERT assay suggests that cells incubated at 37°C for one hour have increased virus internalization after flagellin treatment (**Fig.5.5**), which could support this hypothesis.

While investigating the mechanism through which flagellin increases lung epithelial cell permissivity to viruses, we assessed a panel of cellular uptake inhibitors, alongside measuring the uptake of soluble ligands transferrin and dextran. Using these techniques we observed a minimal effect for altered virus uptake pathways following flagellin treatment. Transferrin uptake increased over the first 20 min as previously reported (Junutula et al., 2004), however the decline noted after the first 20 min was not previously reported and is likely to reflect cell-type specific differences and saturation of the pathway. Using this extended time course we failed to detect any effect of flagellin on transferrin uptake kinetics (**Fig.5.8c**).

Previous studies have reported that, following dextran addition, macropinosome formation increases over time (Falcone et al., 2006) as we observed. However, there was no change with flagellin treatment (**Fig.5.9c**). Falcone et al., 2006, reported comparable macropinocytic uptake of FITC-labeled 20 nm latex beads to 70 kDa dextran. As our dextran molecules were only 10 kDa it may be informative to test higher molecular weight structures that may mimic virus particles, such as latex beads. Another inhibitor that would be interesting to test with flagellin and pseudoparticles is nystatin. One study reports that nystatin, a lipid raft inhibitor, can reduce flagellin-induced IL-8 secretion by A549 cells (Im et al., 2009). It is known that non-enveloped viruses utilize lipid rafts to enter cells (Pelkmans, 2005). Although the role of lipid rafts in enveloped virus entry is still to be determined, influenza may also use this area of the plasma membrane to internalize (Ohkura et al., 2014).

VSV-G mediated, acid-dependent fusion of virus particles in the endosome is an inefficient process and many virus particles internalized are degraded prior to fusion by proteases (Hastie et al., 2013). A genome-wide functional analysis of the human kinome used siRNA to target 590 kinases and identified a small number that enhanced VSV entry when they were silenced through altered endocytosis (Pelkmans, 2005). To determine whether flagellin increases virus escape from the endosome, the proteases involved in degradation of attached and internalized VSV-G particles could be targeted with siRNAs and further experiments could determine whether any kinases involved in endocytosis are affected downstream of NF-κB activation by flagellin. Furthermore, it would be important to confirm that the effect of flagellin on VSV-G-dependent entry is present in full-length VSV infection.

5.10 Summary

In this chapter, we present that the pro-viral activity of flagellin occurs via TLR5 and NF-κB signaling (**Fig.5.11c**), to increase virus internalization post-binding (**Fig.5.5**). While attempting to define the mechanism of increased virus entry we found that flagellin had a minimal effect on clathrin-mediated endocytosis of transferrin (**Fig.5.8c**) or macropinocytosis of dextran molecules (**Fig.5.9c**), suggesting a requirement for particulate or multi-valent structures. In future experiments it will be important to determine whether the effect of flagellin occurs during VSV-G mediated membrane fusion in the endosome and to assess the effect of flagellin on the entry of other viruses to determine whether the same mechanism applies. These findings highlight a new role for flagellin, although more work is needed to define the mechanism leading from NF-κB activation to increased virus entry.

6. THE EFFECT OF FLAGELLIN ON HIV-1 REPLICATION

6.1 Introduction

To extend our earlier findings that flagellin promotes epithelial permissivity to support the entry of a panel of viruses; we selected to study the effect of flagellin on HIV-1 infection.

HIV-1 can infect T cells and macrophages using the primary attachment receptor CD4 and chemokine receptors CXCR4 or CCR5 (Clapham and McKnight, 2001). Entry is mediated by the virally encoded glycoproteins gp120 and gp41 (**Fig.6.1a**) and is mediated via the fusion of viral and host cell membranes (**Fig.6.1b**; reviewed by (Aiamkitsumrit et al., 2014). The early phase of HIV-1 replication includes RTase-mediated conversion of viral RNA into a dsDNA pro-viral genome whilst the capsid core is released into the cytoplasm. The virus uncoats and the DNA is imported into the nucleus, where it can integrate via the activity of a virally encoded integrase. The late phase of the life cycle comprises transcription of the integrated proviral genome, expression of viral proteins and the assembly of nascent viral particles that are secreted from the cell (reviewed by (Freed, 2015).

HIV-1 transcription is regulated by LTRs that contain an enhancer element comprising two binding sites for NF-κB, which can initiate transcription in concert with with other cellular transcription factors. The virally encoded transactivator of transcription (Tat) protein is expressed early in the HIV-1 life cycle and has many

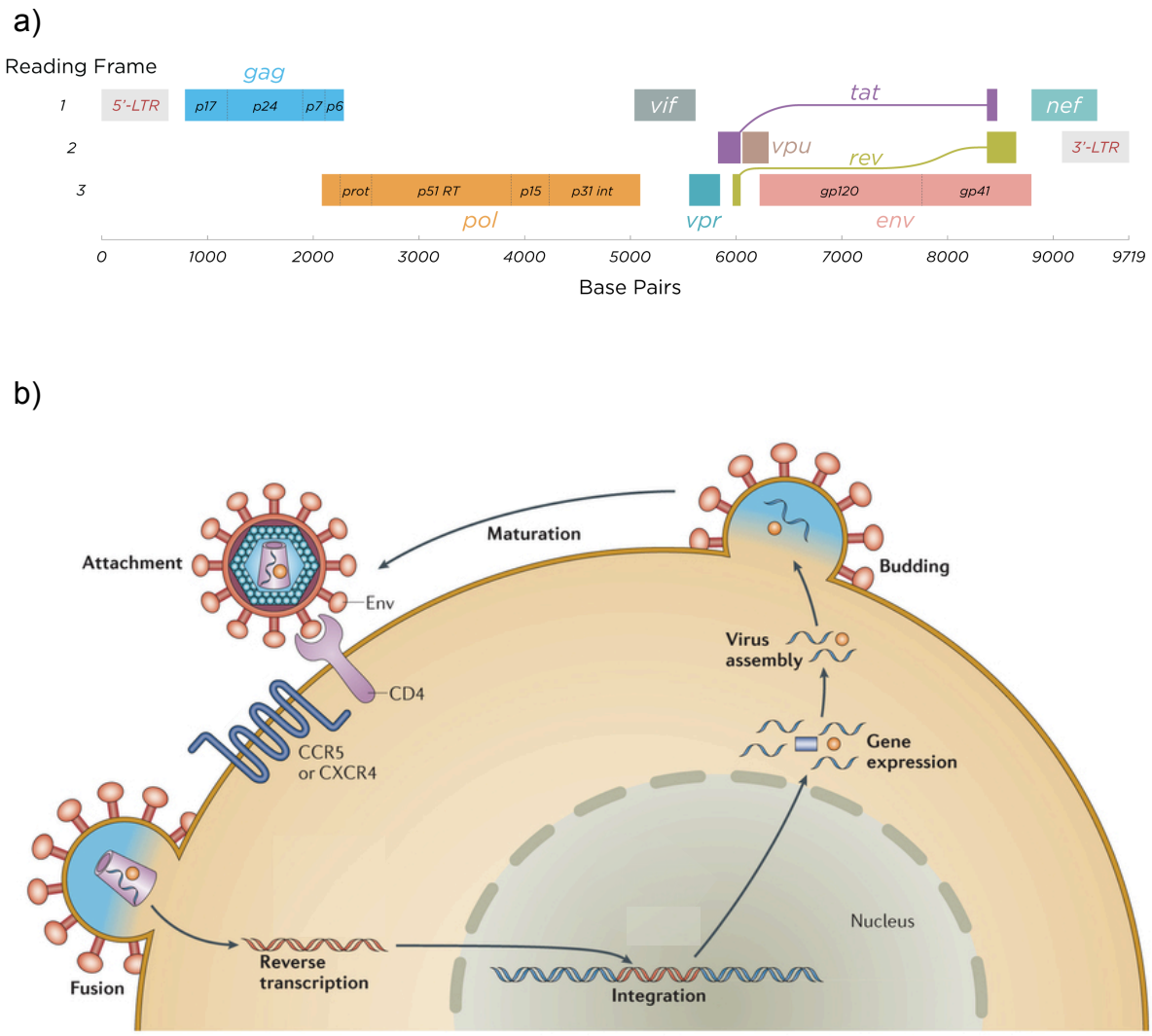

Figure 6.1 **The HIV genome and lifecycle.**

a) The HIV genome, from Thomas Splettstoesser (www.scistyle.com). The envelope glycoproteins, gp41 and gp120, are encoded by *env* late in the viral life cycle. Expression of Tat requires splicing early in the viral life cycle to create *tat* transcripts. b) The HIV lifecycle, adapted from (Laskey and Siliciano, 2014). Fusion occurs at the plasma membrane, following attachment using CD4 and CXCR4 or CCR5. Reverse transcription of viral RNA allows integration and viral gene expression to assemble new viral particles and bud from the host cell.

roles including enhancement of transcription, between 10- and 100-times higher than levels using host cell transcription factors alone (Li et al., 2012). This virally encoded transactivator forms the basis of LTR-reporter cell lines that are sensitive to HIV-dependent Tat expression (Aguilar-Cordova et al., 1994, Wei et al., 2002).

As well as being present on epithelial cell barriers colonized by bacteria, flagellin can be detected in the blood when gut barrier integrity is compromised. Indeed, HIV-1 infection may be associated with increased flagellin levels in the serum (Svärd et al., 2015). Previous studies assessing the role of TLR agonists on HIV replication have shown that flagellin increases LTR activity (Ferreira et al., 2011). Thibault *et al*., 2009, reported that flagellin could reactivate latent HIV-1 in a model cell line, J-Lat, derived from Jurkat cells. Treatment with an NF-κB inhibitor, weledolactone, reduced this reactivation, suggesting an NF-κB dependent process. Brichacek *et al*., 2010, reported that flagellin induced a two-fold increase in the replication of CXCR4- or CCR5-tropic HIV-1 strains infecting *ex vivo* lymphoid tissue. Furthermore, HIV-1 LTR activity can be promoted by flagellin, using a reporter T cell line, 1G5 (Ferreira et al., 2011).

Given our earlier studies showing a role for flagellin to promote viral entry through NF-κB signaling, we were interested to determine whether flagellin could modulate HIV-1 entry into T cells and whether the reported effects of flagellin on LTR-transcription could augment infectious virus production.

Results

6.2 Flagellin increases HIVpp entry

We were interested to determine whether flagellin could increase HIV-1 entry into T cells. Our initial experiments assessed the sensitivity of the PM1 T cell line to support VSV-Gpp infection and its response to flagellin. We observed a modest increase in VSV-Gpp entry (**Fig.6.2a**), demonstrating that the pro-viral activity of flagellin signaling observed in epithelial cells is present in T cells.

We generated HIVpp using the pNL4.3e⁻r⁻luciferase plasmid used for all previous single-round pseudoparticle infections and a plasmid encoding HIV-1 env from the LAI strain, which uses the CXCR4 co-receptor (Aiamkitsumrit et al., 2015). Flagellin increased HIVpp dependent reporter activity three-fold (**Fig.6.2a**). Primary CD4+ T cells were isolated to confirm the pro-viral activity of flagellin on HIVpp entry and two concentrations of flagellin were assessed. Treating primary cells with flagellin (10 µg/mL) increased HIVpp and VSV-Gpp infection (**Fig.6.2b**). However, the increase was not statistically significant. This result supported the finding in PM1 cells that flagellin can increase HIV-1 entry into T cells.

6.3 Flagellin promotes HIV-1 replication

After demonstrating that flagellin promotes HIV-1 entry, we were interested to investigate its effect on the full-length HIV-1 replicative life cycle. Two LTR-reporter cell lines were available to us: TZM-bl cells are derived from HeLa cervical epithelial cells and are engineered to express the viral receptors CD4/CXCR4/CCR5 and a luciferase reporter under transcriptional control of the HIV-1 LTR promoter

a) PM1

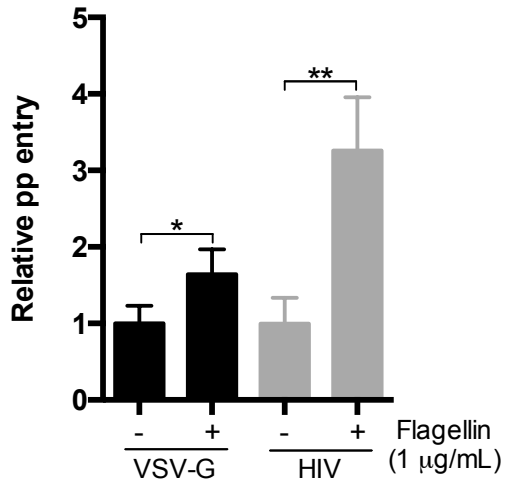

b) Primary CD4+

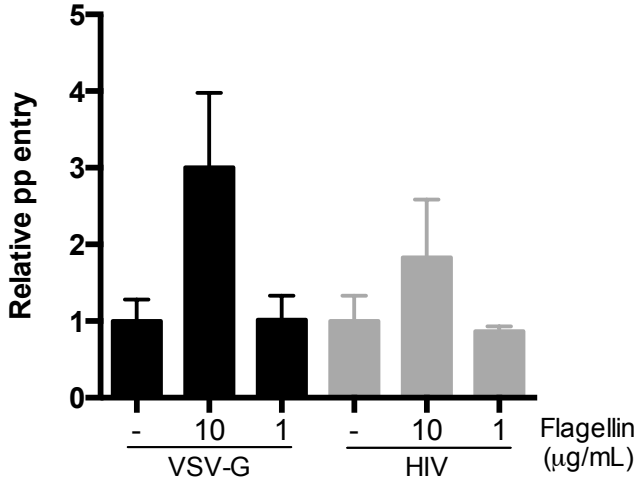

Figure 6.2 **Flagellin increases HIVpp entry into T cells.**

a-b) Cells were incubated with flagellin at stated concentration for 1h prior to infecting with VSV-G or HIV pseudoparticles. Entry was quantified by luciferase assay at 48h. Data are presented as relative to pseudoparticle entry into untreated cells. Error bars show SD of 3 technical replicates, statistical comparison by Unpaired t test: * = $P \leq 0.05$, ** = $P \leq 0.01$.

(Wei et al., 2002); 1G5 cells are derived from the Jurkat CD4 and CXCR4 expressing T cell line and also LTR-luciferase (Aguilar-Cordova et al., 1994).

Initial studies compared the sensitivity of the TZM-bl and 1G5 reporter cells to support HIV-1 infection. Both cell lines were infected with a dilution series of HIV-1 NL4.3 and the data are presented as net luciferase values, where the uninfected basal LTR activity is annotated using a dotted line. We noted a linear relationship between virus dose and reporter activity in both cell lines. TZM-bl cells are more sensitive than 1G5 cells, yielding higher luciferase values and detecting infectivity with a lower viral inoculum (**Fig.6.3a-b**). However, TZM-bl cells have high basal LTR activity. We assessed the effect of media on LTR activity and determined that lower serum concentrations reduced basal levels (data not shown). To maintain low basal levels, TZM-bl cells experiments were carried out with 3% FBS/DMEM. To generate maximum luciferase output from 1G5 cells they were incubated for 48h. However, incubation with HIV-1 for longer than 48h affected cell viability (data not shown). These data demonstrate that both reporter cell lines are valuable but may be used for different experimental protocols: TZM-bl cells are able to detect low quantities of HIV-1, whereas 1G5 cells are T cells and a more physiological cell type.

We then confirmed that flagellin increases HIV-1 infectivity in 1G5 cells as previously reported (Ferreira et al., 2011) and tested the effect of flagellin on HIV-1 infectivity in TZM-bl cells. As determined in previous chapters, flagellin can modulate virus infection through NF-κB signaling and we hypothesized that this would increase LTR-reporter activity. TNF was included as a positive control for NF-κB mediated

a) TZM-bl

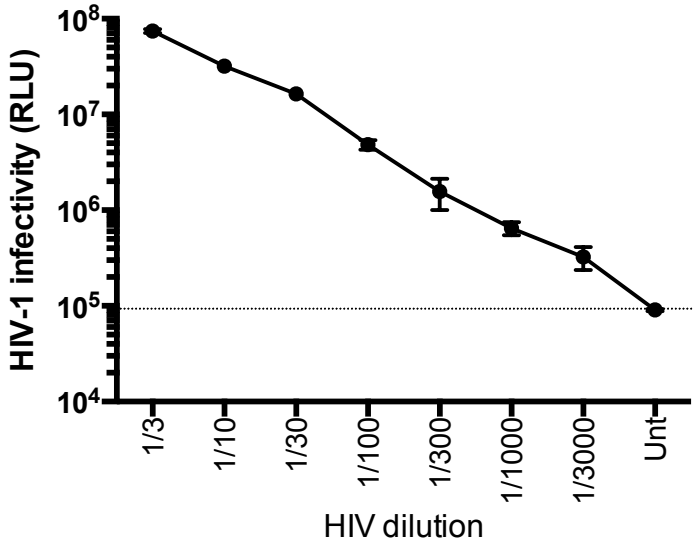

b) 1G5

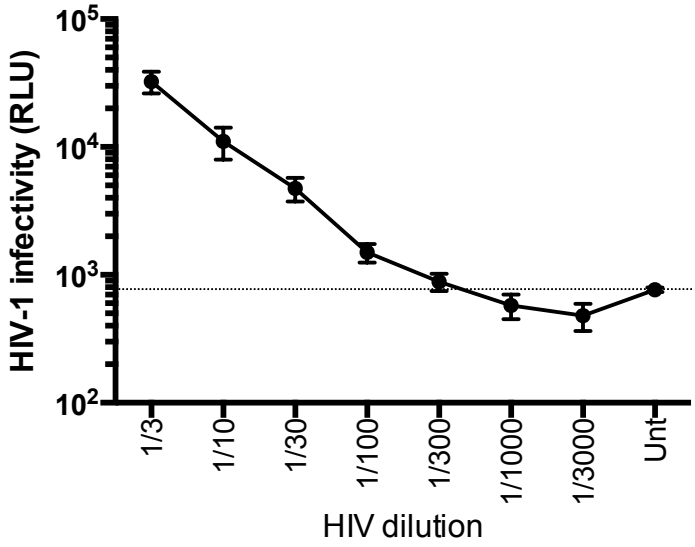

Figure 6.3 **Sensitivity of HIV-1 reporter cell lines.**

a-b) A serial dilution of HIV-1 (strain NL4.3) was added to cells. TZM-bl cells were lysed at 24h, 1G5 cells were lysed at 48h and HIV-1 infectivity was quantified by luciferase assay. Data are presented as relative luciferase units (RLU). Error bars show SD of 3 technical replicates. Dotted lines show the mean RLU of uninfected cells +2 SD.

upregulation of virus infectivity (Li et al., 2012) and this was observed in both cell lines (**Fig.6.4a-b**). Interestingly, flagellin has different effects depending on the cell line. While the basal levels of transcription are increased by flagellin treatment of both TZM-bl and 1G5 cells, it has a negligible effect on HIV-1 infection in TZM-bl cells. However, flagellin increases HIV-1 infection 30-fold in 1G5 cells. These data suggest that TZM-bl cells and 1G5 cells respond differently to flagellin stimulation and we chose to focus on 1G5 cells as a more physiologically relevant model. We determined that the pro-viral activity of flagellin in 1G5 cells occurs in a dose-responsive manner (**Fig.6.5a**) as seen previously.

While our results and previous studies show increased HIV-1 infectivity after flagellin treatment of T cells, we were interested to determine whether this lead to increased infectious virus particle production. To quantify this, 1G5 cells were pre-treated with flagellin, infected with HIV-1 and extracellular media containing newly generated virus particles was collected for titration on TZM-bl cells and lysis for analysis of RTase activity by PERT assay. Flagellin increased extracellular HIV-1 infectivity as determined by titration on TZM-bl cells in a dose-responsive manner, up to eight-fold (**Fig.6.5b**). This pattern is comparable to the effect of flagellin on HIV-1 infectivity in 1G5 cells (**Fig.6.5a**), suggesting that increased transcription does lead to increased production of infectious virus particles. This result is supported by the PERT assay results, which show a 17-fold increase in RTase activity for particles produced by 1G5 cells pre-treated with flagellin (**Fig.6.4c**). Interestingly, although TNF increases HIV-1 infectivity, this does not lead to an augmentation of infectious virus particle production. Together, the data in **Fig.6.4** and **Fig.6.5** demonstrate that increased

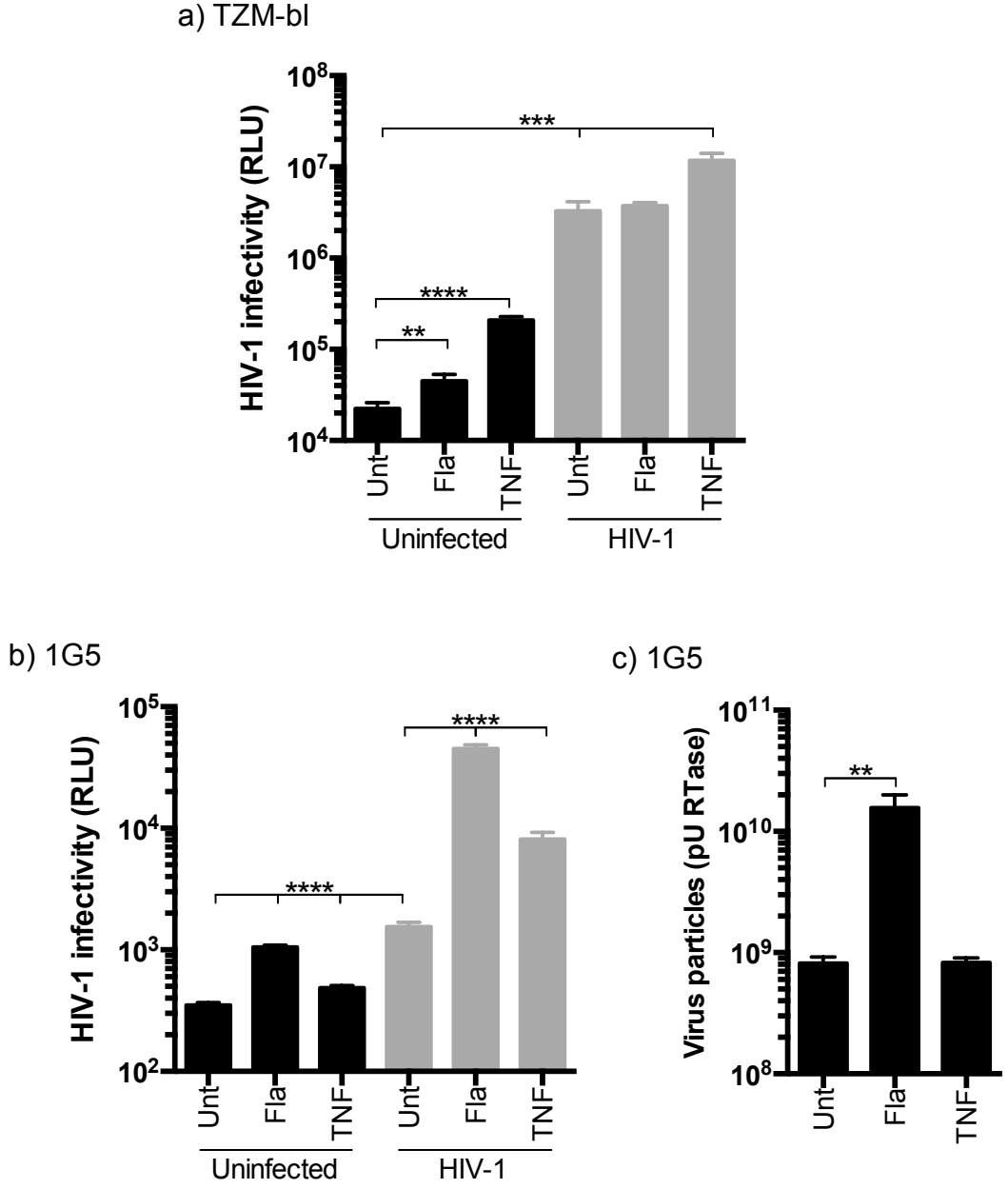

Figure 6.4 **The effect of flagellin on HIV-1 infection of reporter cell lines.**

a-b) Cells were incubated with flagellin (1 µg/mL) or TNF (10 ng/mL) for 1h prior to infection with HIV-1 (NL4.3) and lysed at 24h (TZM-bl) or 48h (1G5). HIV-1 infectivity was quantified by luciferase assay. Data are presented as relative luciferase units (RLU). Representative of 3 biological replicates, error bars show SD of 4 technical replicates, statistical comparison by Unpaired t test: ** = P ≤ 0.01, *** = P ≤ 0.001, **** = P ≤ 0.0001. c) Extracellular media from HIV-1 infected 1G5 cells treated as in (b) was collected and assessed for RTase activity by PERT assay. Data presented are viral particles as determined by units of RTase. Error bars show SD of 3 technical replicates, statistical comparison by Unpaired t test: ** = P ≤ 0.01.

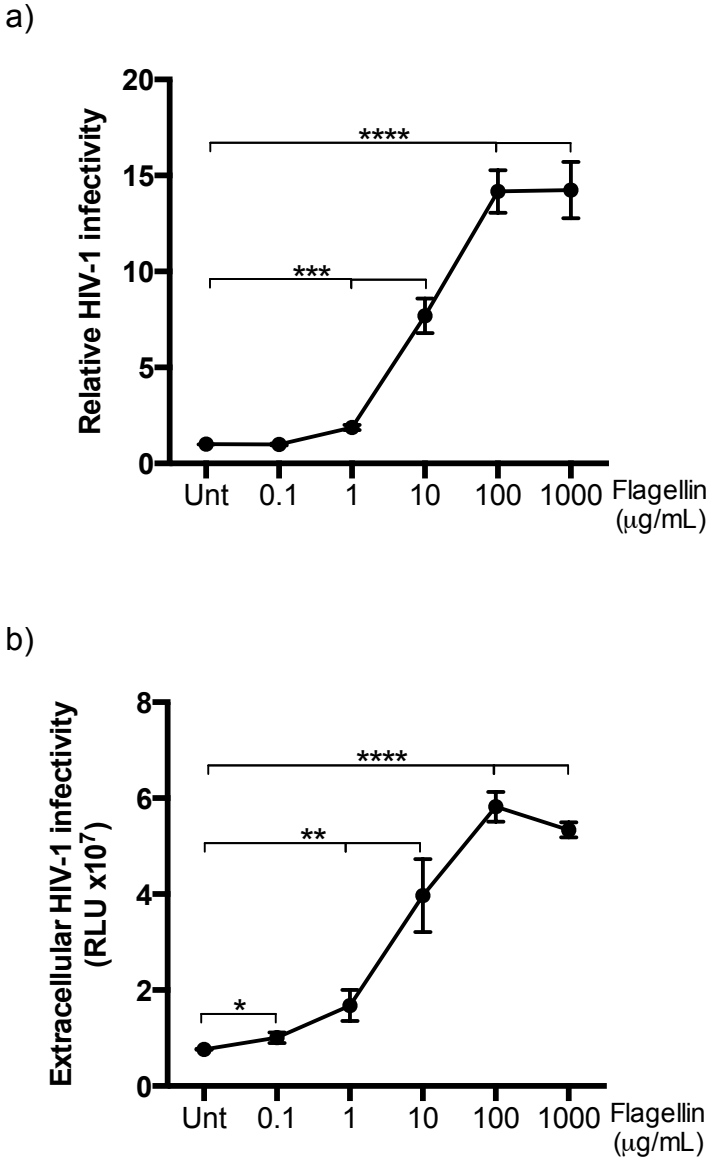

Figure 6.5 **Flagellin increases *de novo* HIV-1 particle production.**

a) 1G5 cells were treated with flagellin at stated concentrations for 1h prior to infection with HIV-1 (NL4.3) for 3h. Cells were washed to remove unbound virus, incubated for 48h. HIV-1 infectivity was quantified by luciferase assay. Data are presented as relative to untreated HIV-1 infectivity. b) Infectivity of the extracellular medium from infected 1G5 cells treated as in (a) when titrated on TZM-bl cells. Data are presented as RLU. Representative of 3 biological replicates, error bars show SD of 3 technical replicates, statistical comparison by Unpaired t test: * = $P \leq 0.05$, ** = $P \leq 0.01$, *** = $P \leq 0.001$, **** = $P \leq 0.0001$.

Tat-dependent transcription in the presence of flagellin augments virus particle production from T cells, which has not been previously reported and suggests that flagellin can modulate virus spread.

Given the different responses of TZM-bl and 1G5 HIV-1 reporter cells to flagellin, we confirmed the pro-viral activity seen in the T cell reporter line using another T cell line, SupT1 cells. In support of the results seen with 1G5 cells, there is a significant increase in extracellular virus infectivity with flagellin treatment when supernatant from SupT1 cells is titred on TZM-bl cells (**Fig.6.6a**) and there is augmented RTase activity by PERT assay (**Fig.6.6b**). Using these data we calculated the specific infectivity and see a 10-fold change (**Table 6.1**), which demonstrates that while more particles are produced, they may be less infectious.

Finally, we assessed the effect of the NF-κB inhibitor, MLN4924, which blocks the pro-viral activity of flagellin in A549 cells (**Fig.5.10b**). Pre-treating 1G5 cells with a concentration of MLN4924 previously reported to inhibit T cell signaling without inducing cell death (Jin et al., 2013) had a minimal effect on the pro-viral activity of flagellin on HIV-1 infectivity (**Fig.6.7**). This suggests that the pro-viral activity of flagellin in T cells may use a different signaling pathway or other factors may be at play.

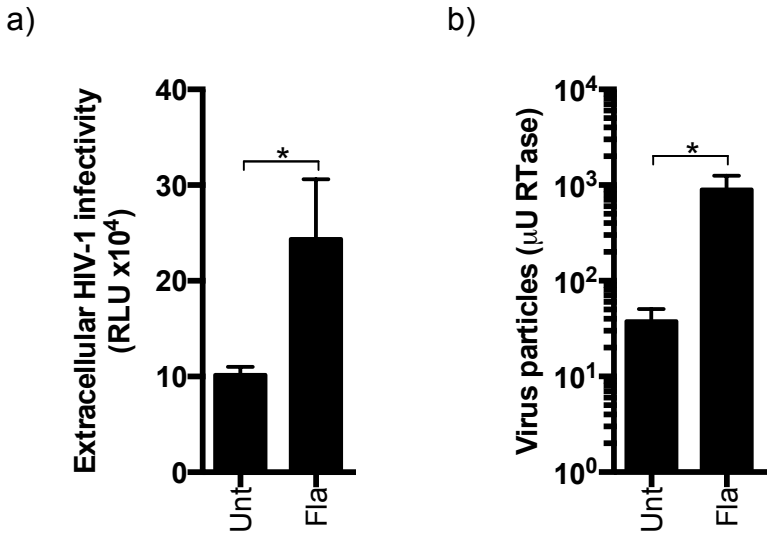

Figure 6.6 **Flagellin increases infectious HIV-1 secretion.**

SupT1 cells were treated with flagellin (0.3 µg/mL) for 1h prior to infection with HIV-1 (NL4.3) and extracellular media was collected at 48h to determine (a) virus infectivity by titration on TZM-bl cells, data are presented as relative luciferase units (RLU), and (b) RTase activity by PERT assay, data presented are viral particles as determined by units of RTase. Error bars show SD of 3 technical replicates, statistical comparison by Unpaired t test: * = $P \leq 0.05$.

Sample	Specific infectivity (RLU x10^4/µU)
Unt	0.30
Fla	0.03

Table 6.1 **Specific infectivity of HIV-1 particles produced by SupT1 cells.**

Specific infectivity was calculated by dividing luciferase activity, as demonstrated in Fig.6.6a, by RTase activity, as demonstrated in Fig.6.6b.

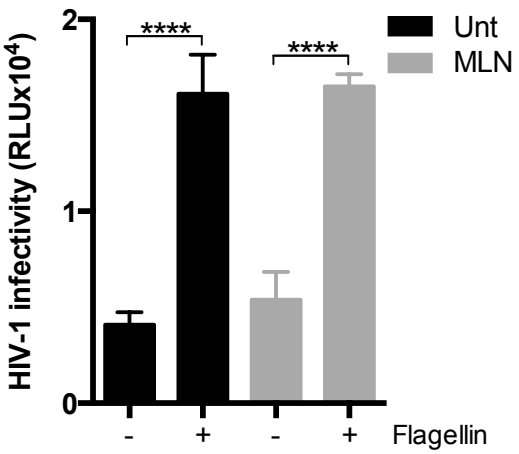

Figure 6.7 **The pro-viral activity of flagellin on HIV-1 transcription is not blocked by MLN4924.**

1G5 cells were treated with MLN4924 (100 nM) for 15 min prior to flagellin addition (10 µg/mL) for 1h. Flagellin was removed and cells were infected with HIV-1 (NL4.3) for 3h. MLN4924 concentration was kept constant throughout this time. Cells were washed to remove unbound virus and incubated for 48h. HIV-1 infectivity was quantified by luciferase assay. Data are presented as relative luciferase units (RLU). Error bars show SD of 3 technical replicates, statistical comparison by Unpaired t test: **** = $P \leq 0.0001$.

6.4 Discussion

In this chapter we aimed to expand the model system we have used to identify a role for flagellin in viral entry, by investigating the role of flagellin in full-length virus infection. Firstly, we observed that flagellin has pro-viral activity in T cells. It can increase HIV-1 entry (**Fig.6.2**), infection of reporter cells (**Fig.6.4**) and the production of infectious virus particles (**Fig.6.6**). Interestingly, this may not be through the same NF-κB signaling mechanism we identified for A549 lung epithelial cells (**Fig.6.7**). However, further experiments are needed to define the mechanism of flagellin pro-viral activity in the HIV-1 replicative lifecycle.

We chose to assess the effect of flagellin on HIV-1 infection, as there were well-characterized reagents available to study at different stages of the viral lifecycle. Initial experiments focused on whether flagellin has pro-viral activity in CD4+ T cells, the main reservoir of HIV-1 infection. As seen with epithelial cells, flagellin can increase virus entry into T cells using the pseudoparticle system (**Fig.6.2**). The HIVpp tested uses the CXCR4 receptor. It will be important to determine the effect of flagellin on CCR5-tropic HIV-1 strains that are involved in the early transmission stages of HIV-1 infection (Aiamkitsumrit et al., 2015). Furthermore, we tested one primary cell donor. There is wide variation in permissivity to HIV-1 infection between primary CD4+ T cell donors (Ciuffi et al., 2004) and it is important to use many different donors to draw conclusions. The effect of flagellin on primary T cells is also likely to vary between donors and TLR responses can be affected by differences in cell purity (Lancioni et al., 2009). The pro-viral activity of flagellin in primary cells required a higher concentration than in the PM1 T cell line.

Another factor to consider when using T cells is their activation status, as the HIV lifecycle may differ depending on whether CD4+ cells are active or quiescent, with activated T cells allowing more productive HIV-1 infection (Zack et al., 2013). We saw higher levels of HIV-1 infection in resting primary CD4+ T cells than in anti-CD3/anti-CD28 activated cells (data not shown) and used resting cells for the flagellin treatment experiment. However, TLRs can act as co-stimulators for TCR signaling, although TLR ligands such as flagellin cannot activate T cells alone (Caron et al., 2005; Rahman et al., 2009). It would be interesting to assess the effect of flagellin alongside TCR-activating anti-CD3 prior to HIV-1 infection, as flagellin and anti-CD3 can increase proliferation of CD4+ T cells (Caron et al., 2005) potentially giving the HIV-1 more target cells to infect. However, Caron et al., 2005, also reported increased cytokine production following flagellin stimulation, including IFNγ.

The effect of flagellin on HIV-1 infectivity in 1G5 cells shows a comparable boost to that reported by Ferreira et al., 2011, of around seven-fold, using 10 μg/mL, after 24 hours. Depending on the concentration of flagellin and whether the experimental protocol required leaving flagellin and HIV-1 on the cells throughout the assay, or removal after 4 hours, we saw an increase between two- and 30-fold after 48 hours (**Fig.6.4b**, **Fig.6.5a**). Previous reports have identified increased HIV p24 (capsid protein) release after flagellin treatment and HIV-1 infection of tonsil explants (Brichacek et al., 2010). P24 release signifies that the virus has reached the late stage of its lifecycle, viral genes have been transcribed and new virus particles have been formed to exit the cell (Freed, 2015). However, p24 can also be released independent of particle formation. We report that there is increased virus particle

release from flagellin pre-treated T cells, using titration on TZM-bl cells and the PERT assay (**Fig.6.4c**, **Fig.6.5b, Fig.6.6**). However, the particles released may not be as infectious and more investigation is needed to determine the effect of flagellin.

Surprisingly, preliminary results suggest that the ability of flagellin to increase HIV-1 infectivity is not through NF-κB signaling (**Fig.6.7**), although flagellin can increase both NF-κB promoter activity and HIV-1 promoter activity in T cells (Thibault et al., 2009). There are also differences in the effect of flagellin or TNF pre-treatment on HIV-1 particle production from 1G5 (**Fig.6.4c**) and SupT1 cells (**Fig.6.6**), although TNF activates NF-κB signaling. Previous studies have found an anti-viral effect of TNF on HIV-1 infection of various cell types (Herbein et al., 1996; Lane et al., 1999) but it is also able to activate HIV-1 in chronically infected T cells and this is through NF-κB-mediated activation of the HIV-1 LTR (Kumar et al., 2013). It will be important to investigate the role of NF-κB in flagellin-associated HIV-1 infection further.

HIV-1 infection can occur through two pathways: cell-free virus encountering a target cell, or cell-cell transmission from an infected cell to a target cell. The second pathway of cell-associated transmission is between 10 and 1000 times more effective than cell-free transmission (Anderson, 2014). We have found that flagellin can increase HIV-1 infection and with the experimental design we used this could be via cell-free or cell-cell transmission routes. Interestingly, flagellin pre-treatment of DCs incubated with HIV-1 prior to co-culture with T cells increased cell-associated transmission, as measured by p24 release (Côté et al., 2013). It would be interesting to investigate further whether flagellin could increase cell-associated transmission, as

it is one pathway thought to contribute to HIV-1 persistence (Kulpa et al., 2013). Flagellin has been reported to reactivate latent HIV-1 (Thibault et al., 2009). To investigate a role for flagellin in cell-associated transmission, it could be added to co-cultures of HIV-infected and uninfected, target CD4+ T cells.

6.5 Summary

Together, these data suggest multiple ways for flagellin to increase virus infection in different cell types throughout the body that may be exposed to flagellin during coinfection or microbial translocation. More experiments are necessary to determine the mechanisms involved. However, it will also be important to expand this model system to include the innate immune cells that will be present *in vivo*. Flagellin can be used as an effective adjuvant, inducing an innate immune response (Lu and Swartz, 2016; Porte et al., 2015). Thus, its role in coinfection may be complex.

7. DISCUSSION

The data presented in this thesis highlight a new role for bacteria to promote enveloped virus infection of epithelial cells, in the presence a low-dose of bacteria. In lung epithelial cells this can be specifically mediated by a single bacterial protein; flagellin. We observed the pro-viral activity of STm to be long lasting, which may be explained by continued host cell signaling or the release of flagellin, suggesting that sparsely bacterially colonized areas of the body may replicate this effect and enhance the infectivity of incoming viruses. We noted that flagellin increased the ability of T cells to support HIV entry and the secretion of infectious particles, demonstrating additional roles in the HIV replicative life cycle beyond entry. These studies implicate a role for flagellin to enhance HIV transmission and infection of new target cells.

The biological relevance of our observations with flagellin may be reflected in the observation that no common bacterial pathogen of the healthy lung is flagellated. *P. aeruginosa*, though flagellated, is a pathogen of immunocompromised individuals, such as those with bronchiectasis or CF (Pfaller et al., 2015, Elborn, 2016). In an individual with bronchiectasis, the burden of *P. aeruginosa* in the lung can often reach $>10^8$ bacteria/mL of sputum (Tunney et al., 2013), providing a reservoir of flagellin production that could contribute to the increased burden of viral infections seen in the immunocompromised lung (Renk et al., 2014; Gao et al., 2015). Furthermore, *P. aeruginosa* has been reported to express low levels of flagellin in the

chronically infected lung (Wolfgang et al., 2004). This is thought to occur because aflagellate bacteria survive longer in the host than flagellated bacteria, most likely mediated by reduced immune recognition, such that many bacterial species down-regulate flagellin expression during infection (Rossez et al., 2015).

Our data suggest a role for TLR5 in the pro-viral activity of flagellin. This receptor has been reported to facilitate flagellin antigen presentation, from DCs to T cells, through MHCII, to induce an adaptive immune response (Letran et al., 2011). Interestingly, MyD88 is not involved in this mechanism, suggesting that there is no involvement of NF-κB signaling. However, this finding led the authors to suggest that increased internalization of the antigen by TLR5 enhances the processing of flagellin into epitopes, to deliver to MHCII. The A549 lung epithelial cells we used are type II alveolar epithelial cells and express both MHCI and MHCII, although expression of the latter is minimal compared to primary cells (Corbière et al., 2011). Relating this theory to our model may be of interest, as this function of TLR5 could allow increased internalization of adhered virus particles into the cell.

The epithelial model system we have used thus far only comprises one host cell type. However, to fully define the effect of flagellin on virus infection it will be important to assess the role of innate immune cells that are also present on epithelial barriers. *In vivo* studies report that the administration of flagellin can limit influenza or rotavirus infection via the increased recruitment and cytokine activity of innate immune cells (Zhang et al., 2014; Porte et al., 2015). Furthermore, flagellin is known to be a potent adjuvant and can enhance the efficacy of viral vaccines, including influenza (Kim et

al., 2015). However, all of these studies used supra-physiological doses of flagellin to enhance the anti-viral immune response. We have found that low doses of flagellin promote virus infection of epithelial cells and T cells, suggesting that the outcome from flagellin challenge will be cell-type and context dependent. Our observations highlight the need for further studies to assess the impact of flagellin on the viral lifecycle *in vivo*, where it has the potential to induce particle uptake into epithelial cells and thereby promote viral spread as well as induce uptake into innate immune cells that may mount an anti-viral response.

Flagellin is an unusual TLR ligand that can elicit responses from both the innate and adaptive immune systems (Letran et al., 2011). We observed a pro-viral effect of flagellin in T cells that may contribute to cell-free HIV-1 infectivity during infection with flagellated pathogens, or microbial translocation. Flagellin has been reported to augment cell-cell transmission (Côté et al., 2013) and reactivate latent HIV-1 in a cellular population that is insensitive to ART, quiescent central memory CD4+ T cells (Thibault et al., 2009). Interestingly, this effect on reactivation can be used to the host's advantage; HIV latency is now being targeted to clear these viral reservoirs during treatment, by reactivating the virus with cytokines or TLR agonists (Sebastian and Collins, 2014).

If the pro-viral activity of flagellin is solely mediated through TLR5, its effect(s) may be most prominent in the aged, where there is a relative decrease in the functionality of TLRs with the exception of TLR5 (Kollmann et al., 2012). It could be that flagellin

enhances susceptibility to viral uptake in individuals who have a reduced capacity to mount an immune response due to age related immune senescence. Our data suggest a dual role of flagellin in enveloped virus entry: while previous studies report a reduction in virus infection (Porte et al., 2015), the cell type that encounters both a virus and flagellin may determine the infection outcome. In conclusion, coinfection research has determined that our past infection history, but also the microbes that we currently carry, can alter the course of incoming infections. By detecting and understanding these interactions better, we may reduce the burden of infectious disease on human health.

7.1 Future work

While these data have uncovered a novel role for flagellin, more investigation is necessary to validate that flagellin has pro-viral activity in primary human cells, using both epithelial and T cells, which may vary in their responses between donors (Ciuffi et al., 2004). Furthermore, there is a need to increase our understanding of coinfection using complex models (Rall and Knoll, 2016) and previous experiments have identified that flagellin can increase HIV cell-cell transmission (Côté et al., 2013). It would be interesting to explore the role of innate immune cell recognition of flagellin in co-culture with epithelial cells, to determine whether virus infection increases or the anti-viral response is augmented. As well as complex *in vitro* models, the role of flagellated vs aflagellate bacteria using *in vivo* virus infection could be assessed, to examine whether the flagellin produced alters the outcome of coinfection.

When considering immune cells to examine in this model, the highest expression of TLR5 mRNA in the mouse is in intestinal DCs (Uematsu et al., 2006). DCs can be targeted by viruses, including HIV-1, to enter the body (Rinaldo and Piazza, 2004). However, this also allows the cells to present viral antigens to the adaptive immune system. By incubating DCs with both flagellin and enveloped viruses, the pro-viral activity of flagellin could be assessed as well as whether viral antigen presentation is increased, to determine the potential role of DCs *in vivo*. Furthermore, the anti-viral effect of flagellin during rotavirus infection in mice is mediated by DC secretion of anti-viral cytokines (Zhang et al., 2014), which may counteract the pro-viral effect of

flagellin. Interestingly, during *P. aeruginosa* infection of individuals with CF, TLR5 is upregulated on neutrophils (Koller et al., 2008). TLR5 upregulation, together with the presence of flagellin, could increase virus entry into neutrophils and it would be interesting to determine whether this results in increased virus infection or increased viral clearance.

Although we observed decreased pro-viral activity in TLR5-silenced epithelial cells, the role of this receptor could be further studied using non-functioning TLR5 (Gewirtz et al., 2001) or flagellin from bacterial species such as *H. pylori*, which does not interact with TLR5 (Eaves-Pyles, 2001). Furthermore, TLR5 is reported to be expressed on the basolateral surface of gut epithelial cells (Gewirtz, 2001a). It would be informative to assess whether basolaterally-administered flagellin can increase the entry of viruses into the apical, or basolateral, surface of polarized gut epithelial monolayers, which have been thus far unresponsive to flagellin. If flagellin addition to the basolateral surface of gut epithelia does not promote virus entry, we could assess whether the addition of multiple MAMPs replicates the pro-viral activity seen with whole bacteria.

We found that the pro-viral activity of flagellin and whole bacteria occurs through NF-κB signalling in epithelial cells. The difference between flagellin being sufficient for lung epithelial cells but the presence of whole bacteria being necessary for pro-viral activity in gut epithelial cells could suggest that the gut cells require more MAMPs to

allow pro-inflammatory activation, which may be predicted given their increased burden of bacteria and need for tolerance.

Through NF-κB signaling, epithelial cells allow more virus particles to enter cells. However, this is not mediated via increased adhesion of particles, as determined by measuring viral particles with the PERT assay following 4°C incubation, leading us to propose that either more virus particles are internalized post-attachment, or more virus particles are able to escape from the endosome. To determine whether adhered particle uptake, or endosomal fusion, is increased we could assess the role of flagellin on GFP-labelled virus trafficking with NH_4Cl to block endosomal acidification. After NH_4Cl is added on a time course, virus uptake can be determined by flow cytometry to create a kinetic profile (Johannsdottir et al., 2009). These techniques are optimized for VSV-G mediated entry, but we see an effect on various virus entry pathways. The effect of flagellin on other viral entry pathways could be investigated by using the PERT adhesion assay to assess the full panel of viral pseudoparticles available. It would also be interesting to examine the role of TLR5 internalization in the context of MHCII expression. However, there are currently no reliable reagents to visualize TLR5 that are readily available.

The pro-viral effect of flagellin on HIV-1 replication is considered to be through NF-κB signaling (Brichacek et al., 2010; Ferreira et al., 2011). We observed a negligible effect of the inhibitor, MLN4924, reported to prevent RelA translocation to the nucleus (Milhollen et al., 2010). Further work is necessary to determine whether MLN4924 has this effect in T cells and the role of NF-κB signaling could be

determined by silencing RelA. Flagellin may also help to activate T cells, which could induce proliferation and enhance HIV-1 spread (Caron et al.; 2005, Zack et al., 2013). We could combine flagellin with anti-CD3 to activate T cells prior to HIV-1 infection and assess whether virus infection is increased, or whether activation induced anti-viral responses such as IFN.

We tested an HIV-1 strain with CXCR4 co-receptor usage. As the shift from CCR5 to CXCR4 is associated with the loss of CD4+ T cells, this suggests that the pro-viral activity of flagellin could speed up progression to the low T cell numbers associated with AIDS by promoting infection with CXCR4-tropic particles (Aiamkitsumrit et al., 2014). CXCR4 and CCR5 tropic viruses can be differentially modulated by the presence other microbes (Kannangara et al., 2005). Although Brichacek el al., 2010, reported that replication was increased for both CCR5 and CXCR4 virus strains following flagellin treatment of *ex vivo* lymphoid tissue, it would be interesting to assess the effect of flagellin on a CCR5 tropic virus, to determine whether flagellin may increase the production of the viral strain associated with HIV-1 transmission (Aiamkitsumrit et al., 2014).

Finally, this study has addressed the role of flagellin on enveloped virus entry and found that flagellin has pro-viral activity on a range of entry pathways. It will be important to test flagellin with non-enveloped viruses, which can enter cells through similar pathways, to determine whether the effect of flagellin is pan-viral.

List of references

Aaron, S.D. (2014) Management and prevention of exacerbations of COPD. **BMJ (Clinical Research Ed.)**, 349: g5237

Aguilar-Cordova, E., Chinen, J., Donehower, L., et al. (1994) A sensitive reporter cell line for HIV-1 tat activity, HIV-1 inhibitors, and T cell activation effects. **AIDS Research and Human Retroviruses**, 10 (3): 295–301

Aiamkitsumrit, B., Dampier, W., Antell, G., et al. (2014) Bioinformatic analysis of HIV-1 entry and pathogenesis. **Current HIV Research**, 12 (2): 132–161

Albertini, A.A., Baquero, E., Ferlin, A., et al. (2012) Molecular and cellular aspects of rhabdovirus entry. **Viruses**, 4 (1): 117–139

Aleksandrowicz, P., Marzi, A., Biedenkopf, N., et al. (2011) Ebola virus enters host cells by macropinocytosis and clathrin-mediated endocytosis. **The Journal of Infectious Diseases**, 204 Suppl 3: S957–67

Amieva, M.R., Vogelmann, R., Covacci, A., et al. (2003) Disruption of the epithelial apical-junctional complex by Helicobacter pylori CagA. **Science (New York)**, 300 (5624): 1430–1434

Andersen-Nissen, E., Smith, K.D., Strobe, K.L., et al. (2005) Evasion of Toll-like receptor 5 by flagellated bacteria. **Proceedings of the National Academy of Sciences of the United States of America**, 102 (26): 9247–9252

Anderson, D.J. (2014) Modeling mucosal cell-associated HIV type 1 transmission in vitro. **The Journal of Infectious Diseases**, 210 Suppl 3: S648–53

Aujla, S.J., Dubin, P.J. and Kolls, J.K. (2007) Th17 cells and mucosal host defense. **Seminars in Immunology**, 19 (6): 377–382

Bardoel, B.W., van der Ent, S., Pel, M.J., et al. (2011) Pseudomonas evades immune recognition of flagellin in both mammals and plants. **PLoS Pathogens**, 7 (8): e1002206

Barlag, B. and Hensel, M. (2015) The giant adhesin SiiE of Salmonella enterica. **Molecules (Basel, Switzerland)**, 20 (1): 1134–1150

Bergelson, J.M. (2009) Intercellular junctional proteins as receptors and barriers to virus infection and spread. **Cell Host & Microbe**, 5 (6): 517–521

Berger, S.B., Romero, X., Ma, C., et al. (2010) SLAM is a microbial sensor that regulates bacterial phagosome functions in macrophages. **Nature Immunology**, 11 (10): 920–927

Bertsche, U., Mayer, C., Götz, F., et al. (2015) Peptidoglycan perception--sensing bacteria by their common envelope structure. **International Journal of Medical Microbiology**, 305 (2): 217–223

Bhavnani, D., Goldstick, J.E., Cevallos, W., et al. (2012) Synergistic effects between rotavirus and coinfecting pathogens on diarrheal disease: evidence from a community-based study in northwestern Ecuador. **American Journal of Epidemiology**, 176 (5): 387–395

Bishop, J.R., Schuksz, M. and Esko, J.D. (2007) Heparan sulphate proteoglycans fine-tune mammalian physiology. **Nature**, 446 (7139): 1030–1037

Blair, J.M., Richmond, G.E., Bailey, A.M., et al. (2013) Choice of bacterial growth medium alters the transcriptome and phenotype of Salmonella enterica Serovar Typhimurium. **Plos One**, 8 (5): e63912

Bobat, S., Flores-Langarica, A., Hitchcock, J., et al. (2011) Soluble flagellin, FliC, induces an Ag-specific Th2 response, yet promotes T-bet-regulated Th1 clearance of Salmonella typhimurium infection. **European Journal of Immunology**, 41 (6): 1606–1618

Bosch, A.A., Biesbroek, G., Trzcinski, K., et al. (2013) Viral and bacterial interactions in the upper respiratory tract. **PLoS Pathogens**, 9 (1): e1003057

Boyle, E.C., Brown, N.F. and Finlay, B.B. (2006) Salmonella enterica serovar Typhimurium effectors SopB, SopE, SopE2 and SipA disrupt tight junction structure and function. **Cellular Microbiology**, 8 (12): 1946–1957

Brichacek, B., Vanpouille, C., Kiselyeva, Y., et al. (2010) Contrasting roles for TLR ligands in HIV-1 pathogenesis. **Plos One**, 5 (9)

Buchacz, K., Lau, B., Jing, Y., et al. (2016) Incidence of AIDS-Defining Opportunistic Infections in a Multicohort Analysis of HIV-infected Persons in the United States and Canada, 2000-2010. **The Journal of Infectious Diseases**, 214 (6): 862–872

Buckner, L.R., Amedee, A.M., Albritton, H.L., et al. (2016) Chlamydia trachomatis Infection of Endocervical Epithelial Cells Enhances Early HIV Transmission Events. **Plos One**, 11 (1): e0146663

Bukreyev, A., Skiadopoulos, M.H., Murphy, B.R., et al. (2006) Nonsegmented negative-strand viruses as vaccine vectors. **Journal of Virology**, 80 (21): 10293–10306

Campellone, K.G. (2010) Cytoskeleton-modulating effectors of enteropathogenic and enterohaemorrhagic Escherichia coli: Tir, EspFU and actin pedestal assembly. **The FEBS Journal**, 277 (11): 2390–2402

Cao, W., Henry, M.D., Borrow, P., et al. (1998) Identification of alpha-dystroglycan as a receptor for lymphocytic choriomeningitis virus and Lassa fever virus. **Science (New York)**, 282 (5396): 2079–2081

Caron, G., Duluc, D., Frémaux, I., et al. (2005) Direct stimulation of human T cells via TLR5 and TLR7/8: flagellin and R-848 up-regulate proliferation and IFN-gamma production by memory CD4+ T cells. **Journal of Immunology**, 175 (3): 1551–1557

Caron, T.J., Scott, K.E., Fox, J.G., et al. (2015) Tight junction disruption: Helicobacter pylori and dysregulation of the gastric mucosal barrier. **World Journal of Gastroenterology**, 21 (40): 11411–11427

Casilag, F., Lorenz, A., Krueger, J., et al. (2016) The LasB Elastase of Pseudomonas aeruginosa Acts in Concert with Alkaline Protease AprA To Prevent Flagellin-Mediated Immune Recognition. **Infection and Immunity**, 84 (1): 162–171

Cauley, L.S. and Vella, A.T. (2015) Why is coinfection with influenza virus and bacteria so difficult to control? **Discovery medicine**, 19 (102): 33–40

Chang, F.M., Reyna, S.M., Granados, J.C., et al. (2012) Inhibition of neddylation represses lipopolysaccharide-induced proinflammatory cytokine production in macrophage cells. **The Journal of Biological Chemistry**, 287 (42): 35756–35767

Chattoraj, S.S., Ganesan, S., Faris, A., et al. (2011a) Pseudomonas aeruginosa suppresses interferon response to rhinovirus infection in cystic fibrosis but not in normal bronchial epithelial cells. **Infection and Immunity**, 79 (10): 4131–4145

Chattoraj, S.S., Ganesan, S., Jones, A.M., et al. (2011b) Rhinovirus infection liberates planktonic bacteria from biofilm and increases chemokine responses in cystic fibrosis airway epithelial cells. **Thorax**, 66 (4): 333–339

Chopra, I. and Roberts, M. (2001) Tetracycline antibiotics: mode of action, applications, molecular biology, and epidemiology of bacterial resistance. **Microbiology and Molecular Biology Reviews**, 65 (2): 232–60 ; second page, table of contents

Ciuffi, A., Bleiber, G., Muñoz, M., et al. (2004) Entry and transcription as key determinants of differences in CD4 T-cell permissiveness to human immunodeficiency virus type 1 infection. **Journal of Virology**, 78 (19): 10747–10754

Clapham, P.R. and McKnight, A. (2001) HIV-1 receptors and cell tropism. **British Medical Bulletin**, 58: 43–59

Cohen, C.J., Shieh, J.T., Pickles, R.J., et al. (2001) The coxsackievirus and adenovirus receptor is a transmembrane component of the tight junction. **Proceedings of the National Academy of Sciences of the United States of America**, 98 (26): 15191–15196

Cohen, M.S., Hellmann, N., Levy, J.A., et al. (2008) The spread, treatment, and prevention of HIV-1: evolution of a global pandemic. **The Journal of Clinical Investigation**, 118 (4): 1244–1254

Corbière, V., Dirix, V., Norrenberg, S., et al. (2011) Phenotypic characteristics of human type II alveolar epithelial cells suitable for antigen presentation to T lymphocytes. **Respiratory Research**, 12: 15

Cossart, P. and Helenius, A. (2014) Endocytosis of viruses and bacteria. **Cold Spring Harbor Perspectives in Biology**, 6 (8)

Cosset, F.L., Marianneau, P., Verney, G., et al. (2009) Characterization of Lassa virus cell entry and neutralization with Lassa virus pseudoparticles. **Journal of Virology**, 83 (7): 3228–3237

Côté, S.C., Plante, A., Tardif, M.R., et al. (2013) Dectin-1/TLR2 and NOD2 agonists render dendritic cells susceptible to infection by X4-using HIV-1 and promote cis-infection of CD4(+) T cells. **Plos One**, 8 (7): e67735

Coyne, C.B. and Bergelson, J.M. (2006) Virus-induced Abl and Fyn kinase signals permit coxsackievirus entry through epithelial tight junctions. **Cell**, 124 (1): 119–131

Crowe, S.M., Vardaxis, N.J., Kent, S.J., et al. (1994) HIV infection of monocyte-derived macrophages in vitro reduces phagocytosis of Candida albicans. **Journal of Leukocyte Biology**, 56 (3): 318–327

Cunningham, A.F., Khan, M., Ball, J., et al. (2004) Responses to the soluble flagellar protein FliC are Th2, while those to FliC on Salmonella are Th1. **European Journal of Immunology**, 34 (11): 2986–2995

Cureton, D.K., Massol, R.H., Saffarian, S., et al. (2009) Vesicular stomatitis virus enters cells through vesicles incompletely coated with clathrin that depend upon actin for internalization. **PLoS Pathogens**, 5 (4): e1000394

Datsenko, K.A. and Wanner, B.L. (2000) One-step inactivation of chromosomal genes in Escherichia coli K-12 using PCR products. **Proceedings of the National Academy of Sciences of the United States of America**, 97 (12): 6640–6645

Dean, P., Young, L., Quitard, S., et al. (2013) Insights into the pathogenesis of enteropathogenic E. coli using an improved intestinal enterocyte model. **Plos One**, 8 (1): e55284

Deffur, A., Mulder, N.J. and Wilkinson, R.J. (2013) Co-infection with Mycobacterium tuberculosis and human immunodeficiency virus: an overview and motivation for systems approaches. **Pathogens and disease**, 69 (2): 101–113

Dickson, R.P. and Huffnagle, G.B. (2015) The Lung Microbiome: New Principles for Respiratory Bacteriology in Health and Disease. **PLoS Pathogens**, 11 (7): e1004923

Didierlaurent, A., Goulding, J. and Hussell, T. (2007) The impact of successive infections on the lung microenvironment. **Immunology**, 122 (4): 457–465

Didierlaurent, A., Goulding, J., Patel, S., et al. (2008) Sustained desensitization to bacterial Toll-like receptor ligands after resolution of respiratory influenza infection. **The Journal of Experimental Medicine**, 205 (2): 323–329

Dörig, R.E., Marcil, A., Chopra, A., et al. (1993) The human CD46 molecule is a receptor for measles virus (Edmonston strain). **Cell**, 75 (2): 295–305

Eaves-Pyles, T.D., Wong, H.R., Odoms, K., et al. (2001) Salmonella flagellin-dependent proinflammatory responses are localized to the conserved amino and carboxyl regions of the protein. **Journal of Immunology**, 167 (12): 7009–7016

Eckmann, L., Kagnoff, M.F. and Fierer, J. (1993) Epithelial cells secrete the chemokine interleukin-8 in response to bacterial entry. **Infection and Immunity**, 61 (11): 4569–4574

Edinger, T.O., Pohl, M.O. and Stertz, S. (2014) Entry of influenza A virus: host factors and antiviral targets. **The Journal of General Virology**, 95 (Pt 2): 263–277

Elborn, J.S. (2016) Cystic fibrosis. **The Lancet**

Elsinghorst, E.A. (1994) Measurement of invasion by gentamicin resistance. **Methods in Enzymology**, 236: 405–420

Engel, J. and Eran, Y. (2011) Subversion of mucosal barrier polarity by pseudomonas aeruginosa. **Frontiers in microbiology**, 2: 114

Ernst, J.D. (2012) The immunological life cycle of tuberculosis. **Nature Reviews. Immunology**, 12 (8): 581–591

Evans, L.D., Hughes, C. and Fraser, G.M. (2014) Building a flagellum in biological outer space. **Microbial cell**, 1 (2): 64–66

Fàbrega, A. and Vila, J. (2013) Salmonella enterica serovar Typhimurium skills to succeed in the host: virulence and regulation. **Clinical Microbiology Reviews**, 26 (2): 308–341

Falcone, S., Cocucci, E., Podini, P., et al. (2006) Macropinocytosis: regulated coordination of endocytic and exocytic membrane traffic events. **Journal of Cell Science**, 119 (Pt 22): 4758–4769

Feasey, N.A., Dougan, G., Kingsley, R.A., et al. (2012) Invasive non-typhoidal salmonella disease: an emerging and neglected tropical disease in Africa. **The Lancet**, 379 (9835): 2489–2499

Ferreira, V.H., Nazli, A., Khan, G., et al. (2011) Endometrial epithelial cell responses to coinfecting viral and bacterial pathogens in the genital tract can activate the HIV-1 LTR in an NF{kappa}B-and AP-1-dependent manner. **The Journal of Infectious Diseases**, 204 (2): 299–308

Fink, S.L. and Cookson, B.T. (2007) Pyroptosis and host cell death responses during Salmonella infection. **Cellular Microbiology**, 9 (11): 2562–2570

Finkelshtein, D., Werman, A., Novick, D., et al. (2013) LDL receptor and its family members serve as the cellular receptors for vesicular stomatitis virus. **Proceedings of the National Academy of Sciences of the United States of America**, 110 (18): 7306–7311

Finlay, B.B. and Falkow, S. (1990) Salmonella interactions with polarized human intestinal Caco-2 epithelial cells. **The Journal of Infectious Diseases**, 162 (5): 1096–1106

Fletcher, N.F., Howard, C. and McKeating, J.A. (2012) Over the fence or through the gate: how viruses infect polarized cells. **Immunotherapy**, 4 (3): 249–251

Fletcher, N.F., Sutaria, R., Jo, J., et al. (2014) Activated macrophages promote hepatitis C virus entry in a tumor necrosis factor-dependent manner. **Hepatology**, 59 (4): 1320–1330

Flores-Langarica, A., Bobat, S., Marshall, J.L., et al. (2015) Soluble flagellin coimmunization attenuates Th1 priming to Salmonella and clearance by modulating dendritic cell activation and cytokine production. **European Journal of Immunology**, 45 (8): 2299–2311

Freed, E.O. (2015) HIV-1 assembly, release and maturation. **Nature Reviews. Microbiology**, 13 (8): 484–496

Freedman, J.C., Shrestha, A. and McClane, B.A. (2016) Clostridium perfringens Enterotoxin: Action, Genetics, and Translational Applications. **Toxins**, 8 (3)

Furrer, H. (2016) Opportunistic Diseases During HIV Infection-Things Aren't What They Used to Be, or Are They? **The Journal of Infectious Diseases**, 214 (6): 830–831

Galdiero, S., Falanga, A., Cantisani, M., et al. (2012) Microbe-host interactions: structure and role of Gram-negative bacterial porins. **Current Protein & Peptide Science**, 13 (8): 843–854

Gallo, R.L. and Hooper, L.V. (2012) Epithelial antimicrobial defence of the skin and intestine. **Nature Reviews. Immunology**, 12 (7): 503–516

Gao, Y.H., Guan, W.J., Xu, G., et al. (2015) The role of viral infection in pulmonary exacerbations of bronchiectasis in adults: a prospective study. **Chest**, 147 (6): 1635–1643

Garai, P., Gnanadhas, D.P. and Chakravortty, D. (2012) Salmonella enterica serovars Typhimurium and Typhi as model organisms: revealing paradigm of host-pathogen interactions. **Virulence**, 3 (4): 377–388

Gewirtz, A.T., Navas, T.A., Lyons, S., et al. (2001a) Cutting edge: bacterial flagellin activates basolaterally expressed TLR5 to induce epithelial proinflammatory gene expression. **Journal of Immunology**, 167 (4): 1882–1885

Gewirtz, A.T., Simon, P.O., Schmitt, C.K., et al. (2001b) Salmonella typhimurium translocates flagellin across intestinal epithelia, inducing a proinflammatory response. **The Journal of Clinical Investigation**, 107 (1): 99–109

Glod, J., Kobiler, D., Noel, M., et al. (2006) Monocytes form a vascular barrier and participate in vessel repair after brain injury. **Blood**, 107 (3): 940–946

Gordon, M.A., Banda, H.T., Gondwe, M., et al. (2002) Non-typhoidal salmonella bacteraemia among HIV-infected Malawian adults: high mortality and frequent recrudescence. **AIDS**, 16 (12): 1633–1641

Goulding, J., Snelgrove, R., Saldana, J., et al. (2007) Respiratory infections: do we ever recover? **Proceedings of the American Thoracic Society**, 4 (8): 618–625

Griffiths, E.C., Pedersen, A.B., Fenton, A., et al. (2011) The nature and consequences of coinfection in humans. **The Journal of Infection**, 63 (3): 200–206

Gruber, A., Lell, C.P., Spruth, M., et al. (2003) HIV-1 and its transmembrane protein gp41 bind to different Candida species modulating adhesion. **FEMS Immunology and Medical Microbiology**, 37 (1): 77–83

Gupta, R.K., Lucas, S.B., Fielding, K.L., et al. (2015) Prevalence of tuberculosis in post-mortem studies of HIV-infected adults and children in resource-limited settings: a systematic review and meta-analysis. **AIDS**, 29 (15): 1987–2002

Guttenplan, S.B., Shaw, S. and Kearns, D.B. (2013) The cell biology of peritrichous flagella in Bacillus subtilis. **Molecular Microbiology**, 87 (1): 211–229

Guy, R.L., Gonias, L.A. and Stein, M.A. (2000) Aggregation of host endosomes by Salmonella requires SPI2 translocation of SseFG and involves SpvR and the fms-aroE intragenic region. **Molecular Microbiology**, 37 (6): 1417–1435

Guyader, M., Kiyokawa, E., Abrami, L., et al. (2002) Role for human immunodeficiency virus type 1 membrane cholesterol in viral internalization. **Journal of Virology**, 76 (20): 10356–10364

Hastie, E., Cataldi, M., Marriott, I., et al. (2013) Understanding and altering cell tropism of vesicular stomatitis virus. **Virus Research**, 176 (1-2): 16–32

Hastie, E. and Grdzelishvili, V.Z. (2012) Vesicular stomatitis virus as a flexible platform for oncolytic virotherapy against cancer. **The Journal of General Virology**, 93 (Pt 12): 2529–2545

Hatziioannou, T., Perez-Caballero, D., Cowan, S., et al. (2005) Cyclophilin interactions with incoming human immunodeficiency virus type 1 capsids with opposing effects on infectivity in human cells. **Journal of Virology**, 79 (1): 176–183

Herbein, G., Montaner, L.J. and Gordon, S. (1996) Tumor necrosis factor alpha inhibits entry of human immunodeficiency virus type 1 into primary human macrophages: a selective role for the 75-kilodalton receptor. **Journal of Virology**, 70 (11): 7388–7397

Hoffmann, J., Rabezanahary, H., Randriamarotia, M., et al. (2012) Viral and atypical bacterial etiology of acute respiratory infections in children under 5 years old living in a rural tropical area of Madagascar. **Plos One**, 7 (8): e43666

Hoiseth, S.K. and Stocker, B.A. (1981) Aromatic-dependent Salmonella typhimurium are non-virulent and effective as live vaccines. **Nature**, 291 (5812): 238–239

Hooshyar, D., Hanson, D.L., Wolfe, M., et al. (2007) Trends in perimortal conditions and mortality rates among HIV-infected patients. **AIDS**, 21 (15): 2093–2100

Hsu, M., Zhang, J., Flint, M., et al. (2003) Hepatitis C virus glycoproteins mediate pH-dependent cell entry of pseudotyped retroviral particles. **Proceedings of the National Academy of Sciences of the United States of America**, 100 (12): 7271–7276

Hughson, E.J. and Hopkins, C.R. (1990) Endocytic pathways in polarized Caco-2 cells: identification of an endosomal compartment accessible from both apical and basolateral surfaces. **The Journal of Cell Biology**, 110 (2): 337–348

Hussell, T. and Cavanagh, M.M. (2009) The innate immune rheostat: influence on lung inflammatory disease and secondary bacterial pneumonia. **Biochemical Society Transactions**, 37 (Pt 4): 811–813

Hussell, T., Wissinger, E. and Goulding, J. (2009) Bacterial complications during pandemic influenza infection. **Future Microbiology**, 4 (3): 269–272

Im, J., Jeon, J.H., Cho, M.K., et al. (2009) Induction of IL-8 expression by bacterial flagellin is mediated through lipid raft formation and intracellular TLR5 activation in A549 cells. **Molecular Immunology**, 47 (2-3): 614–622

Imperiali, F.G., Zaninoni, A., La Maestra, L., et al. (2001) Increased Mycobacterium tuberculosis growth in HIV-1-infected human macrophages: role of tumour necrosis factor-alpha. **Clinical and Experimental Immunology**, 123 (3): 435–442

Jin, H.S., Liao, L., Park, Y., et al. (2013) Neddylation pathway regulates T-cell function by targeting an adaptor protein Shc and a protein kinase Erk signaling. **Proceedings of the National Academy of Sciences of the United States of America**, 110 (2): 624–629

Johannsdottir, H.K., Mancini, R., Kartenbeck, J., et al. (2009) Host cell factors and functions involved in vesicular stomatitis virus entry. **Journal of Virology**, 83 (1): 440–453

Jones, M.K., Watanabe, M., Zhu, S., et al. (2014) Enteric bacteria promote human and mouse norovirus infection of B cells. **Science (New York)**, 346 (6210): 755–759

Junutula, J.R., Schonteich, E., Wilson, G.M., et al. (2004) Molecular characterization of Rab11 interactions with members of the family of Rab11-interacting proteins. **The Journal of Biological Chemistry**, 279 (32): 33430–33437

Kane, M., Case, L.K., Kopaskie, K., et al. (2011) Successful transmission of a retrovirus depends on the commensal microbiota. **Science (New York)**, 334 (6053): 245–249

Kannangara, S., DeSimone, J.A. and Pomerantz, R.J. (2005) Attenuation of HIV-1 infection by other microbial agents. **The Journal of Infectious Diseases**, 192 (6): 1003–1009

Kaparakis-Liaskos, M. and Ferrero, R.L. (2015) Immune modulation by bacterial outer membrane vesicles. **Nature Reviews. Immunology**, 15 (6): 375–387

Karlström, A., Boyd, K.L., English, B.K., et al. (2009) Treatment with protein synthesis inhibitors improves outcomes of secondary bacterial pneumonia after influenza. **The Journal of Infectious Diseases**, 199 (3): 311–319

Karst, S.M. (2015) Identification of a novel cellular target and a co-factor for norovirus infection - B cells & commensal bacteria. **Gut microbes**, 6 (4): 266–271

Kazmierczak, B.I., Mostov, K. and Engel, J.N. (2001) Interaction of bacterial pathogens with polarized epithelium. **Annual Review of Microbiology**, 55: 407–435

Khameneh, H.J. and Mortellaro, A. (2014) NLRC4 gets out of control. **Nature Genetics**, 46 (10): 1048–1049

Kim, J.R., Holbrook, B.C., Hayward, S.L., et al. (2015) Inclusion of Flagellin during Vaccination against Influenza Enhances Recall Responses in Nonhuman Primate Neonates. **Journal of Virology**, 89 (14): 7291–7303

Klasse, P.J. (2012) The molecular basis of HIV entry. **Cellular Microbiology**, 14 (8): 1183–1192

Koller, B., Kappler, M., Latzin, P., et al. (2008) TLR expression on neutrophils at the pulmonary site of infection: TLR1/TLR2-mediated up-regulation of TLR5 expression in cystic fibrosis lung disease. **Journal of Immunology**, 181 (4): 2753–2763

Kollmann, T.R., Levy, O., Montgomery, R.R., et al. (2012) Innate immune function by Toll-like receptors: distinct responses in newborns and the elderly. **Immunity**, 37 (5): 771–783

Kondo, Y., Higa-Nakamine, S., Noguchi, N., et al. (2012) Induction of epithelial-mesenchymal transition by flagellin in cultured lung epithelial cells. **American Journal of Physiology. Lung Cellular and Molecular Physiology**, 303 (12): L1057–69

Koo, H.L., Neill, F.H., Estes, M.K., et al. (2013) Noroviruses: The Most Common Pediatric Viral Enteric Pathogen at a Large University Hospital After Introduction of Rotavirus Vaccination. **Journal of the Pediatric Infectious Diseases Society**, 2 (1): 57–60

Krzyzaniak, M.A., Zumstein, M.T., Gerez, J.A., et al. (2013) Host cell entry of respiratory syncytial virus involves macropinocytosis followed by proteolytic activation of the F protein. **PLoS Pathogens**, 9 (4): e1003309

Kudva, A., Scheller, E.V., Robinson, K.M., et al. (2011) Influenza A inhibits Th17-mediated host defense against bacterial pneumonia in mice. **Journal of Immunology**, 186 (3): 1666–1674

Kulpa, D.A., Brehm, J.H., Fromentin, R., et al. (2013) The immunological synapse: the gateway to the HIV reservoir. **Immunological Reviews**, 254 (1): 305–325

Kumar, A., Abbas, W. and Herbein, G. (2013) TNF and TNF receptor superfamily members in HIV infection: new cellular targets for therapy? **Mediators of Inflammation**, 2013: 484378

Kuss, S.K., Best, G.T., Etheredge, C.A., et al. (2011) Intestinal microbiota promote enteric virus replication and systemic pathogenesis. **Science (New York)**, 334 (6053): 249–252

Lai, S.K., Hida, K., Shukair, S., et al. (2009) Human immunodeficiency virus type 1 is trapped by acidic but not by neutralized human cervicovaginal mucus. **Journal of Virology**, 83 (21): 11196–11200

Lancioni, C.L., Thomas, J.J. and Rojas, R.E. (2009) Activation requirements and responses to TLR ligands in human CD4+ T cells: comparison of two T cell isolation techniques. **Journal of Immunological Methods**, 344 (1): 15–25

Lane, B.R., Markovitz, D.M., Woodford, N.L., et al. (1999) TNF-alpha inhibits HIV-1 replication in peripheral blood monocytes and alveolar macrophages by inducing the production of RANTES and decreasing C-C chemokine receptor 5 (CCR5) expression. **Journal of Immunology**, 163 (7): 3653–3661

Laskey, S.B. and Siliciano, R.F. (2014) A mechanistic theory to explain the efficacy of antiretroviral therapy. **Nature Reviews. Microbiology**, 12 (11): 772–780

Lee, B., Robinson, K.M., McHugh, K.J., et al. (2015) Influenza-induced type I interferon enhances susceptibility to gram-negative and gram-positive bacterial pneumonia in mice. **American Journal of Physiology. Lung Cellular and Molecular Physiology**, 309 (2): L158–67

Lee, V.T. and Schneewind, O. (2001) Protein secretion and the pathogenesis of bacterial infections. **Genes & Development**, 15 (14): 1725–1752

Letran, S.E., Lee, S.J., Atif, S.M., et al. (2011) TLR5 functions as an endocytic receptor to enhance flagellin-specific adaptive immunity. **European Journal of Immunology**, 41 (1): 29–38

Lévy, C., Verhoeyen, E. and Cosset, F.L. (2015) Surface engineering of lentiviral vectors for gene transfer into gene therapy target cells. **Current Opinion in Pharmacology**, 24: 79–85

Li, L., Dahiya, S., Kortagere, S., et al. (2012) Impact of Tat Genetic Variation on HIV-1 Disease. **Advances in virology**, 2012: 123605

Liberati, N.T., Urbach, J.M., Miyata, S., et al. (2006) An ordered, nonredundant library of Pseudomonas aeruginosa strain PA14 transposon insertion mutants. **Proceedings of the National Academy of Sciences of the United States of America**, 103 (8): 2833–2838

Long, J., Wright, E., Molesti, E., et al. (2015) Antiviral therapies against Ebola and other emerging viral diseases using existing medicines that block virus entry. [version 2; referees: 2 approved]. **F1000Research**, 4: 30

López-Yglesias, A.H., Zhao, X., Quarles, E.K., et al. (2014) Flagellin induces antibody responses through a TLR5- and inflammasome-independent pathway. **Journal of Immunology**, 192 (4): 1587–1596

Lozupone, C.A., Li, M., Campbell, T.B., et al. (2013) Alterations in the gut microbiota associated with HIV-1 infection. **Cell Host & Microbe**, 14 (3): 329–339

Lu, Y. and Swartz, J.R. (2016) Functional properties of flagellin as a stimulator of innate immunity. **Scientific reports**, 6: 18379

Lütschg, V., Boucke, K., Hemmi, S., et al. (2011) Chemotactic antiviral cytokines promote infectious apical entry of human adenovirus into polarized epithelial cells. **Nature Communications**, 2: 391

Majde, J.A. (1993) Microbial cell-wall contaminants in peptides: a potential source of physiological artifacts. **Peptides**, 14 (3): 629–632

Maldonado, R.F., Sá-Correia, I. and Valvano, M.A. (2016) Lipopolysaccharide modification in Gram-negative bacteria during chronic infection. **FEMS Microbiology Reviews**, 40 (4): 480–493

Marchetti, G., Tincati, C. and Silvestri, G. (2013) Microbial translocation in the pathogenesis of HIV infection and AIDS. **Clinical Microbiology Reviews**, 26 (1): 2–18

Marom, T., Nokso-Koivisto, J. and Chonmaitree, T. (2012) Viral-bacterial interactions in acute otitis media. **Current allergy and asthma reports**, 12 (6): 551–558

Maxfield, F.R. and McGraw, T.E. (2004) Endocytic recycling. **Nature Reviews. Molecular Cell Biology**, 5 (2): 121–132

McClure, R. and Massari, P. (2014) TLR-Dependent Human Mucosal Epithelial Cell Responses to Microbial Pathogens. **Frontiers in immunology**, 5: 386

McGhie, E.J., Brawn, L.C., Hume, P.J., et al. (2009) Salmonella takes control: effector-driven manipulation of the host. **Current Opinion in Microbiology**, 12 (1): 117–124

Mee, C.J., Grove, J., Harris, H.J., et al. (2008) Effect of cell polarization on hepatitis C virus entry. **Journal of Virology**, 82 (1): 461–470

Mercer, J. and Helenius, A. (2012) Gulping rather than sipping: macropinocytosis as a way of virus entry. **Current Opinion in Microbiology**, 15 (4): 490–499

Milhollen, M.A., Traore, T., Adams-Duffy, J., et al. (2010) MLN4924, a NEDD8-activating enzyme inhibitor, is active in diffuse large B-cell lymphoma models: rationale for treatment of NF-{kappa}B-dependent lymphoma. **Blood**, 116 (9): 1515–1523

Miller, S.I., Ernst, R.K. and Bader, M.W. (2005) LPS, TLR4 and infectious disease diversity. **Nature Reviews. Microbiology**, 3 (1): 36–46

Mirmonsef, P., Krass, L., Landay, A., et al. (2012) The role of bacterial vaginosis and trichomonas in HIV transmission across the female genital tract. **Current HIV Research**, 10 (3): 202–210

Mitiku, H., Weldegebreal, F. and Teklemariam, Z. (2015) Magnitude of opportunistic infections and associated factors in HIV-infected adults on antiretroviral therapy in eastern Ethiopia. **HIV/AIDS (Auckland, N.Z.)**, 7: 137–144

Moller-Tank, S. and Maury, W. (2015) Ebola virus entry: a curious and complex series of events. **PLoS Pathogens**, 11 (4): e1004731

Monaco, C.L., Gootenberg, D.B., Zhao, G., et al. (2016) Altered Virome and Bacterial Microbiome in Human Immunodeficiency Virus-Associated Acquired Immunodeficiency Syndrome. **Cell Host & Microbe**, 19 (3): 311–322

Morens, D.M., Taubenberger, J.K. and Fauci, A.S. (2008) Predominant role of bacterial pneumonia as a cause of death in pandemic influenza: implications for pandemic influenza preparedness. **The Journal of Infectious Diseases**, 198 (7): 962–970

Motta, V., Soares, F., Sun, T., et al. (2015) NOD-like receptors: versatile cytosolic sentinels. **Physiological Reviews**, 95 (1): 149–178

Mudd, J.C. and Brenchley, J.M. (2016) Gut Mucosal Barrier Dysfunction, Microbial Dysbiosis, and Their Role in HIV-1 Disease Progression. **The Journal of Infectious Diseases**, 214 Suppl 2: S58–66

Mühlebach, M.D., Mateo, M., Sinn, P.L., et al. (2011) Adherens junction protein nectin-4 is the epithelial receptor for measles virus. **Nature**, 480 (7378): 530–533

Nakatsu, Y., Takeda, M., Ohno, S., et al. (2006) Translational inhibition and increased interferon induction in cells infected with C protein-deficient measles virus. **Journal of Virology**, 80 (23): 11861–11867

Naniche, D., Varior-Krishnan, G., Cervoni, F., et al. (1993) Human membrane cofactor protein (CD46) acts as a cellular receptor for measles virus. **Journal of Virology**, 67 (10): 6025–6032

Natoli, M., Leoni, B.D., D'Agnano, I., et al. (2012) Good Caco-2 cell culture practices. **Toxicology in Vitro**, 26 (8): 1243–1246

Noyce, R.S., Bondre, D.G., Ha, M.N., et al. (2011) Tumor cell marker PVRL4 (nectin 4) is an epithelial cell receptor for measles virus. **PLoS Pathogens**, 7 (8): e1002240

Nusbaum, R.J., Calderon, V.E., Huante, M.B., et al. (2016) Pulmonary Tuberculosis in Humanized Mice Infected with HIV-1. **Scientific reports**, 6: 21522

Obasi, C.N., Barrett, B., Brown, R., et al. (2014) Detection of viral and bacterial pathogens in acute respiratory infections. **The Journal of Infection**, 68 (2): 125–130

Ohkura, T., Momose, F., Ichikawa, R., et al. (2014) Influenza A virus hemagglutinin and neuraminidase mutually accelerate their apical targeting through clustering of lipid rafts. **Journal of Virology**, 88 (17): 10039–10055

Ohuchi, M., Cramer, A., Vey, M., et al. (1994) Rescue of vector-expressed fowl plague virus hemagglutinin in biologically active form by acidotropic agents and coexpressed M2 protein. **Journal of Virology**, 68 (2): 920–926

Opal, S.M. (2007) The host response to endotoxin, antilipopolysaccharide strategies, and the management of severe sepsis. **International Journal of Medical Microbiology**, 297 (5): 365–377

Palgen, J.L., Jurgens, E.M., Moscona, A., et al. (2015) Unity in diversity: shared mechanism of entry among paramyxoviruses. **Progress in molecular biology and translational science**, 129: 1–32

Palmer, B.E., Li, S.X. and Lozupone, C.A. (2016) The hIV-Associated enteric microbiome has gone viral. **Cell Host & Microbe**, 19 (3): 270–272

Panda, S., Mohakud, N.K., Pena, L., et al. (2014) Human metapneumovirus: review of an important respiratory pathogen. **International Journal of Infectious Diseases**, 25: 45–52

Pantaleo, G., Graziosi, C. and Fauci, A.S. (1993) New concepts in the immunopathogenesis of human immunodeficiency virus infection. **The New England Journal of Medicine**, 328 (5): 327–335

Papi, A., Bellettato, C.M., Braccioni, F., et al. (2006) Infections and airway inflammation in chronic obstructive pulmonary disease severe exacerbations. **American Journal of Respiratory and Critical Care Medicine**, 173 (10): 1114–1121

Pasqual, G., Rojek, J.M., Masin, M., et al. (2011) Old world arenaviruses enter the host cell via the multivesicular body and depend on the endosomal sorting complex required for transport. **PLoS Pathogens**, 7 (9): e1002232

Pawlowski, A., Jansson, M., Sköld, M., et al. (2012) Tuberculosis and HIV co-infection. **PLoS Pathogens**, 8 (2): e1002464

Pelkmans, L. (2005) Secrets of caveolae- and lipid raft-mediated endocytosis revealed by mammalian viruses. **Biochimica et Biophysica Acta**, 1746 (3): 295–304

Peltola, V.T. and McCullers, J.A. (2004) Respiratory viruses predisposing to bacterial infections: role of neuraminidase. **The Pediatric Infectious Disease Journal**, 23 (1 Suppl): S87–97

Peterson, L.W. and Artis, D. (2014) Intestinal epithelial cells: regulators of barrier function and immune homeostasis. **Nature Reviews. Immunology**, 14 (3): 141–153

Pfaller, M.A., Richter, S.S., Funke, G., et al. (2015) **Manual of Clinical Microbiology, 11th Edition**. American Society of Microbiology

Pizzato, M., Erlwein, O., Bonsall, D., et al. (2009) A one-step SYBR Green I-based product-enhanced reverse transcriptase assay for the quantitation of retroviruses in cell culture supernatants. **Journal of Virological Methods**, 156 (1-2): 1–7

Porte, R., Fougeron, D., Muñoz-Wolf, N., et al. (2015) A Toll-Like Receptor 5 Agonist Improves the Efficacy of Antibiotics in Treatment of Primary and Influenza Virus-Associated Pneumococcal Mouse Infections. **Antimicrobial Agents and Chemotherapy**, 59 (10): 6064–6072

Prince, P.D., Matser, A., van Tienen, C., et al. (2014) Mortality rates in people dually infected with HIV-1/2 and those infected with either HIV-1 or HIV-2: a systematic review and meta-analysis. **AIDS**, 28 (4): 549–558

Rahal, J.J. and Simberkoff, M.S. (1979) Bactericidal and bacteriostatic action of chloramphenicol against memingeal pathogens. **Antimicrobial Agents and Chemotherapy**, 16 (1): 13–18

Rahman, A.H., Taylor, D.K. and Turka, L.A. (2009) The contribution of direct TLR signaling to T cell responses. **Immunologic Research**, 45 (1): 25–36

Rall, G. and Knoll, L.J. (2016) Development of Complex Models to Study Co- and Polymicrobial Infections and Diseases. **PLoS Pathogens**, 12 (9): e1005858

Renk, H., Regamey, N. and Hartl, D. (2014) Influenza A(H1N1)pdm09 and cystic fibrosis lung disease: a systematic meta-analysis. **Plos One**, 9 (1): e78583

De Repentigny, L., Goupil, M. and Jolicoeur, P. (2015) Oropharyngeal Candidiasis in HIV Infection: Analysis of Impaired Mucosal Immune Response to Candida albicans in Mice Expressing the HIV-1 Transgene. **Pathogens (Basel, Switzerland)**, 4 (2): 406–421

Rinaldo, C.R. and Piazza, P. (2004) Virus infection of dendritic cells: portal for host invasion and host defense. **Trends in Microbiology**, 12 (7): 337–345

Robinson, C.M., Jesudhasan, P.R. and Pfeiffer, J.K. (2014) Bacterial lipopolysaccharide binding enhances virion stability and promotes environmental fitness of an enteric virus. **Cell Host & Microbe**, 15 (1): 36–46

Rodriguez Rodrigues, C., Remes Lenicov, F., Jancic, C., et al. (2013) Candida albicans delays HIV-1 replication in macrophages. **Plos One**, 8 (8): e72814

Rossez, Y., Wolfson, E.B., Holmes, A., et al. (2015) Bacterial flagella: twist and stick, or dodge across the kingdoms. **PLoS Pathogens**, 11 (1): e1004483

Le Roy, C. and Wrana, J.L. (2005) Clathrin- and non-clathrin-mediated endocytic regulation of cell signalling. **Nature Reviews. Molecular Cell Biology**, 6 (2): 112–126

Rybtke, M., Hultqvist, L.D., Givskov, M., et al. (2015) Pseudomonas aeruginosa Biofilm Infections: Community Structure, Antimicrobial Tolerance and Immune Response. **Journal of Molecular Biology**, 427 (23): 3628–3645

Sajjan, U.S., Jia, Y., Newcomb, D.C., et al. (2006) H. influenzae potentiates airway epithelial cell responses to rhinovirus by increasing ICAM-1 and TLR3 expression. **The FASEB Journal**, 20 (12): 2121–2123

Salazar-Gonzalez, R.M. and McSorley, S.J. (2005) Salmonella flagellin, a microbial target of the innate and adaptive immune system. **Immunology Letters**, 101 (2): 117–122

Sambe-Ba, B., Espié, E., Faye, M.E., et al. (2013) Community-acquired diarrhea among children and adults in urban settings in Senegal: clinical, epidemiological and microbiological aspects. **BMC Infectious Diseases**, 13: 580

Santos, R.L. and Bäumler, A.J. (2004) Cell tropism of Salmonella enterica. **International Journal of Medical Microbiology**, 294 (4): 225–233

Schlee, M., Wehkamp, J., Altenhoefer, A., et al. (2007) Induction of human beta-defensin 2 by the probiotic Escherichia coli Nissle 1917 is mediated through flagellin. **Infection and Immunity**, 75 (5): 2399–2407

Schmiedel, Y. and Zimmerli, S. (2016) Common invasive fungal diseases: an overview of invasive candidiasis, aspergillosis, cryptococcosis, and Pneumocystis pneumonia. **Swiss Medical Weekly**, 146: w14281

Schoenhals, M., Frecha, C., Bruyer, A., et al. (2012) Efficient transduction of healthy and malignant plasma cells by lentiviral vectors pseudotyped with measles virus glycoproteins. **Leukemia**, 26 (7): 1663–1670

Sebastian, N.T. and Collins, K.L. (2014) Targeting HIV latency: resting memory T cells, hematopoietic progenitor cells and future directions. **Expert Review of Anti-Infective Therapy**, 12 (10): 1187–1201

Secor, W.E. (2012) The effects of schistosomiasis on HIV/AIDS infection, progression and transmission. **Current Opinion in HIV and AIDS**, 7 (3): 254–259

Sekirov, I., Russell, S.L., Antunes, L.C., et al. (2010) Gut microbiota in health and disease. **Physiological Reviews**, 90 (3): 859–904

Shan, L. and Siliciano, R.F. (2014) Unraveling the relationship between microbial translocation and systemic immune activation in HIV infection. **The Journal of Clinical Investigation**, 124 (6): 2368–2371

Shankar, E.M., Vignesh, R., Ellegård, R., et al. (2014) HIV-Mycobacterium tuberculosis co-infection: a “danger-couple model” of disease pathogenesis. **Pathogens and disease**, 70 (2): 110–118

Shimojima, M., Ströher, U., Ebihara, H., et al. (2012) Identification of cell surface molecules involved in dystroglycan-independent Lassa virus cell entry. **Journal of Virology**, 86 (4): 2067–2078

Short, K.R., Habets, M.N., Hermans, P.W., et al. (2012) Interactions between Streptococcus pneumoniae and influenza virus: a mutually beneficial relationship? **Future Microbiology**, 7 (5): 609–624

Shu, Q., Lennemann, N.J., Sarkar, S.N., et al. (2015) ADAP2 Is an Interferon Stimulated Gene That Restricts RNA Virus Entry. **PLoS Pathogens**, 11 (9): e1005150

Simon, R. and Levine, M.M. (2012) Glycoconjugate vaccine strategies for protection against invasive Salmonella infections. **Human vaccines & immunotherapeutics**, 8 (4): 494–498

Singh, P.K., Tack, B.F., McCray, P.B., et al. (2000a) Synergistic and additive killing by antimicrobial factors found in human airway surface liquid. **American Journal of Physiology. Lung Cellular and Molecular Physiology**, 279 (5): L799–805

Singh, U., Van Itallie, C.M., Mitic, L.L., et al. (2000b) CaCo-2 cells treated with Clostridium perfringens enterotoxin form multiple large complex species, one of which contains the tight junction protein occludin. **The Journal of Biological Chemistry**, 275 (24): 18407–18417

Skehel, J.J. and Wiley, D.C. (2000) Receptor binding and membrane fusion in virus entry: the influenza hemagglutinin. **Annual Review of Biochemistry**, 69: 531–569

Van der Sluijs, K.F., van Elden, L.J., Nijhuis, M., et al. (2004) IL-10 is an important mediator of the enhanced susceptibility to pneumococcal pneumonia after influenza infection. **Journal of Immunology**, 172 (12): 7603–7609

Smith, K.D., Andersen-Nissen, E., Hayashi, F., et al. (2003) Toll-like receptor 5 recognizes a conserved site on flagellin required for protofilament formation and bacterial motility. **Nature Immunology**, 4 (12): 1247–1253

Song, H., Huai, W., Yu, Z., et al. (2016) MLN4924, a First-in-Class NEDD8-Activating Enzyme Inhibitor, Attenuates IFN-β Production. **Journal of Immunology**, 196 (7): 3117–3123

Sonoda, N., Furuse, M., Sasaki, H., et al. (1999) Clostridium perfringens enterotoxin fragment removes specific claudins from tight junction strands: Evidence for direct involvement of claudins in tight junction barrier. **The Journal of Cell Biology**, 147 (1): 195–204

Soucy, T.A., Smith, P.G. and Rolfe, M. (2009) Targeting NEDD8-activated cullin-RING ligases for the treatment of cancer. **Clinical Cancer Research**, 15 (12): 3912–3916

Steele-Mortimer, O. (2008) The Salmonella-containing vacuole: moving with the times. **Current Opinion in Microbiology**, 11 (1): 38–45

Sun, Y.H., Rolán, H.G. and Tsolis, R.M. (2007) Injection of flagellin into the host cell cytosol by Salmonella enterica serotype Typhimurium. **The Journal of Biological Chemistry**, 282 (47): 33897–33901

Svärd, J., Paquin-Proulx, D., Buggert, M., et al. (2015) Role of translocated bacterial flagellin in monocyte activation among individuals with chronic HIV-1 infection. **Clinical Immunology**, 161 (2): 180–189

Tallant, T., Deb, A., Kar, N., et al. (2004) Flagellin acting via TLR5 is the major activator of key signaling pathways leading to NF-kappa B and proinflammatory gene program activation in intestinal epithelial cells. **BMC Microbiology**, 4: 33

Taylor, A.C. (1962) Responses of cells to pH changes in the medium. **The Journal of Cell Biology**, 15: 201–209

Thibault, S., Imbeault, M., Tardif, M.R., et al. (2009) TLR5 stimulation is sufficient to trigger reactivation of latent HIV-1 provirus in T lymphoid cells and activate virus gene expression in central memory CD4+ T cells. **Virology**, 389 (1-2): 20–25

Törmäkangas, L., Markkula, E., Lounatmaa, K., et al. (2010) Chlamydia pneumoniae infection in polarized epithelial cell lines. **Infection and Immunity**, 78 (6): 2714–2722

Tunney, M.M., Einarsson, G.G., Wei, L., et al. (2013) Lung microbiota and bacterial abundance in patients with bronchiectasis when clinically stable and during exacerbation. **American Journal of Respiratory and Critical Care Medicine**, 187 (10): 1118–1126

Uchiyama, R., Chassaing, B., Zhang, B., et al. (2014) Antibiotic treatment suppresses rotavirus infection and enhances specific humoral immunity. **The Journal of Infectious Diseases**, 210 (2): 171–182

Uematsu, S., Jang, M.H., Chevrier, N., et al. (2006) Detection of pathogenic intestinal bacteria by Toll-like receptor 5 on intestinal CD11c+ lamina propria cells. **Nature Immunology**, 7 (8): 868–874

Vardakas, K.Z., Theocharis, G., Tansarli, G.S., et al. (2016) Impact of oseltamivir use on the reduction of complications in patients with influenza: a prospective study. **Archives of Virology**, 161 (9): 2511–2518

Velge, P., Wiedemann, A., Rosselin, M., et al. (2012) Multiplicity of Salmonella entry mechanisms, a new paradigm for Salmonella pathogenesis. **MicrobiologyOpen**, 1 (3): 243–258

Verkaik, N.J., Nguyen, D.T., de Vogel, C.P., et al. (2011) Streptococcus pneumoniae exposure is associated with human metapneumovirus seroconversion and increased susceptibility to in vitro HMPV infection. **Clinical Microbiology and Infection**, 17 (12): 1840–1844

Verma, A., Arora, S.K., Kuravi, S.K., et al. (2005) Roles of specific amino acids in the N terminus of Pseudomonas aeruginosa flagellin and of flagellin glycosylation in the innate immune response. **Infection and Immunity**, 73 (12): 8237–8246

Vermeire, J., Naessens, E., Vanderstraeten, H., et al. (2012) Quantification of reverse transcriptase activity by real-time PCR as a fast and accurate method for titration of HIV, lenti- and retroviral vectors. **Plos One**, 7 (12): e50859

Viasus, D., Paño-Pardo, J.R., Pachón, J., et al. (2011) Pneumonia complicating pandemic (H1N1) 2009: risk factors, clinical features, and outcomes. **Medicine**, 90 (5): 328–336

Vijay-Kumar, M. and Gewirtz, A.T. (2009) Flagellin: key target of mucosal innate immunity. **Mucosal Immunology**, 2 (3): 197–205

Vinzing, M., Eitel, J., Lippmann, J., et al. (2008) NAIP and Ipaf control Legionella pneumophila replication in human cells. **Journal of Immunology**, 180 (10): 6808–6815

Walker, S.L., Brocklehurst, T.F. and Wimpenny, J.W. (1997) The effects of growth dynamics upon pH gradient formation within and around subsurface colonies of Salmonella typhimurium. **Journal of Applied Microbiology**, 82 (5): 610–614

Walters, R.W., van't Hof, W., Yi, S.M., et al. (2001) Apical localization of the coxsackie-adenovirus receptor by glycosyl-phosphatidylinositol modification is sufficient for adenovirus-mediated gene transfer through the apical surface of human airway epithelia. **Journal of Virology**, 75 (16): 7703–7711

Wei, X., Decker, J.M., Liu, H., et al. (2002) Emergence of resistant human immunodeficiency virus type 1 in patients receiving fusion inhibitor (T-20) monotherapy. **Antimicrobial Agents and Chemotherapy**, 46 (6): 1896–1905

Whitsett, J.A. and Alenghat, T. (2015) Respiratory epithelial cells orchestrate pulmonary innate immunity. **Nature Immunology**, 16 (1): 27–35

Wilks, J., Beilinson, H. and Golovkina, T.V. (2013) Dual role of commensal bacteria in viral infections. **Immunological Reviews**, 255 (1): 222–229

Wilks, J., Lien, E., Jacobson, A.N., et al. (2015) Mammalian Lipopolysaccharide Receptors Incorporated into the Retroviral Envelope Augment Virus Transmission. **Cell Host & Microbe**, 18 (4): 456–462

Wissinger, E., Goulding, J. and Hussell, T. (2009) Immune homeostasis in the respiratory tract and its impact on heterologous infection. **Seminars in Immunology**, 21 (3): 147–155

Wolfgang, M.C., Jyot, J., Goodman, A.L., et al. (2004) Pseudomonas aeruginosa regulates flagellin expression as part of a global response to airway fluid from cystic fibrosis patients. **Proceedings of the National Academy of Sciences of the United States of America**, 101 (17): 6664–6668

Wu, Z., Nybom, P. and Magnusson, K.E. (2000) Distinct effects of Vibrio cholerae haemagglutinin/protease on the structure and localization of the tight junction-associated proteins occludin and ZO-1. **Cellular Microbiology**, 2 (1): 11–17

Yamamoto, S. and Kutsukake, K. (2006) FljA-mediated posttranscriptional control of phase 1 flagellin expression in flagellar phase variation of Salmonella enterica serovar Typhimurium. **Journal of Bacteriology**, 188 (3): 958–967

Yamauchi, Y. and Helenius, A. (2013) Virus entry at a glance. **Journal of Cell Science**, 126 (Pt 6): 1289–1295

Yu, Y., Nagai, S., Wu, H., et al. (2006) TLR5-mediated phosphoinositide 3-kinase activation negatively regulates flagellin-induced proinflammatory gene expression. **Journal of Immunology**, 176 (10): 6194–6201

Yu, Y., Zeng, H., Lyons, S., et al. (2003) TLR5-mediated activation of p38 MAPK regulates epithelial IL-8 expression via posttranscriptional mechanism. **American Journal of Physiology. Gastrointestinal and Liver Physiology**, 285 (2): G282–90

Zack, J.A., Kim, S.G. and Vatakis, D.N. (2013) HIV restriction in quiescent $CD4^+$ T cells. **Retrovirology**, 10: 37

Zeng, H., Carlson, A.Q., Guo, Y., et al. (2003) Flagellin is the major proinflammatory determinant of enteropathogenic Salmonella. **Journal of Immunology**, 171 (7): 3668–3674

Zhang, B., Chassaing, B., Shi, Z., et al. (2014) Viral infection. Prevention and cure of rotavirus infection via TLR5/NLRC4-mediated production of IL-22 and IL-18. **Science (New York)**, 346 (6211): 861–865

Zhang, F., Sodroski, C., Cha, H., et al. (2016) Infection of Hepatocytes with HCV Increases Cell Surface Levels of Heparan Sulfate Proteoglycans, Uptake of Cholesterol and Lipoprotein, and Virus Entry by Upregulating SMAD6 and SMAD7. **Gastroenterology**

Zhang, S., Kingsley, R.A., Santos, R.L., et al. (2003) Molecular pathogenesis of Salmonella enterica serotype typhimurium-induced diarrhea. **Infection and Immunity**, 71 (1): 1–12

Zhang, Y.G., Wu, S., Xia, Y., et al. (2013) Salmonella infection upregulates the leaky protein claudin-2 in intestinal epithelial cells. **Plos One**, 8 (3): e58606

Zhao, Y. and Shao, F. (2015) The NAIP-NLRC4 inflammasome in innate immune detection of bacterial flagellin and type III secretion apparatus. **Immunological Reviews**, 265 (1): 85–102